

# UNCLASSIFIED

AD NUMBER
AD266714
NEW LIMITATION CHANGE
TO Approved for public release, distribution unlimited
FROM Distribution: Further dissemination only as directed by Aeronautical Systems Division, AFSC, USAF, Wright -Patterson AFB, Ohio 45433; Jun 1961 or higher DoD authority.
AUTHORITY
ASD, USAF itr, 6 Aug 1974.

THIS PAGE IS UNCLASSIFIED

UNCLASSIFIED

---

AD 266 714

*Reproduced  
by the*

ARMED SERVICES TECHNICAL INFORMATION AGENCY  
ARLINGTON HALL STATION  
ARLINGTON 12, VIRGINIA



---

UNCLASSIFIED

NOTICE: When government or other drawings, specifications or other data are used for any purpose other than in connection with a definitely related government procurement operation, the U. S. Government thereby incurs no responsibility, nor any obligation whatsoever; and the fact that the Government may have formulated, furnished, or in any way supplied the said drawings, specifications, or other data is not to be regarded by implication or otherwise as in any manner licensing the holder or any other person or corporation, or conveying any rights or permission to manufacture, use or sell any patented invention that may in any way be related thereto.

WADD TECHNICAL REPORT 58-284  
PART IV

CATALOGED BY ASTIA  
AS AD NO. 266714

**PERFORMANCE OF TRAILING AERODYNAMIC  
DECELERATORS AT HIGH DYNAMIC PRESSURES**  
**PHASE IV**

B. A. ENGSTROM  
R. P. LANG

COOK RESEARCH LABORATORIES  
A DIVISION OF COOK ELECTRIC COMPANY  
CHICAGO, ILLINOIS

JUNE 1961

NOX

This report is not to be announced  
or distributed automatically  
to foreign governments  
(AFR 205-43A, paragraph 6d).

AERONAUTICAL SYSTEMS DIVISION

## NOTICES

When Government drawings, specifications, or other data are used for any purpose other than in connection with a definitely related Government procurement operation, the United States Government thereby incurs no responsibility nor any obligation whatsoever; and the fact that the Government may have formulated, furnished, or in any way supplied the said drawings, specifications, or other data, is not to be regarded by implication or otherwise as in any manner licensing the holder or any other person or corporation, or conveying any rights or permission to manufacture, use, or sell any patented invention that may in any way be related thereto.

ASTIA release to OTS not authorized.

Qualified requesters may obtain copies of this report from the Armed Services Technical Information Agency, (ASTIA), Arlington Hall Station, Arlington 12, Virginia.

Copies of ASD Technical Reports and Technical Notes should not be returned to the Aeronautical Systems Division unless return is required by security considerations, contractual obligations, or notice on a specific document.

WADD TECHNICAL REPORT 58-284  
PART IV

# **PERFORMANCE OF TRAILING AERODYNAMIC DECELERATORS AT HIGH DYNAMIC PRESSURES**

## **PHASE IV**

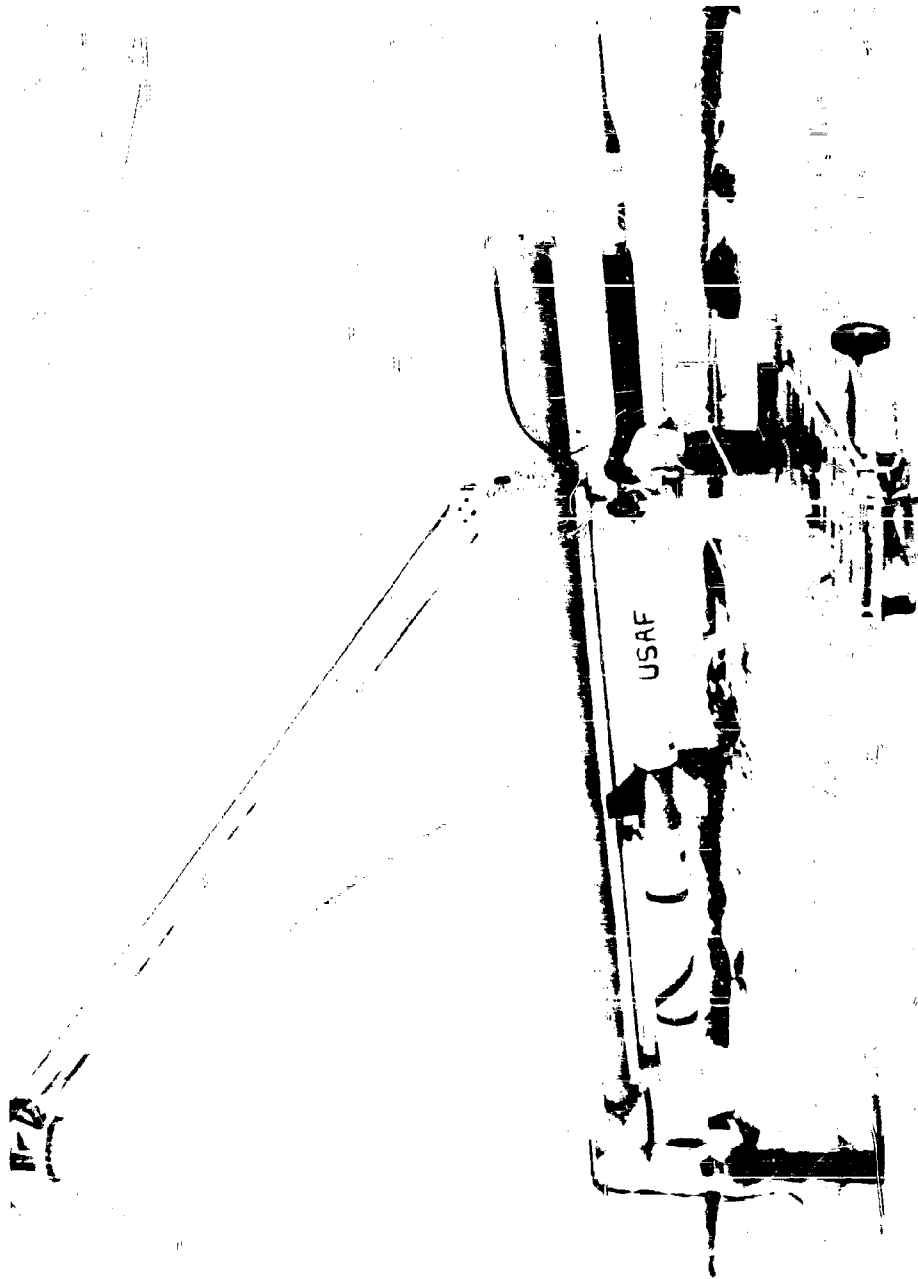
**B. A. ENGSTROM  
R. P. LANG**

**COOK RESEARCH LABORATORIES  
A DIVISION OF COOK ELECTRIC COMPANY  
CHICAGO, ILLINOIS**

**JUNE 1961**

**AERODYNAMIC DECELERATOR BRANCH  
FLIGHT ACCESSORIES LABORATORY  
CONTRACT No. AF 33(616)-5507  
PROJECT No. 6065-61525**

**AERONAUTICAL SYSTEMS DIVISION  
AIR FORCE SYSTEMS COMMAND  
UNITED STATES AIR FORCE  
WRIGHT-PATTERSON AIR FORCE BASE, OHIO**



Frontispiece

## FOREWORD

This report was prepared by the Cook Research Laboratories, a division of the Cook Electric Company, Chicago, Illinois, in compliance with Contract No. AF 33(616)-5507, Project No. 6065 and Task No. 61525. The Parachute Branch, Aeronautical Accessories Laboratory, Wright Air Development Division, was the initiating agency with Mr. Rudi Berndt serving as project officer. The work at the Cook Research Laboratories on Phase IV of Project P-1031E was under the supervision of Dr. J. R. Downing, Director; Dr. H. V. Hawkins, Assistant Director; and B. A. Engstrom, Project Engineer. The work was initiated on 1 February 1959 and completed on 15 October 1959.

Staff members who contributed to the project include: L. J. Lorenz Executive Engineer; S. C. Henjum, Staff Engineer; K. J. Allen, Senior Engineer; L. W. Sims, Senior Engineer; G. A. Allred, Senior Engineer; R. Golbach, Designer; R. P. Lang, Engineer.



## ABSTRACT

A method for the testing of Aerodynamic decelerators utilizing a ground launch technique was developed. Suitable test equipment and launch hardware was selected. Test methods and procedures were established. Test missiles capable of over water operation were designed and fabricated.

A field test program consisting of five missions was performed over a test regime of altitudes between 25,000 and 70,000 feet and Mach numbers from 1.1 to 1.83.

A shaped parachute canopy in the form of a hemispherical ribbon type with 10% extensions (Hemisflo) was found to perform satisfactorily at a Mach number of 1.83.

## PUBLICATION REVIEW

This report has been reviewed and is approved.

FOR THE COMMANDER:



GEORGE A. SOLT, JR.  
Chief, Aerodynamic Decelerator Branch  
Flight Accessories Laboratory

## TABLE OF CONTENTS

<u>Section</u>	<u>Page</u>
I. INTRODUCTION . . . . .	1
A. General . . . . .	1
B. Background. . . . .	1
II. OPERATIONAL RESULTS. . . . .	4
A. Test Mission 28-1 . . . . .	4
B. Test Mission 29-2 . . . . .	8
C. Test Mission 30-3 . . . . .	9
D. Test Mission 31-4 . . . . .	12
E. Test Mission 32-5 . . . . .	14
III. TEST MISSILE DEVELOPMENT . . . . .	16
A. Background. . . . .	16
B. General Description. . . . .	16
1. Missile Structure . . . . .	17
2. Nose Assembly . . . . .	19
a. Nose Probe . . . . .	19
b. Air Storage . . . . .	19
c. Nose Structure . . . . .	20
3. Forward Instrumentation Compartment. . . . .	21
4. Recovery Compartment. . . . .	21
5. Aft Instrumentation Compartment . . . . .	23
6. Test Parachute Assembly. . . . .	23

# TABLE OF CONTENTS (cont'd)

<u>Section</u>	<u>Page</u>
C. Missile Subsystems . . . . .	25
1. Instrumentation . . . . .	25
a. Programming . . . . .	25
b. Data Acquisition . . . . .	27
c. Tracking Aids . . . . .	29
2. Recovery . . . . .	30
3. Flotation . . . . .	30
D. Systems Testing . . . . .	31
1. Recovery . . . . .	31
2. Instrumentation . . . . .	36
3. Camera. . . . .	37
E. Aerodynamic Considerations . . . . .	38
1. Stability Characteristics . . . . .	38
2. Dispersion . . . . .	42
3. Aerodynamic Heating. . . . .	45
IV. TEST METHODS, PROCEDURES AND FACILITIES .	48
A. Test Facilities . . . . .	48
1. General. . . . .	48
2. Launch Site . . . . .	48
B. Launch Equipment . . . . .	49
1. Launcher . . . . .	49
2. Launch Fittings . . . . .	50

# TABLE OF CONTENTS (cont'd)

<u>Section</u>	<u>Page</u>
3. Booster Hardware . . . . .	51
4. Booster to Missile Adaptor . . . . .	53
5. Second Stage Igniter. . . . .	54
C. Test Procedures . . . . .	55
1. Preparation . . . . .	55
2. Count Down Procedure . . . . .	56
D. Data Reduction and Analysis . . . . .	58
1. General . . . . .	58
2. Telemetry Data. . . . .	59
3. Film Data . . . . .	64
V. DISCUSSION OF TEST RESULTS . . . . .	68
A. General . . . . .	68
B. Missile Performance . . . . .	68
C. Test Parachute Performance . . . . .	85
VI. CONCLUSIONS AND RECOMMENDATIONS. . . . .	95

# LIST OF ILLUSTRATIONS

<u>Figure</u>		<u>Page</u>
1	Single Stage Type III Cree Launch, Mission 28-1 . . . . .	6
2	Two Stage Type III Cree Loading Operation, Mission 30-3	10
3	Two Stage Type III Cree Elevated to a Launch Angle of 79° . . . . .	11
4	Two Stage Type III Cree Launch, Mission 30-3 . . . . .	11
5	Two Stage Type III Cree Launch, Mission 31-4 . . . . .	13
6	Model 59 Cree Missile Structure . . . . .	17
7	General Assembly of Model 59 Cree Missile . . . . .	18
8	Main Instrumentation System Details . . . . .	22
9	Details of Cree Missile Aft End and Faired Last Stage Adaptor . . . . .	24
10	Block Diagram - Programming System . . . . .	26
11	Block Diagram - Data Acquisition System . . . . .	28
12	Cree Flotation Balloon . . . . .	32
13	Flotation System Test Method . . . . .	32
14	Crash Boat Approaching Floating Balloon . . . . .	33
15	Type I and II Cree Missiles - Center of Pressure and Center of Gravity vs. Mach Number . . . . .	38
16	Drag Coefficient vs. Mach Number Cree Types I, II and III . . . . .	39
17	Single Stage Type III Cree Center of Gravity and Center of Pressure vs. Mach Number . . . . .	39
18	Drag Coefficient vs. Mach Number - Single Stage Type III Cree . . . . .	40

# LIST OF ILLUSTRATIONS (cont'd)

<u>Figure</u>		<u>Page</u>
19	Two Stage Type III Cree Center of Gravity and Center of Pressure vs. Mach Number . . . . .	40
20	Drag Coefficient vs. Mach Number - Two Stage Type III Cree . . . . .	42
21	Two Stage Type I Cree Center of Gravity and Center of Pressure vs. Mach Number . . . . .	42
22	Three Stage Type III Cree Center of Gravity and Center of Pressure vs. Mach Number . . . . .	41
23	Drag Coefficient vs Mach Number - Cree Type III with Three Nike Stages . . . . .	42
24	Drag Coefficient vs. Mach Number - Cree Type III with Two Nike Stages . . . . .	42
25	Drag Coefficient vs. Mach Number - Cree Type III with Single Nike Stage . . . . .	42
26	Three Stage Two Missile Cree Cluster Center of Gravity and Center of Pressure vs. Mach Number . . . . .	43
27	Drag Coefficient vs. Mach Number - Cree Two Missile Cluster with Three Nike Stages . . . . .	43
28	Drag Coefficient vs. Mach Number - Cree Two Missile Cluster with Two Nike Stages . . . . .	44
29	Drag Coefficient vs. Mach Number - Cree Two Missile Cluster with One Nike Stage . . . . .	44
30	Skin Temperature vs. Time, Two Stage Type I Cree (Turbulent Heating) . . . . .	46
31	Cree Multistage Rocket Launcher . . . . .	49
32	Cree Zero Length Launching Fittings . . . . .	51
33	Cree Launcher with Two Nike Boosters Ready to Receive Payload . . . . .	52

# LIST OF ILLUSTRATIONS (cont'd)

<u>Figure</u>		<u>Page</u>
34	Nike Interstage Hardware . . . . .	52
35	Missile to Booster Unfaired Intertie Structure . . . .	53
36	Schematic Diagram - Second Stage Ignition System . .	55
37	Typical Pressure Transducer Calibration . . . . .	61
38	Film Data Reduction Table . . . . .	65
39	Predicted Missile Performance for a Single Stage, Type III Configuration . . . . .	69
40	Predicted Missile Performance for a Two Stage, Type III Configuration . . . . .	70
41	Data Collected on Phase I, Phase II, and Phase IV . .	71
42	Predicted and Actual Trajectories for Cree Mission 28-1 . . . . .	74
43	Wind Velocity vs. Altitude During Cree Mission 28-1 .	75
44	Missile Performance Data for Cree Mission 28-1 . . .	76
45	Predicted Trajectory for Cree Mission 29-2 . . . . .	78
46	Predicted and Actual Trajectory for Cree Mission 30-3	79
47	Missile Performance Data for Cree Mission 30-3 . . .	80
48	Predicted and Actual Trajectories for Cree Mission 31-4	82
49	Missile Performance Data for Cree Mission 31-4 . . .	83
50	Altitude vs. Time for Cree Mission 31-4 . . . . .	84
51	Predicted and Actual Trajectories for Cree Mission 32-5	84
52	Missile Performance Data for Cree Mission 32-5 . . .	86

# LIST OF ILLUSTRATIONS (cont'd)

<u>Figure</u>		<u>Page</u>
53	Typical Test Parachute Gore Layouts . . . . .	87
54	Parachute Test Data vs. Time for Cree Mission 30-3 .	88
55	Equiflo Parachute Inflation Characteristics. . . . .	90
56	Parachute Test Data vs. Time for Cree Mission 29-2 .	91
57	Film Data for Cree Mission 32-5 . . . . .	92
58	Hemisflo Parachute Inflation Characteristics. . . . .	93



# LIST OF TABLES

<u>Table</u>		<u>Page</u>
1	Field Test Program Outline . . . . .	3
2	Summary of Operational Results . . . . .	5
3	Parachute Physical Details . . . . .	72
4	Summary of Test Results. . . . .	73

## SECTION I

### INTRODUCTION

#### A. General

The following represents Part IV of WADD Technical Report 58-284 entitled, "Performance of Trailing Aerodynamic Decelerators at High Dynamic Pressures." The work reported on herein is Phase IV of a continuing effort in the study of the behavior of fabric parachutes at high altitudes and high velocities. The pertinent contract was AF 33(616)-5507.

Test vehicles were developed and fabricated, test hardware and launch equipment were selected and installed, and a series of tests were conducted. All testing was accomplished at the Air Proving Ground Center, Eglin Air Force Base, Florida.

Test data were collected on several basic types of parachutes. These were:

- (1) FIST ribbon
- (2) Conical ribbon
- (3) Equiflo ribbon
- (4) Hemisflo ribbon.

Test missions were accomplished over a velocity regime from Mach 1.1 to Mach 1.83 and at altitudes from 25,000 feet to 70,000 feet. The test vehicles were all launched from the ground and all except the first mission employed two stages of boost.

#### B. Background

Phases I and II of the program involved testing with both aircraft and balloons serving as launching platforms. A total of 27 missions were accomplished during these previous phases. The results were reported in Parts I and II of this report.

---

Manuscript released by the author February 1961 for publication as a WADD Technical Report

Before the end of Phase II the limitations of the launch methods being used became apparent. Range limitations, weather restrictions, and other difficulties made it necessary to adopt ground-launch techniques. No suitable land range was available and, therefore, an over-water range was selected. As a result the basic missile had to be redesigned for water recovery. This involved the inclusion of a balloon flotation system and the arrangement of all instrumentation components in watertight compartments.

The redesign of the test vehicle was partially accomplished during Phase II. Also, some progress was made on the fabrication of the necessary quantity of these test vehicles. A launcher was selected, ordered, received, and installed at the test site. Launch techniques and procedures were tentatively established. The necessary launch hardware was determined and either fabrication initiated or vendors contacted.

Phase III was a wind tunnel study which was conducted concurrently with Phase II and was reported as Part III of this report.

Table 1 presents an over-all picture of the testing during Phase I, II and IV.

TABLE 1  
FIELD TEST PROGRAM OUTLINE

Test No.	Phase No.	Mission No.	Test Date	Mach No.	Altitude (ft)	Test Site	Type of Launch	Missile Type
1	I	1	6/19/57	0.5	15,000	El Centro	Aircraft	I
2	I	2	6/28/57	0.75	15,000	El Centro	Aircraft	II
3	I	3	7/9/57	0.75	15,000	El Centro	Aircraft	II
4	I	4	8/2/57	0.75	15,000	El Centro	Aircraft	I
5	I	5	8/27/57	0.75	15,000	El Centro	Aircraft	I
6	I	6	9/18/57	0.5	15,000	El Centro	Aircraft	I
7	I	7	10/18/57	0.5	15,000	El Centro	Aircraft	I
8	I	8	11/1/57	0.5	15,000	El Centro	Aircraft	I
9	I	9	11/15/57	0.75	30,000	El Centro	Aircraft	II
10	I	10	11/25/57	0.5	30,000	El Centro	Aircraft	III
11	I	11	12/13/57	0.75	30,000	El Centro	Aircraft	I
12	I	12	1/10/58	0.75	30,000	El Centro	Aircraft	III
13	I	13	2/16/58	0.5	30,000	El Centro	Aircraft	II
14	I	14	2/24/58	0.75	15,000	El Centro	Aircraft	II
15	I	15	3/3/58	0.75	30,000	El Centro	Aircraft	I
16	II	-	5/22/58	0.75	30,000	El Centro	Aircraft	II
17	II	1	6/27/58	0.75	15,000	El Centro	Aircraft	Cluster
18	II	3	7/31/58	0.75	15,000	El Centro	Aircraft	Cluster
19	II	6	8/7/58	0.5	70,000	AFMDC	Balloon	Cluster
20	II	7	9/17/58	0.5	70,000	AFMDC	Balloon	Cluster
21	II	8	10/9/58	0.75	70,000	AFMDC	Balloon	Cluster
22	II	3	10/24/58	2.0	30,000	El Centro	Aircraft	Cluster
23	II	4	10/28/58	2.0	30,000	El Centro	Aircraft	Cluster
24	II	9	11/4/58	0.75	70,000	AFMDC	Balloon	Cluster
25	II	13	11/14/58	0.75	100,000	AFMDC	Balloon	Cluster
26	II	5	12/2/58	2.0	30,000	El Centro	Aircraft	Cluster
27	II	10	12/16/58	0.5	100,000	AFMDC	Balloon	Cluster
28	IV	1	3/10/59	1.5	25,000	APGC	Ground	III
29	IV	2	4/23/59	1.5	66,000	APGC	Ground	III
30	IV	3	6/19/59	1.5	66,000	APGC	Ground	III
31	IV	4	7/10/59	1.87	50,000	APGC	Ground	II
32	IV	5	9/2/59	1.87	50,000	APGC	Ground	III

## SECTION II

### OPERATIONAL RESULTS

This section presents primarily an over-all evaluation of the relative performance of the five ground launch test missions of Phase IV. Included herein are general descriptions of launch and flight characteristics, instrumentation efficiency, and the success of recovery operations. Table 2 introduces in summary form the operational results of test missions 28-1 through 32-5. Presentation and discussion of test data will be accomplished in detail in Section V.

#### A. Test Mission 28-1

Test Date - 10 March 1959

Configuration - Type III missile (800 lb) with single Nike booster

Mission No. - 28-1

Launch angle -  $79^{\circ}$

Programmed test altitude - 25,000 ft

Anticipated test velocity - Mach 1.5

Test parachute - CRIII C-30 $^{\circ}$  conical ribbon

##### 1. Test Results

The launch was normal and uneventful (see Figure 1). Missile left launcher and climbed on predicted trajectory. Booster burning appeared erratic, but provided a full 3.5 seconds of thrust. At first stage burnout a spin rate of approximately one revolution per second was observed. Ground cameras showed the missile and booster still attached (or in very close proximity to each other) at  $t + 4.0$  seconds or 4.0 seconds after launch. The missile was not visible again until  $t + 5.0$  seconds. By this time separation had occurred and the booster was not seen within the camera's field of view. At  $t + 5.1$  seconds a white object appeared just aft of the test missile. Indications of test parachute deployment at approximately four seconds were noted during the investigation of telemetry records. Booster impact was observed visually from the shore. Several objects, one of them tentatively

TABLE 2

## SUMMARY OF OPERATIONAL RESULTS

Mission No.	28-1	29-2	30-3	31-4	32-5
Launch	Normal	Normal	Normal	Normal	Normal
First Stage Burning	Normal	Normal**	Normal	Normal	Normal
Second Stage Burning	-----	Premature Ignition	Normal	Normal	Late Ignition - Rough Burning
Coast	Normal	Excessively Long	Normal	Normal	Shorter Than Normal
Second Stage Separation	Normal*	Normal	Normal	Normal	Too Close to Burnout - Rough
Test Parachute Deployment	Premature	As Programmed	As Programmed	Unknown	As Programmed
Instrumentation					
Static Pressure	Good	None	None	Good	None
Impact Pressure	Good	Good	None	None	None
Shock Force	None	Good	Good	None	None
Drag Force	None	Good	Good	None	None
Timing Mark Oscillator	Intermittent	Good	Good	Good	None
Camera Data	None	None	Good	None	Good But No Timing Marks
Nose Weight Ejection	As Programmed	Unknown	As Programmed	Unknown	As Programmed
Recovery Parachute Deployment	As Programmed	As Programmed	As Programmed	As Programmed	As Programmed
Balloon Deployment	None	As Programmed	As Programmed	As Programmed	As Programmed
SARAH Signal	None	Briefly	Received by Boat	None	Good
Recovery	None	None	Yes	None	Yes
Conrave Photodolite Tracking	To 4,000 Ft	None	To 54,000 Ft	To 14,000 Ft	To Peak Altitude
Radar					
Beacon Tracking	None	None	Intermittent	None	To Peak Altitude
Skin Tracking	Peak Altitude to Water Impact	None	46,000 Ft to Water Impact	32,000 Ft to Water Impact	43,000 Ft to Water Impact

\*First Stage Separation

\*\*Premature Separation at 0.050 Second

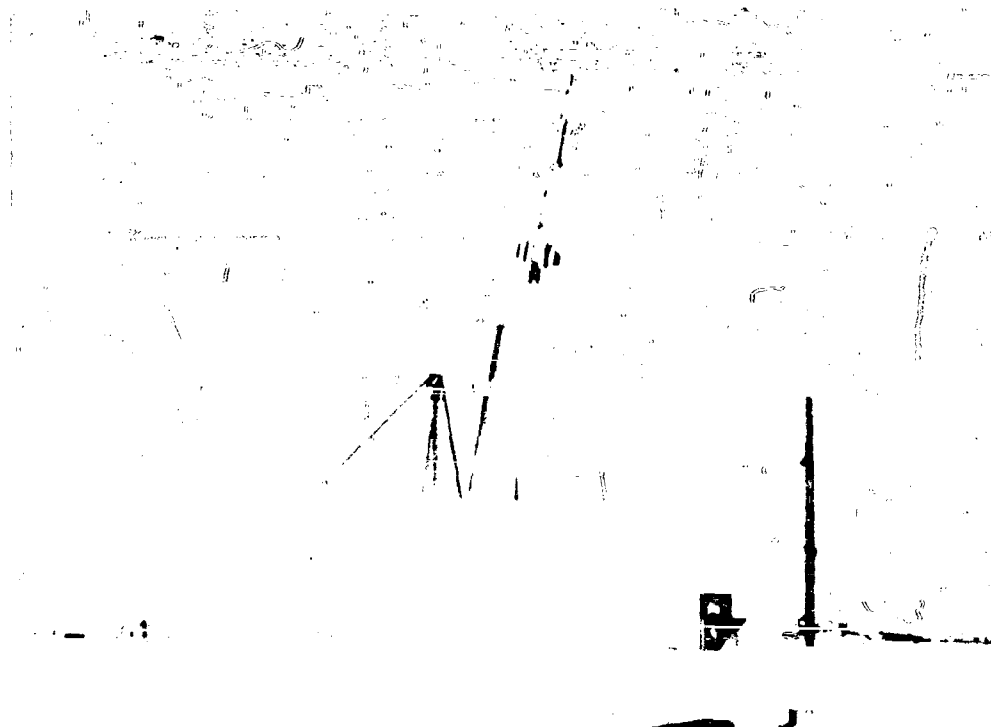


Figure 1. Single Stage Type III Cree Launch, Mission 28-1

identified as a white parachute, were seen to impact along the line of flight within the booster splash point. Search operations initiated immediately following the test mission failed to produce a parachute or any other floating object between shore and booster impact point; however, during diving operations at a later date, the Nike bottle was located and two of its three fins retrieved.

At the time the test parachute was programmed to deploy ( $t + 15.5$  seconds), the telemetry records indicate an event occurred. While the record does look somewhat like a parachute deployment, the ground camera film shows only a puff of smoke. No parachute was visible at this time.

The recovery parachute was deployed at  $t + 28.5$  seconds. Both telemetry records and ground cameras gave evidence that this event occurred on schedule. Contrave phototheodolite film shows a puff of smoke at  $t + 28.4$  seconds. At  $t + 29.5$  seconds two white objects are definitely visible. It can be assumed that one object is the missile,

the other the nose weight.

Recorded time to splash was 288 seconds (approximately eight seconds longer than predicted) at a range of 29,600 feet. Peak altitude attained during the test mission was 33,400 feet. The rate of descent was 100 feet per second at an altitude of 2500 feet. The theoretical value of rate of descent with an eight foot FIST ribbon recovery parachute is 93 feet per second. No SARAH signal was received, no dye marker was observed, and the missile was not recovered.

Telemetry reception was good during the entire flight. At  $t + 3.4$  seconds a zero shift occurred in the pressure channels and the force channels became noisy. The tensiometer channels have what appears to be good data at about  $t + 3.4$  seconds for 0.5 second after which they become noisy. At  $t + 27.4$  seconds the pressure channels recover from the zero shift which occurred at 3.4 seconds and remain at that level for the rest of the flight. At  $t + 27.4$  seconds the noise on the force channels decays to a negligible level where it remains for the rest of the test (to  $t + 288$  seconds).

None of the radar stations were able to pick up the beacon signal. Indications prior to launch were that the beacon was being interrogated and was transmitting.

Contrave phototheodolite tracking of the missile proved to be difficult and several of the cameras followed the booster. While the missile image size was small it was possible to observe smoke from powder charges and other significant events.

A missile trajectory was obtained by radar skin tracking techniques; however, the radar plot indicates an excessive amount of searching was needed.

No evidence could be found to definitely establish that the balloon had emerged from its compartment and inflated. However, the fact that no SARAH signal was received by either the search aircraft or the ships and also since no dye marker was detected, it seems logical to assume that there was no flotation.

Since the mission was initiated shortly after 2:00 P. M. the hours of daylight remaining for a search were somewhat limited. Also, no definite search procedure had been established in the event no SARAH signal was received. It was not until several days after the shot that divers actually conducted a search on the bottom at the splash point as indicated by radar. There is reason to believe that if the diving



operation had been accomplished immediately after the test, the missile would have been found. The extremely strong underwater currents which exist in the Gulf of Mexico could very possibly cause a configuration, such as the Cree missile with recovery parachute attached, to drift a considerable distance each day. Using portable sonar gear, divers searched a 1200 foot diameter circle.

## 2. Conclusions

- (a) The missile programming system functioned satisfactorily at least up to the time of balloon inflation.
- (b) The test parachute was probably deployed prematurely at the time of booster separation.
- (c) The test missile radar beacon apparently did not function.
- (d) The loss of the missile was due to a failure in the flotation system and a lack of coordination of the search activity.
- (e) The spin vanes imparted a spin rate of approximately one revolution per second to the booster-missile combination as predicted.

## B. Test Mission 29-2

Test Date - 23 April 1959

Configuration - Type III missile (800 lb) with two stages of Nike boosters

Mission No. - 29-2

Launch angle -  $79^{\circ}$

Programmed test altitude - 66,000 ft

Anticipated test velocity - Mach 1.5

Test parachute - 6 ft FIST ribbon (Project Mercury)

### 1. Test Results

First stage ignited and missile lifted off launcher. At  $t + 0.050$  second, second stage ignited. Separation of first and second stages occurred immediately. Both second stage with payload and first stage

alone proceeded on separate trajectories. Second stage booster separation from missile was not witnessed but apparently occurred normally at about  $t + 10$  seconds. Telemetry records indicate test parachute deployment occurred at  $t + 43$  seconds.

Recovery parachute operation appeared to be normal with deployment at  $t + 73$  seconds. From the available information it was not possible to determine if nose weight separation or balloon inflation had occurred. Search aircraft reported seeing the test missile on its recovery parachute with two other round objects hanging beneath. They did not witness splash but received a SARAH signal for a very brief period.

Radar tracked missile beacon for the first five seconds. Thereafter skin track was obtained intermittently to  $t + 63$  seconds. All tracking data gathered was exceedingly rough and did not reduce into a usable trajectory. Despite an intensive search the missile was not recovered. The telemetry record on this mission was one of the best obtained in the entire test program.

## 2. Conclusions

- (a) All obtainable information indicates that all missile functions occurred about on schedule. The evidence tends to indicate that the balloon had at least partially inflated.
- (b) It can be assumed with reasonable assurance that the balloon did not float except possibly for a very brief period of time.
- (c) It was not possible to determine why the second stage ignited prematurely.
- (d) Better coordination between the search activity, the radar site, and the mission control points must be attained on future test missions.

## C. Test Mission 30-3

Test Date - 3 June 1959

Configuration - Type III missile (800 lb) with two stages of Nike boosters  
(see Figure 2)

Mission No. - 30-3

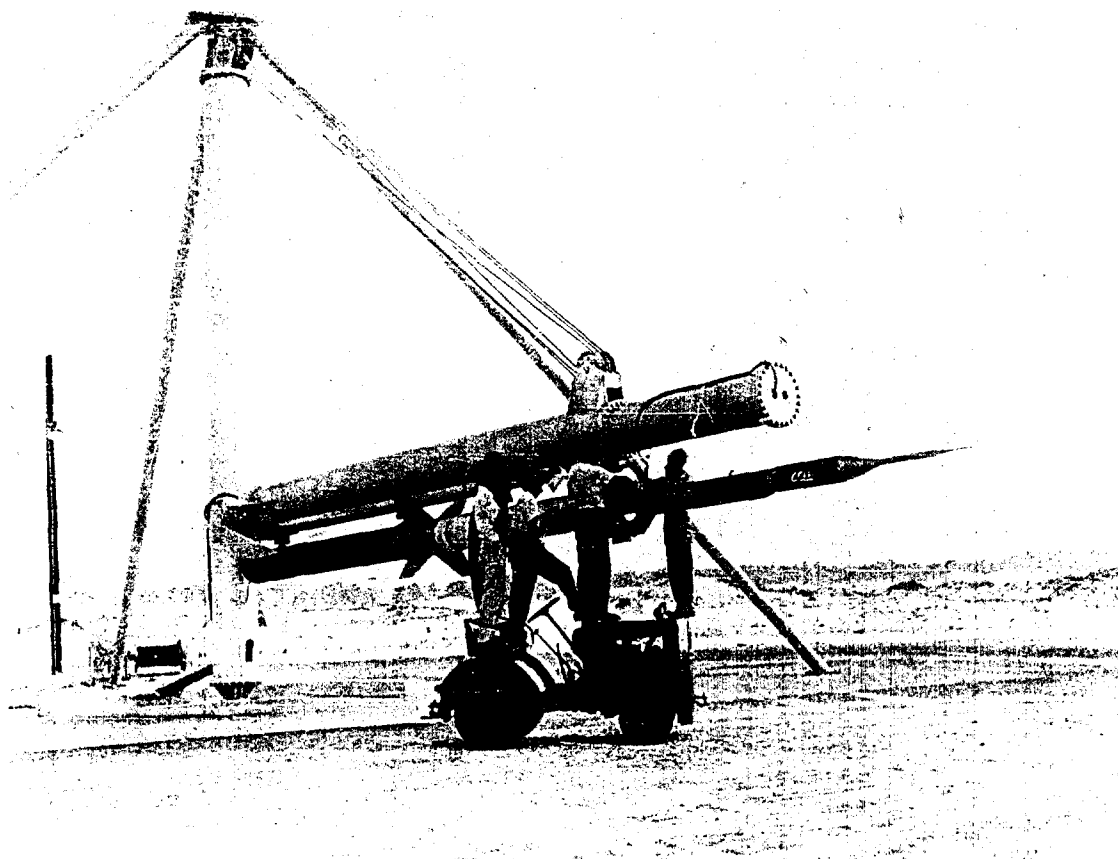


Figure 2. Two Stage Type III Cree Loading Operation, Mission 30-3

Launch angle -  $79^{\circ}$  (see Figure 3)

Programmed test altitude - 66,000 ft

Anticipated test velocity - Mach 1.5

Test parachute - Type IIIA 10% equiflo ribbon

#### 1. Test Results

Launch was smooth and normal as shown in Figure 4. First stage burned evenly and some rotation was noted. Burnout of the first stage ( $t + 3.4$  seconds) and ignition ( $t + 8.8$  seconds) and burnout ( $t + 12.2$  seconds) of the second stage progressed as expected. Missile separation and test parachute deployment occurred as programmed at  $t + 14$  seconds and  $t + 43$  seconds, respectively. Full inflation of the canopy

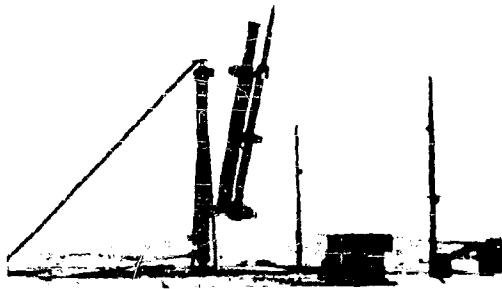


Figure 3. Two Stage Type III Cree  
Elevated to a Launch  
Angle of  $79^{\circ}$ ,  
Mission 30-3

was delayed for approximately 2.13 seconds after deployment. There appeared to be a restriction at the parachute skirt. When the canopy finally blossomed, it filled quickly and appeared to be fully inflated.

Missile camera film was obtained for approximately 18 seconds. Throughout this time, the test parachute performed satisfactorily and exhibited little evidence of breathing or flutter.

A strong telemetry signal was received and good force data recorded. Apparently both pressure channels remained in 100 percent calibrate position and pressure data were not re-

corded. The radar beacon was functioning intermittently and only limited data were obtained. However, at least one radar skin tracked the missile for a considerable portion of the mission. Usable data were also obtained by several contrave theodolite cameras.

Recovery parachute deployment, at  $t + 66.74$  seconds, and flotation balloon inflation appeared to occur properly. The missile was sighted by the recovery boat at about the time of water impact. The search aircraft did not spot the package until recovery was in progress by the boat crew. SARAH signal was received by the aircraft. Recovery of the missile from the water was accomplished within 20 minutes after impact.

Examination of the missile after recovery revealed that water leakage into some of the sealed packages had caused minor damage. However, the

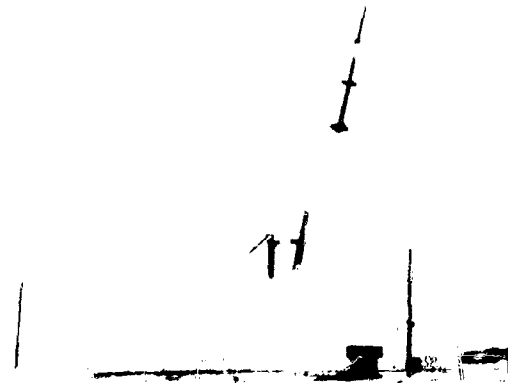


Figure 4. Two Stage Type III Cree  
Launch, Mission 30-3

missile was reusable after limited reworking. No damage was incurred by either the test or recovery parachutes.

## 2. Conclusions

- (a) The missile programming system functioned satisfactorily.
- (b) The radar beacon did not function properly.
- (c) The equiflo parachute functioned very well exhibiting a high degree of stability.
- (d) An improvement in range coordination was noted.

## D. Test Mission 31-4

Test Date - 10 July 1959

Configuration - Type III missile with two stages of Nike boosters

Mission No. - 31-4

Launch angle -  $79^{\circ}$

Programmed test altitude - 50,000 ft

Anticipated test velocity - Mach 1.87

Test parachute - Type IIIB 10% equiflo ribbon

### 1. Test Results

The launch was made at 7:45 A. M. and was apparently normal (see Figure 5). Operation up to ignition of second stage was normal. Second stage appeared to flame out less than one second after ignition. However, it delivered thrust for a full 3.4 seconds. A good telemetry signal was received for about 180 seconds. Radar beacon was not functioning at time of launch. A radar skin track was obtained for the initial 15 seconds and again from an altitude of 32,500 feet on down to splash. Phototheodolites tracked from launch to an altitude of 15,000 feet. Total flight time was 397 seconds.

Investigation of the telemetry records revealed a shift in force channels at about  $t + 4$  seconds, of about 50 percent of full scale on the 40 kilocycle channel and 20 percent of full scale on the 70 kilocycle

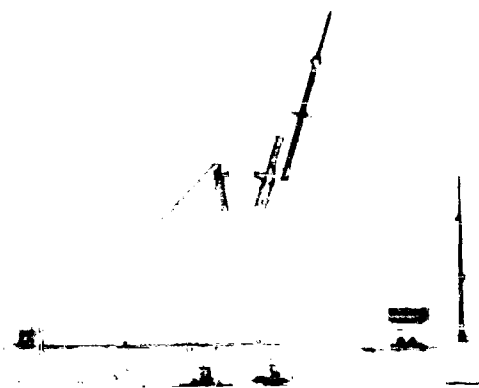


Figure 5. Two Stage Type III Cree  
Launch, Mission 31-4

channel. No data were obtained from either of the force channels. Good static pressures were recorded but no impact pressure data were obtained. Timing marks appeared on all data channels.

The test parachute container was found after the test, indicating the test parachute had deployed. Time of flight indicates recovery parachute also deployed.

A tropical storm was detected in the impact area while the mission was in progress. A water spout was served and all crash boats and arch aircraft were ordered to return to the base immediately. The search aircraft passed over the impact point within one minute of the splash time reported by radar. Marker dye was sighted but no balloon was visible. No SARAH signal was received. The missile was not recovered.

## 2. Conclusions

(a) From the available information, it appears that the mission was very nearly normal with all functions occurring on schedule.

(b) Dye marker on the water tends to indicate that the balloon had either inflated or at least was out of its compartment. The fact that the balloon was not sighted suggests that either it burst upon water impact or the nose weight had not separated.

(c) It is obvious from the results of this mission that adequate weather forecasting must be provided. It is reasonable to assume that had it not been for the sudden intrusion of a tropical storm, the missile would have been recovered. Three radars all tracked the missile to an impact point within a 100 yard circle and a search aircraft had the impact point in view. It was not possible to initiate search operations until three days after the test. The search was abandoned after one square mile around the impact point had been thoroughly combed. Both dragging and diving operations were employed. The impact point as given by radar was considered to be reliable. It must be concluded that the missile drifted after impact.

E. Test Mission 32-5

Test Date - 2 September 1959

Configuration - Type III (800 lb) with two stages of Nike boosters

Mission No. - 32-5

Launch angle - 79°

Programmed test altitude - 50,000 ft

Anticipated test velocity - Mach 1.87

Test parachute - Type IIIB 10% Hemisflo ribbon with 2D suspension lines

1. Test Results

Launch and first stage boost functioned normally. Second stage ignited late, at about  $t + 10$  seconds, and burned out at  $t + 14.5$  seconds. Burning of the second stage was observed to be rough and uneven. Telemetry and radar beacon functioned up to peak altitude of about 74,600 feet. Test parachute was deployed at a Mach number of 1.83 and an altitude of 53,800 feet. Parachute operation, as evidenced by onboard camera film, was very good. Inflation was rapid and parachute oscillation and breathing were limited. Telemetry signal strength was good through the test portion of the flight. However, data record became erratic at ignition of the second stage booster. No data could be reduced from telemetry recordings. Comparatively good radar and contrave data were obtained. After radar beacon fadeout, at  $t + 103.6$  seconds, a skin track was established (at  $t + 177.7$  seconds) and the missile followed to splash.

The test missile was spotted by search aircraft at about the time of splash. SARAH transmitter and location light were functioning properly, but the crash boat did not use the SARAH signal because of the visual sighting. The boat arrived at the impact point within 10 minutes of splash time.

Most missile compartments had some water, but damage was slight. Aft end of the missile showed some structural damage apparently caused by rough burning of the second stage, and the fact that second stage separation occurred before burnout. A considerable number of screws was sheared off at the base of the missile fins.

## 2. Conclusions

- (a) The missile programming system functioned satisfactorily.
- (b) Late ignition and rough burning of second stage did not impair the missile's over-all performance.
- (c) Radar beacon provided good tracking through the test point.
- (d) The type IIIB 10 percent extended hemispherical ribbon showed very good operation.
- (c) The anticipated test conditions had been attained.



## SECTION III

### TEST MISSILE DEVELOPMENT

#### A. Background

The model 59 test missile utilized in this phase of testing was designed and developed during Phase II of the program. As a result the test vehicle was described briefly in Part II of this report although principle attention was devoted to the differences between the new or model 59 version and the original land based type.

In order to make this part of the report complete in itself, the model 59 missile and its various subsystems will now be described in some detail.

#### B. General Description

The model 59 Cree missile is nine inches in diameter and has a total basic length of about 10 feet. The missile body is of semimonocoque construction with three external longerons 120 degrees apart running the full length of the skin panels, or 72 inches. Internal bulkheads are located at various stations in the missile. Missile weight can be increased from its basic type I weight of 230 pounds up to 800 pounds by the addition of a nose ballast section.

The missile contains a four channel telemetry and data acquisition system which gathers and transmits significant data on the performance of the test item. A dual programming system controls the various missile functions. The missile is also equipped with a recovery and flotation system and a number of location aids.

The missile can be physically divided into a number of definite compartments. These are:

- (1) Nose assembly
- (2) Main instrumentation
- (3) Flotation and recovery
- (4) Rear instrumentation
- (5) Test parachute.

The general arrangement of the various compartments and some basic dimensions are shown in Figures 6 and 7.

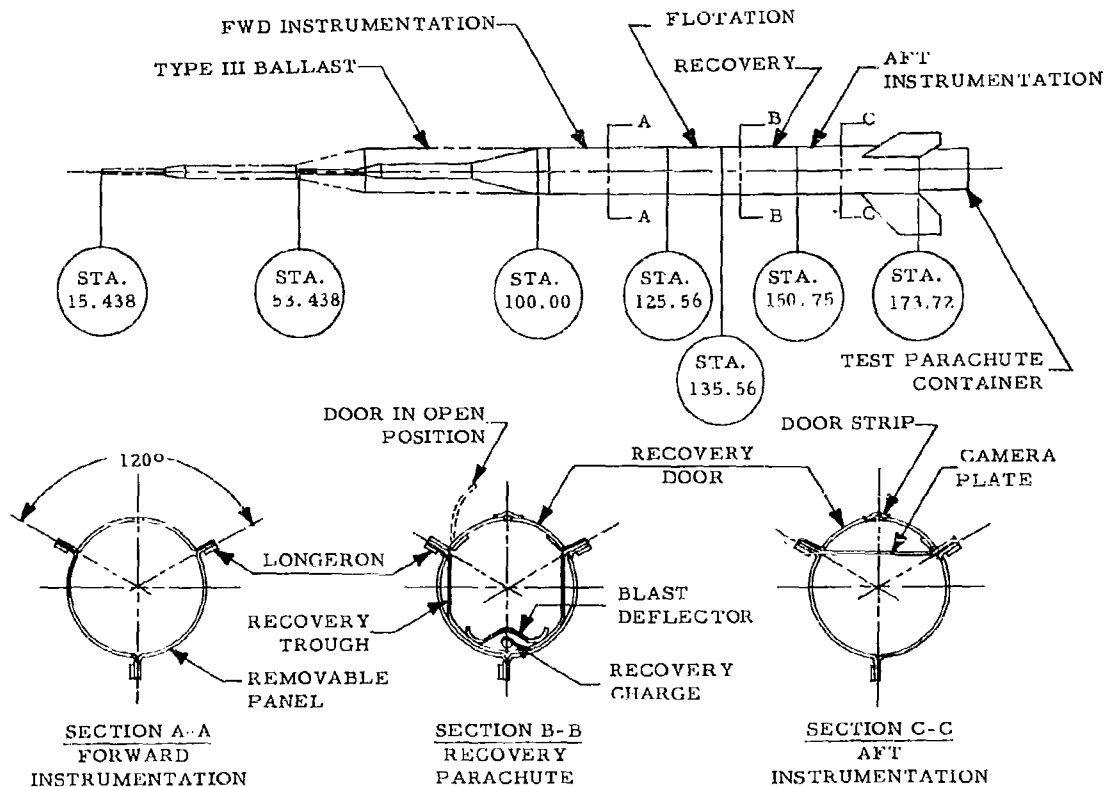


Figure 6. Model 59 Cree Missile Structure

#### 1. Missile Structure

The basic structure of the model 59 Cree missile retains many of the features of the original vehicle. The missile shell consists basically of three skin panels each 72 inches long and extending 120 degrees around the circumference. The skin panels are fabricated from 1/8 inch thick type 7075-T6 aluminum. At the longitudinal juncture of the skins, each panel is bent outward to form an external rib. To provide additional stiffness, an external longeron 1/8 inch thick and one inch wide made of heat treated 4130 steel is provided along each rib. The skins are bolted together with the longerons serving as a nut plate as shown in Figure 6.

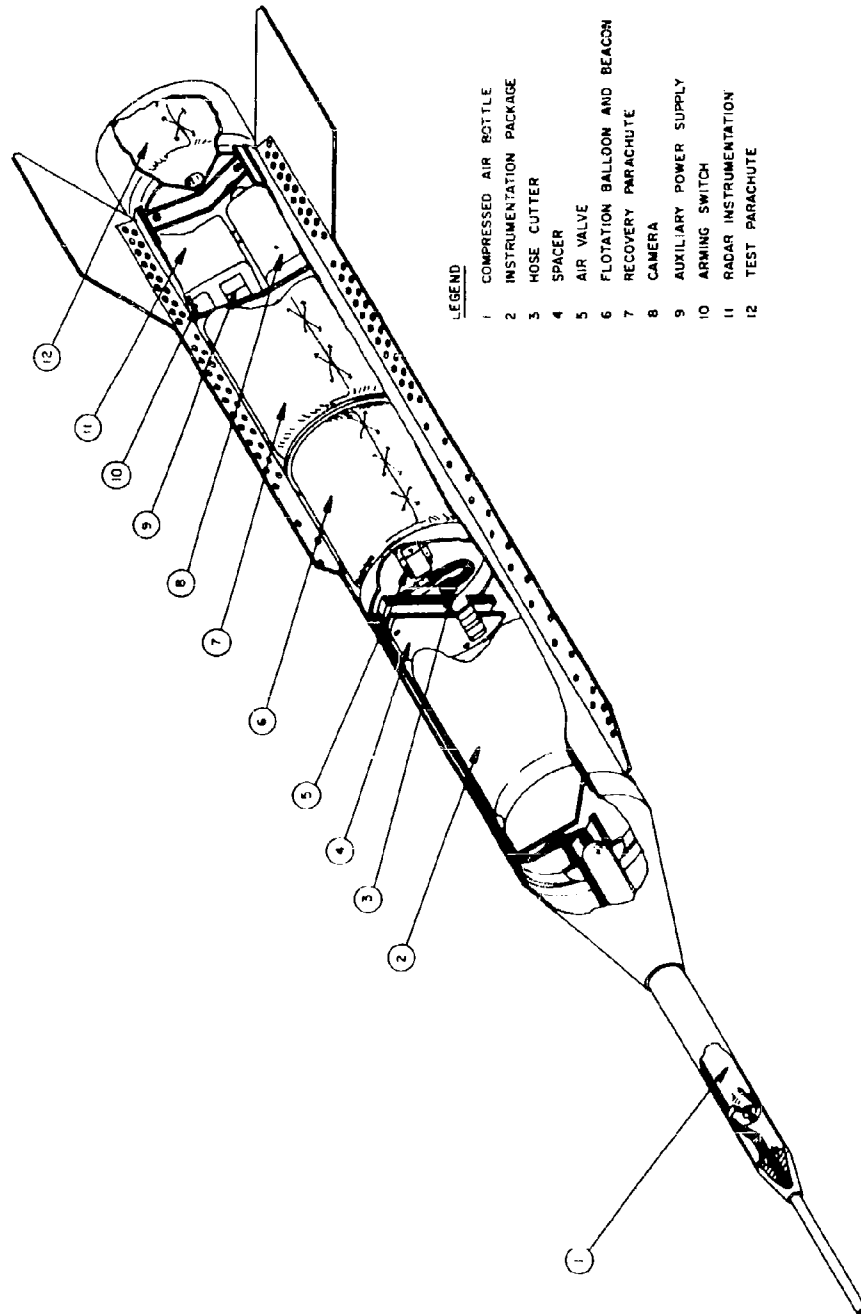


Figure 7. General Assembly of Model 59 Cree Missile

Over the flotation, recovery and rear instrumentation compartments, one of the skin panels acts as a door. The skin panel is split longitudinally along its entire length and each half fastened to one of the longerons through a hinge. Thus each half of the door panel can be opened outward as shown in Figure 6, Section B-B. The doors are kept in the closed position by means of an external strip fastened to both halves of the door. When it is desired to open the doors, the strip is broken by an explosive system.

In order to provide sufficient strength in the sections where the recovery door replaces a skin panel, additional structure was added. This extra structure also serves as the deployment housing for the recovery parachute (see Section B-B, Figure 6). In the rear compartment, additional strength is obtained by means of the camera mounting or wing plate (see Figure 6, Section C-C).

## 2. Nose Assembly

The missile nose assembly consists of a combination pitot tube and telemetry antenna, an air storage bottle, and the housings and fairing required to integrate these elements into the basic recovery package.

### a. Nose Probe

The missile nose probe serves the dual purpose of a telemetry antenna and a pitot tube. The stainless steel pitot tube picks up both total and static pressures. These pressures are ducted into flexible hoses which lead to the main instrumentation compartment where pressure transducers convert the pressure readings to equivalent electrical outputs.

The probe is insulated from the missile itself by a phenolic cone which fastens onto the nose spike. This permits use of the probe as a telemetry antenna. A coaxial cable leads to the main instrumentation compartment from the probe.

### b. Air Storage

The air supply for the flotation balloon is stored in a high pressure air reservoir constructed to ICC specifications, which is located inside of the missile nose spike. Formerly the spike was used as a ground penetration device in order to minimize impact damage. While this capability is no longer required in the water recovery type of vehicle, it is still necessary to provide

a nose spike in order to position the pitot tube a suitable distance forward of the basic vehicle.

The relaxed strength requirements for the spike permitted use of a thin wall tubing thus making available a considerable volume within the spike. A long, slender air storage bottle was selected which would easily fit within the spike and would permit storage of a sufficient quantity of air to provide proper balloon inflation. While the bottle has a proof rating of 5000 pounds per square inch it was found through testing that for the Cree flotation system, 2400 pounds per square inch was more than adequate. Generally, a balloon pressure of from one to two pounds per square inch gage at sea level is considered to be satisfactory.

The air storage bottle is oriented as shown in Figure 7 with the filling valve at the forward end. High pressure air is conducted from the aft end of the bottle through a stainless steel tube to the balloon inflation valve located on the bulkhead at station 125.

#### c. Nose Structure

The 2-1/2 inch diameter nose spike fits into a socket in the forward end of the station 100 bulkhead. The probe assembly fits directly on the front end of the basic spike on the type I or 230 pound vehicle. When a type III or 800 pound configuration is used it is necessary to add an extension to the spike in order to maintain the probe at a sufficient distance in front of the basic vehicle. From Figure 6 it can be seen that for a type III vehicle, the tip of the nose probe is at station 15.438 while for the type I it is 38 inches further aft or at station 53.438.

The ballast necessary to increase the missile weight from 230 to 800 pounds is a cylindrical body the same diameter as the basic missile and approximately three feet long. It attaches to the front bulkhead by means of a special separable ring. After completion of a test, this ring is broken by an explosive system thus releasing the ballast and permitting missile recovery.

A fairing is provided between the 2-1/2 inch spike diameter and the nine inch missile diameter. This fairing is a 15 degree half angle stainless steel cone which attaches directly to the station 100 bulkhead in the case of the type I missile and to the nose ballast section in the case of the type III missile.

### 3. Forward Instrumentation Compartment

The forward instrumentation compartment extends between the bulkheads at stations 100 and 125 as shown in Figure 6. One of the three missile skin panels is removable thus providing access to the compartment. The instrumentation is housed within a sealed container, Figure 8, which can be installed in the missile through the access panel opening. It was necessary to flatten two opposite sides of the container in order to permit installation into the missile shell.

The instrumentation container is a molded Fiberglas cylinder, open at one end. All of the system components are combined in one assembly which is inserted into the container through the open end. An O ring seal and a special clamp ring are incorporated into the endplate thus providing a water tight container. All electrical leads are brought out through a single 81 pin sealed connector located in the end plate. The two pressure taps for the pitot system and a coaxial connector are also located in the end plate. Significant details of the instrumentation compartment are shown in Figure 8.

Once the instrumentation package has been installed in the missile and all connections made, a spacer assembly is inserted between the aft end of the instrumentation package and the forward edge of the station 125 bulkhead. The spacer can be expanded to completely fill the space and hold the package tightly in place.

### 4. Recovery Compartment

The recovery compartment occupies the space between the forward and aft instrumentation sections. The forward portion of the recovery compartment houses the flotation balloon and the SARAH location beacon. The recovery parachute is located in the aft portion.

A trough-like inner section runs the full length of the recovery compartment. The straight sides of this insert permit easy ejection of the flotation balloon and the recovery parachute. Also the spaces between the trough walls and the missile skin serve as wiring tunnels between the forward and aft instrumentation compartments. A thin simple bulkhead separates the recovery and flotation sections.

At the bottom of the recovery section is a blast deflector panel which serves to distribute the pressure developed by the explosive parachute ejection charge. A so-called "blast bag" protects the recovery parachute from the hot gases generated by the explosive charge.

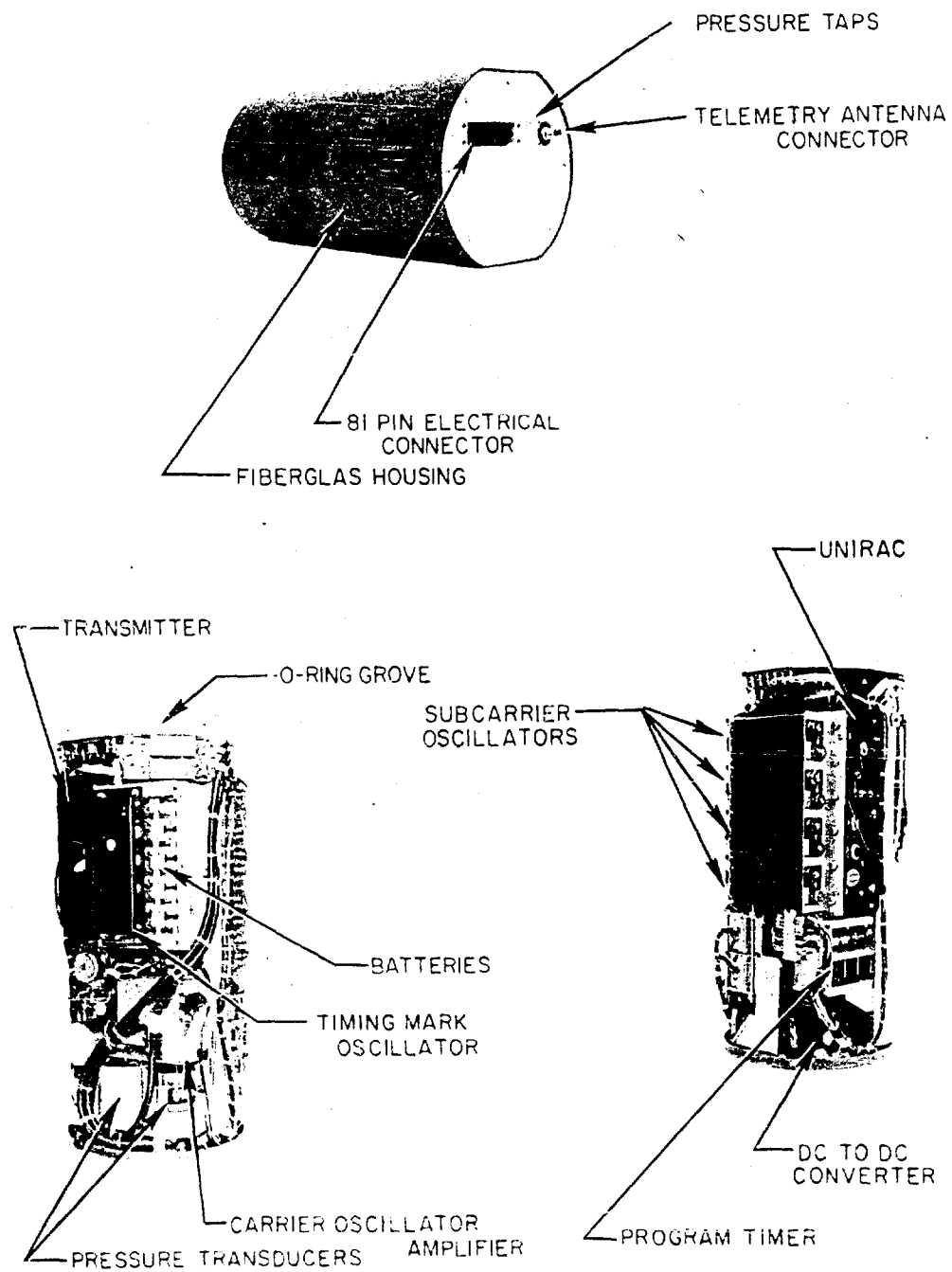


Figure 8. Main Instrumentation System Details

The blast bag is secured in the compartment at its upper end around its entire periphery. The blast bag is inverted by the deployment charge and remains with the vehicle after the deployment of the recovery parachute.

The hinged recovery door extends over the entire recovery compartment as well as the rear instrumentation compartment. This is necessary so that the recovery parachute riser can be brought back to the missile rear bulkhead where attachment is made. This riser passes through the space inside the recovery door and above the camera plate shown in Section C-C of Figure 6.

#### 5. Aft Instrumentation Compartment

Since it was desired that the item undergoing testing should be observed it was necessary to provide space for a high speed motion picture camera. The camera selected was a Fairchild model HS100. This camera had to be located as close to the aft end of the missile as possible. Hence the aft instrumentation or camera compartment occupies the last section of the missile. The camera views the test item through an opening in the rear or station 172 bulkhead.

There were also several other instrumentation system components which could logically be located in the camera compartment. These included such items as arming switches, the auxiliary programming system, an external control connector, arming and shorting plugs and for the model 59 missile a radar tracking beacon and destruct system.

The wing plate (see Figure 6), besides being a structural member, serves as a mounting plate for the camera and several other components. All of the components were housed in sealed containers. The camera was enclosed in a specially fabricated boot. A clear filter backed by an O ring seal was used over the camera lens.

Access doors were provided in the aft instrumentation section so that certain last minute functions could be accomplished easily and safely. Some of these functions are; the insertion and connection of the recovery parachute ejection charge, the insertion of the missile arming plug, and the removal of the explosive system's shorting plug.

#### 6. Test Parachute Assembly

The station 172 bulkhead is actually the aft end of the missile structure. It is a rigid weldment made of 4130 heat treated steel. Attachment points for both the test and the recovery parachutes were built into this bulkhead.



The test parachute container mounts to the rear bulkhead fitting snugly within the bulkhead outer flange. Shear screws through the missile skin, the bulkhead flange and into the test parachute container keep the assembly intact until at the desired time the test parachute deployment squibs are fired. The ejection mortars develop sufficient force to shear the retaining screws thus initiating the deployment of the test item.

The test parachute container is cylindrical in shape and is open at one end. On a segment across the open end two small pistons are attached. These pistons fit into mortar housings which are mounted on the station 172 bulkhead (see Figure 9).

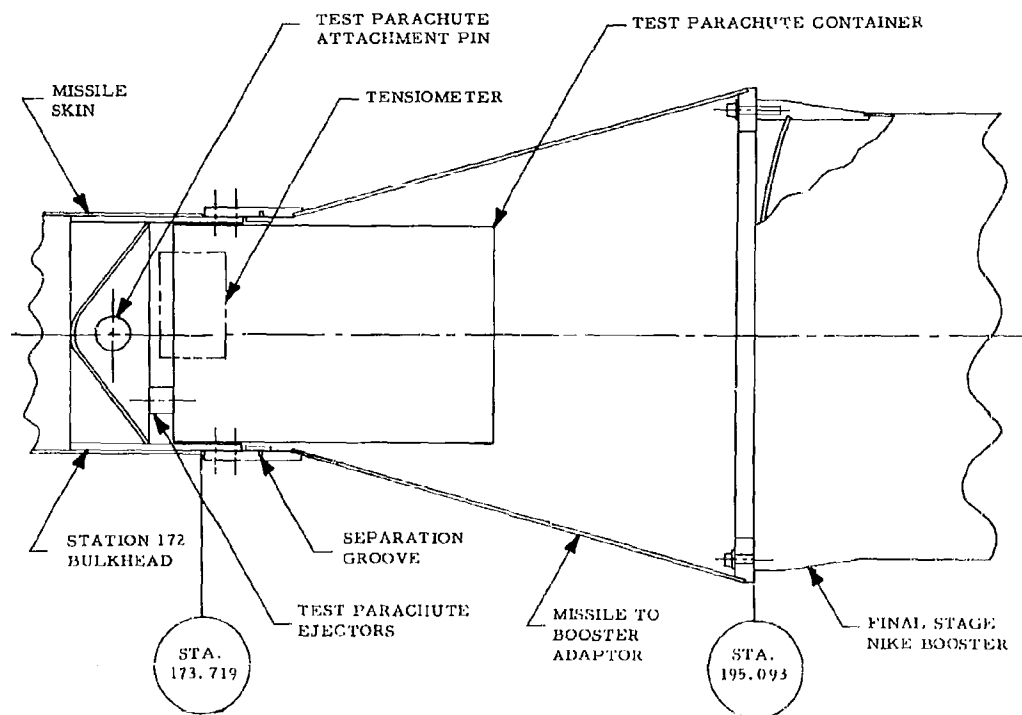


Figure 9. Details of Cree Missile Aft End and Fairing Last Stage Adaptor

The test parachute is packed in a deployment bag which is secured to the inside top of the container. The parachute riser attaches to a load measuring device, or tensiometer, which in turn is attached through a short, flexible link to the center of the station 172 bulkhead.

### C. Missile Systems

The Cree missile contains a number of subsystems each of which contributes to the over-all capability of the test vehicle. These subsystems are described briefly in the following sections.

#### 1. Instrumentation

The instrumentation system can be divided into the three basic categories of

- (a) Programming
- (b) Data acquisition
- (c) Tracking aids.

Most of the system components such as the telemetry, timers and power supply are located in the forward or main instrumentation compartment. The aft compartment houses such components as the high speed camera, radar beacon, arming switches, etc.

##### a. Programming

The Cree missile programming system is composed of a primary and a secondary system as shown in Figure 10. Each of the two systems is completely separated from the other in order to provide the highest possible reliability. Thus, each system has its own power supply and arming switch. Each of the many missile functions is provided with two initiators so that full advantage of the dual programming system can be realized.

Each of the two lanyard operated arming switches are actuated as the missile leaves the launcher. In the primary system the functioning of the lanyard switch starts the motor driven programming timer and also removes electrical shorts from all of the explosive circuits. The timer has 10 cams, each of which controls one missile function. The functions are:

- (1) Timing monitor
- (2) Calibrate sequence
- (3) Booster separate

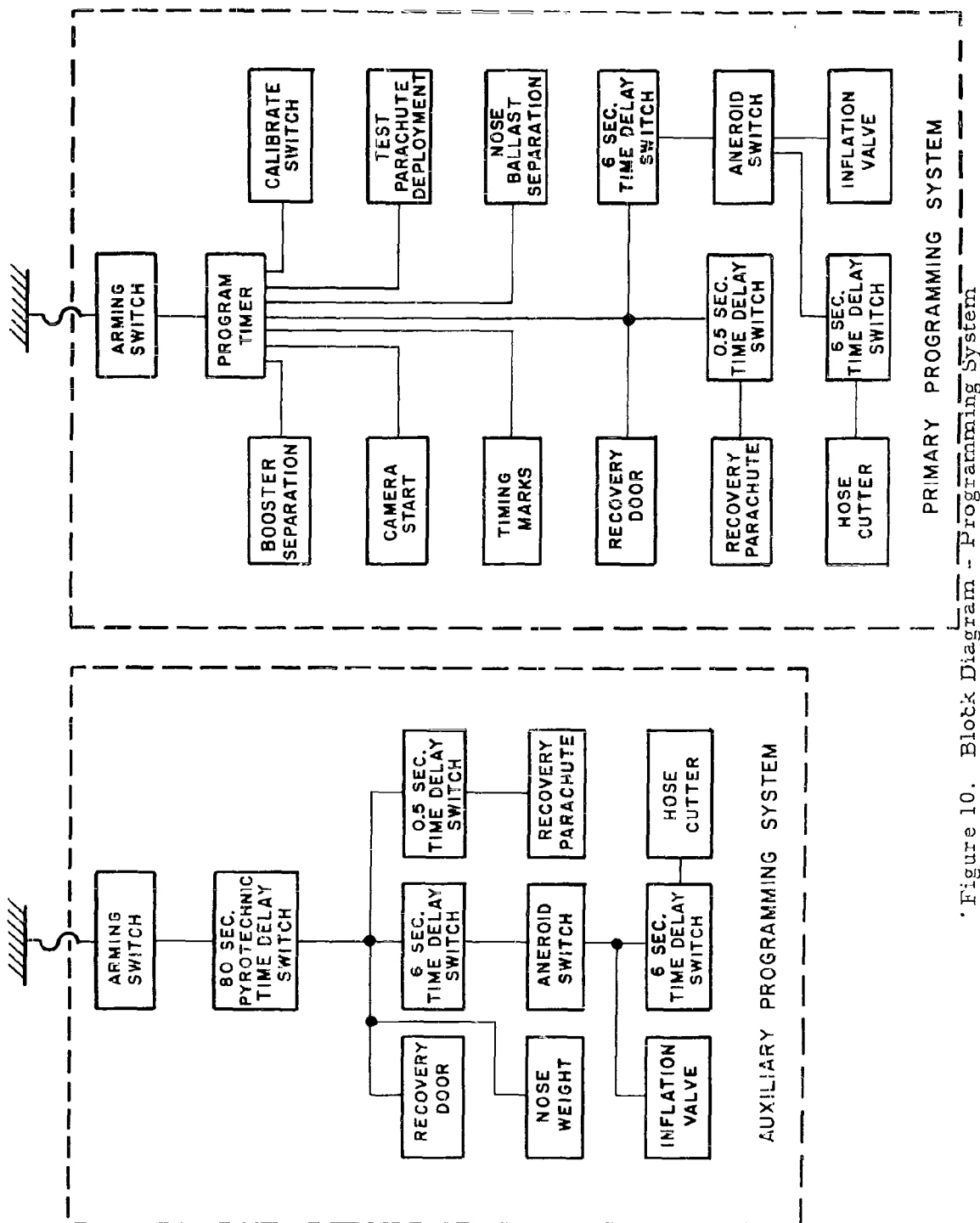


Figure 10. Block Diagram - Programming System

- (4) Camera start
- (5) Test parachute deployment
- (6) Timing mark start
- (7) Nose weight separate
- (8) Recovery system
- (9) Power off
- (10) Timer reset.

The single recovery system input actually controls several functions in this system. The recovery door opens immediately with the closing of the recovery system switch. Two pyrotechnic time delay elements are ignited at the same time. One of these time delay elements (0.5 second) controls the recovery parachute deployment, while the other (6.0 seconds) controls the flotation system inflation valve through an aneroid control. The inflation system completes its operation with no other external control being required.

The auxiliary programming system controls only those functions essential to the successful recovery of the test missile. The arming switch ignites a pyrotechnic time delay switch of such a duration that the recovery sequence will be initiated at the desired time. The longest time delay employed during Phase IV was 80 seconds. The initiation of the recovery phase amounts to opening the recovery door and jettisoning the nose ballast. Additional time delay elements are also set in motion which controls the recovery parachute deployment and the various inflation system functions.

#### b. Data Acquisition

The data gathering system used on the model 59 Cree missile was essentially the same as that used on the previous model. A number of modifications were made to the system in an attempt to improve both the quality and the reliability of the acquired data. Also, the instrumentation components were regrouped and repackaged in water tight compartments. A block diagram of the data acquisition system is shown in Figure 11.

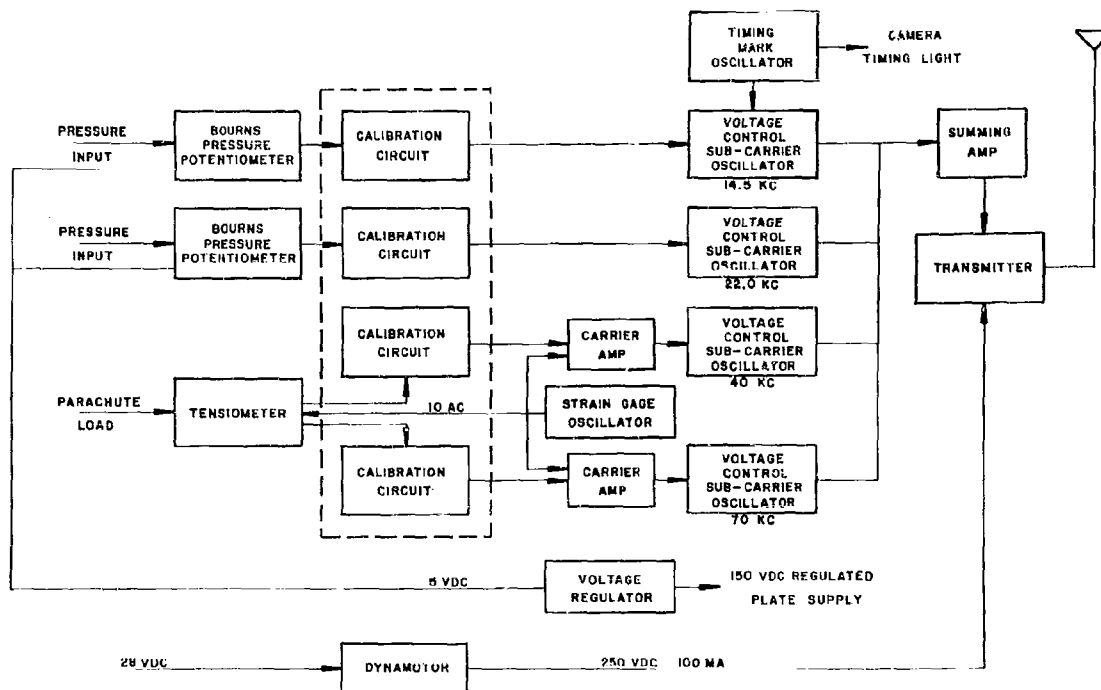


Figure 11. Block Diagram - Data Acquisition System

#### (1) Telemetry

The four channel telemetry system consists basically of a Raymond Rosen Model 1001A, phase modulated, crystal controlled transmitter; four Raymond Rosen Model 957 voltage controlled subcarrier oscillators; and the amplifiers and calibration circuitry necessary to complete the system. The calibration circuitry was provided by a Raymond Rosen Model 1401A Unirac assembly. As previously described, the telemetry antenna is a part of the missile nose probe assembly.

The transmitter has a power output of 3.6 watts in a 215 to 235 megacycle range. The four subcarrier center band frequencies are 14.5 kilocycles, 22.0 kilocycles, 40 kilocycles, and 70 kilocycles. The respective data functions are static pressure, differential pressure, drag force and shock force. The outputs of the four subcarrier oscillators are combined by a summing amplifier and the resultant signal is then transmitted.

## (2) Sensors

The two pressure channels are fed by a potentiometer type of pressure transducer. One such transducer monitors the static or ambient pressure while the other measured the difference between static and total or ram pressure. From these two pressure measurements it is possible to determine both the altitude and the velocity of the missile during a test mission. The output of the potentiometer type pressure transducer is fed directly to the voltage controlled sub-carrier oscillators.

The force measuring device, or tensiometer, is a ring type tension link containing two strain gage bridges each of four active arms. The sensitivity of the drag bridge is twice that of the shock bridge. Thus, on a 3000 pound range tensiometer one strain bridge, the drag channel, reads 100 percent at a load level of 1500 pounds while the second or shock bridge reads 100 percent at a 3000 pound load.

The use of dual bridges provides the desirable capability of being able to measure large parachute opening forces while retaining the capacity to measure steady state drag forces with a reasonable degree of accuracy.

### c. Tracking Aids

The nature of the Phase IV test program was such that missile trajectory determination by ordinary radar skin tracking techniques would be unsatisfactory. An object the size of the Cree missile is difficult to skin track especially when other larger objects such as boosters are in such close proximity as can be expected on most test missions. Therefore, it was decided to improve the tracking capability by incorporating a radar beacon in the missile.

The selected beacon operates on "S" band frequencies (2700 to 2900 megacycles) and is compatible with the MSQ-1A shore based radar. When the beacon is interrogated by a pulse from the radar station, it retransmits a pulse. Either single or double pulse interrogation can be used. A pulse repetition frequency of 410 cycles per second was employed.

It was also intended to provide a destruct capability in conjunction with the radar beacon operation. A destruct receiver was designed to function either by the loss of the beacon signal or by a planned change in the pulse repetition frequency. The requirement for a missile destruct capability was relaxed and the system was never employed.

## 2. Recovery

To accomplish missile recovery it is necessary to (1) open the recovery doors, (2) separate the nose ballast, and (3) deploy the recovery parachute. These functions are controlled by the main programming timer or the auxiliary pyrotechnic system. To initiate recovery, the recovery door is opened. A thermal time delay deploys the recovery parachute 0.1 second later. The separation of the nose ballast is controlled by a separate timer cam.

Opening of the recovery door is accomplished by breaking the door retaining strip by means of a strand of 10 grain per foot primacord. Each end of the primacord is assembled with a blasting cap each of which is initiated by one of the programming systems. Once the primacord has broken the door strip, the force of the explosion causes the doors to open in which position they are held by special spring clips.

The nose ballast is separated by the breaking of the mating ring which attaches the weight to the missile front bulkhead. The ring is grooved to receive a strand of 30 grain per foot primacord. As in the case of the recovery door each of the two ends of the primacord is mated to a blasting cap each of which is activated by one of the programming systems. The nose ballast slides off the nose spike after separation has been accomplished.

The recovery parachute compartment is formed by a trough-like section which provides straight parallel sides so the parachute can be easily ejected and also leaves a cavity under the bottom of the parachute pack. Into this cavity are blasted the expanding gases formed by the ignition of the recovery parachute ejection charge. The charge is a sealed cartridge containing approximately four grams of powder and two electric squibs.

## 3. Flotation

The model 59 Cree missile was provided with an entirely self-contained flotation system. This system consisted of:

- (a) An air storage reservoir
- (b) An explosively actuated air valve
- (c) An explosively operated hose cutter
- (d) An inflatable balloon.

The air storage bottle occupies the empty space inside of the nose spike. A stainless steel tube conducts the high pressure air through the instrumentation compartment to the air valve on the forward side of the bulkhead at station 125. The valve is opened when its plunger is depressed as the cam surface on the actuating rod moves through its travel. Movement of the valve actuator is accomplished by an explosively driven piston. This piston can be actuated by either one of two electric squibs located in the cylinder head.

When the inflation valve opens the high pressure air passes through a short rubber hose to the balloon itself. As the balloon fills, it breaks the tie cords which hold it in place in its compartment. The balloon inflates to full size while held snugly to the side of the missile by six tethering lines.

The tethering lines and the filling hose all pass through a hose cutting device. At a preset time after the initiation of inflation, usually six seconds, the two electric squibs in the hose cutter are ignited and the piston type knife is driven through the hose and the tethering lines. The balloon is thus released from the side of the missile but remains attached by means of a 25 foot riser. A fabric skirt at the equator of the balloon adds to the balloon drag so that it will always remain above the parachute and will thus enter the water last (see Figure 12).

#### D. Systems Testing

##### 1. Recovery

A series of system and component tests were conducted on the missile recovery systems. After ascertaining the proper functioning of each of the individual components, the flotation system consisting of the air storage bottle, the explosive valve, the hose cutter, and the balloon itself were assembled in the missile.

After a series of successful static system tests, a complete missile was mounted on a suitable vehicle and a series of inflation tests



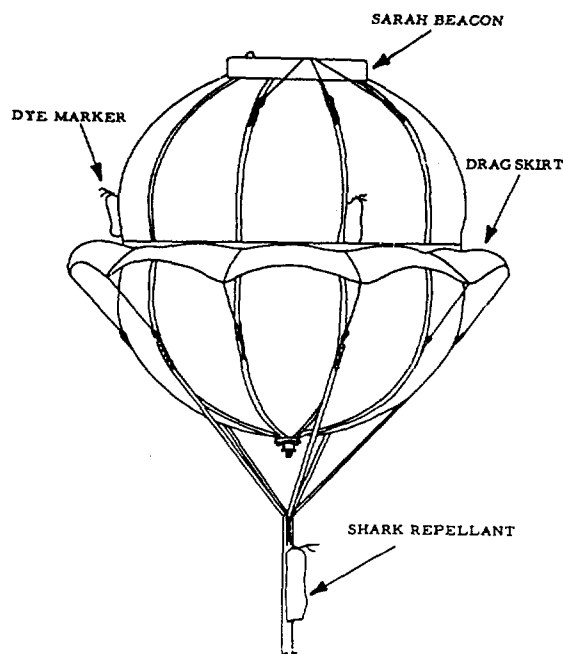


Figure 12. Cree Flotation Balloon

performed at velocities of 80 and 100 feet per second. On all tests, inflation was observed to be very satisfactory. The inflated balloon exhibited little tendency to oscillate and remained quite stable while tethered to the missile. On one test, the hose cutter was actuated and the balloon separated from the missile. The balloon extended to the full length of its riser. The test was completely satisfactory.

A series of three recovery and flotation system tests were conducted at the field test site at Eglin Air Force Base, Florida. For these tests, the recovery and flotation components were assembled in a standard Cree missile shell that had been ballasted to weigh 200 pounds. An Air Force helicopter was used as a launching platform as shown in Figure 13.

These tests will now be described in detail.

The first flotation system test was accomplished on 13 May 1959. The test conditions and results were as follows:

(a) Test Configuration - Standard missile shell without recovery doors and with special programming system and no test parachute.

(b) Test Method - Missile suspended nose down, beneath a helicopter. Recovery parachute was deployed by static line immediately after release. Balloon inflation and cut-off were controlled by the programming system.

(c) Release Altitude - 2500 feet.



Figure 13. Flotation System Test Method

(d) Test Results - Recovery parachute deployed normally. Balloon inflation was uneventful although four second time period allowed for inflation was apparently too short to permit full inflation. The balloon was slightly softer than normal.

During descent the balloon on more than one occasion dropped to the level of the parachute canopy, but each time it returned to a position behind the parachute. However, the balloon riser never became really taut. Missile velocity at the time of balloon inflation was 94.15 feet per second.

At water entry the balloon did not completely submerge. However, rough seas soon wet the entire balloon (see Figure 14). The velocity at the time of water entry was 91.38 feet per second. The impact point was about 1/2 mile off shore directly south of site A-11. The water depth was 50 feet. The marker dye gave excellent results and the impact point was visible for a considerable distance. Recovery was uneventful and was accomplished within 20 minutes after completion of the test.



Figure 14. Crash Boat Approaching Floating Balloon

(e) Conclusions - The test was very successful. The test equipment was undamaged except for corrosion in the programming system and some slight chaffing marks on the balloon riser. The flotation system functioned satisfactorily. The hose cutter operation was successful even though only one squib was employed. However, in future tests, for increased reliability, two squibs will be used.

The excellent visibility of both the floating balloon and the marker dye seem to indicate that on any test where the balloon floats, it would be extremely unlikely that the unit would not be found.

The second flotation test was accomplished on 15 May 1959. The test conditions and results were as follows:

(a) Test Configuration - A standard missile shell with flotation gear and recovery parachute was suspended beneath a helicopter. Recovery doors were installed and the recovery parachute was to be deployed by a powder charge in the normal manner.

(b) Test Results - No events were observed to have occurred. The missile impacted in the water apparently with no recovery parachute or flotation balloon having been deployed. The remains of the missile were recovered by divers. From an examination of the recovered pieces and an analysis of the film coverage of the test, the following conclusions were reached:

(1) The arming lanyard had pulled and all pyrotechnic time delays had ignited, burned through, and all circuits were completed.

(2) The door opening primacord had fired and the door appeared to have opened before water impact.

(3) The recovery parachute charge had fired but the parachute did not emerge from its compartment. The cap end of the recovery charge had broken away from the main body.

(4) The balloon inflation squibs had fired and the valve had opened. In the film, the balloon was visible just before water impact and it is estimated that it was from 1/3 to 1/2 fully inflated. The recovered balloon was split in several places.

(5) The hose cutter squibs did not fire. The missile appeared to enter the water before the time this event was scheduled to occur.

(c) Conclusions - The loss of the missile was due to the failure of the recovery parachute to deploy. This was apparently caused by the head or squib end of the recovery charge blowing off and allowing pressure to escape. The missile impacted with the water before the balloon was fully inflated and before the hose cutter squibs had fired.

On 21 May 1959, two static ground tests of recovery door opening were performed. A single strand of 10 grain per foot LEDC was used in each test. In one test a single E-80 blasting cap was used and in the other, a single X257 igniter was used. In each case the door strip broke down the middle. The two halves of the door strip also pulled loose from the mounting screws and broke up into small pieces three to five inches long. There were no sharp or uneven edges left on the door and the test was considered very successful. Some slight blast damage was noted on the recovery parachute bag and the parachute riser. The damage was not considered serious but on future tests, protective material will be introduced to eliminate the possibility of any damage.

A number of tests were conducted on the flotation system hose cutter. It was found that a single one grain squib was not sufficient to cut the hose while one two grain squib was adequate. When two one grain squibs were used and only one ignited, the second failed to fire. When the same test was performed using two grain squibs, they both fired.

On 22 May 1959, a static ground test of a complete missile was conducted. The missile was suspended, nose down, from the boom of the launcher. The missile had a complete flotation system, recovery system and a type III nose weight. The arming lanyard was pulled and the following results were observed:

- (a) Recovery door opened
- (b) Nose weight separated
- (c) Recovery parachute deployed.

After deployment of recovery parachute, no succeeding events occurred. Examination of the missile revealed that the head end of the recovery charge had blown off and had severed wires which

controlled the balloon inflation and cutoff conditions. The damaged wires were repaired and the test continued. The test was completed uneventfully.

The nose weight separated normally without causing any difficulties with the air supply in the nose spike. No leaks developed. The movement of the missile was very slight after deployment of the recovery parachute.

On 25 May 1959, a second static ground test was performed. Again the missile was suspended, nose down, from the boom of the launcher. No nose weight was used. In both the hose cutter and the air valve, a pair of two grain squibs were used. Only one squib of each pair was wired into the programming system.

The test was very successful. All squibs were ignited. The hose cutter mounting screws were sheared through. The air valve mounting screws were damaged. All functions occurred normally, however.

On 26 May 1959, the third flotation test was accomplished. The test conditions and results were as follows:

(a) Test Configuration - A standard missile shell with a dual programming system. Recovery and flotation systems were complete. No nose weight was used.

(b) Test Results - All functions appeared normal. Recovery doors opened and recovery parachute deployed. Balloon inflation and separation appeared normal. The balloon behaved similar to the first test of this series. At times it was even with the skirt of the parachute, and at other times it was above the parachute. The balloon riser was never under any real tension.

Upon water entry, the balloon did not submerge. The water line was approximately at the balloon equator.

Examination of the missile after the test revealed that again the cap of the recovery charge had blown off. Fortunately, no damage to the instrumentation resulted. For all future tests, a backing block will be used in conjunction with the recovery parachute charge.

## 2. Instrumentation

a. Main Instrumentation Package

A number of pressure tests were conducted wherein the main instrumentation package was sealed in the normal manner and then completely immersed in water. The internal pressure was maintained at 20 pounds per square inch. No leaks were detected.

Next, the completely assembled package was subjected to a vibration test. The unit was mounted in a special fixture on a standard shake table. The setup was such that the output of any one of the four telemetry channels could be monitored. The output was viewed on an oscilloscope and shifts in voltage noted.

For all tests, the force level was set at plus or minus five g's. The frequency of vibrations were increased slowly up to a level of 500 cycles per second. This test was performed on each of the four channels in all three axes for a total of 12 tests. In addition, on one test, the frequency was increased to 2000 cycles per second.

In general the results were satisfactory. Some difficulty was experienced with the pressure transducers but the basic telemetry and programming systems functioned very satisfactorily. The maximum voltage shifts varied between two to four percent.

b. Radar Beacon

Shock and vibration tests of the radar beacon were conducted. No difficulties were encountered when the beacon was held at a steady state of 50 g's on the spin table. The beacon was also subjected to vibrations of plus or minus five g's through a frequency range of 0 to 1500 cycles per second. The only difficulties encountered were at about 800 and again at 1300 cycles per second. At these frequencies, the beacon operated intermittently. It was possible to resolve the difficulty by lowering the g level somewhat, while maintaining the same frequency.

The above situation is not considered too critical since it is expected that any vibrations at the five g level existing in the missile would be at frequencies well under 500 cycles per second.

3. Camera

The camera was encased in its rubber boot and placed in an altitude

chamber. Various tests were conducted; some to altitudes of 80,000 feet. First the boot was allowed to expand freely but this occupied too much space. Then a check valve was used to allow air over a certain pressure to escape. However, after return to atmospheric pressure, air would gradually leak back into the boot. Finally, a method was tried wherein the check valve was eliminated and a nylon case laced around the boot. This system performed the best of all, the rubber boot maintaining a seal and the nylon case retaining the shape.

## E. Aerodynamic Considerations

### 1. Stability Characteristics

#### a. Types I and III Cree Missiles

The large difference in center of gravity position for the types I and III missiles dictate fin size requirements. Appropriate fins for each missile configuration are employed consistent with the test condition. For example, with 12 by 10 inch fins on the type I missile, neutral stability is attained at a Mach number of 5. By the employment of 12 by 12 inch fins, the stability is increased to three percent of the length at this Mach number. For all tests at Mach 4 for this missile, the larger fins will provide a margin of six percent of the length. The type III Cree missile is adequately stabilized up to Mach 6 with 12 by 9 inch fins. Stability characteristics of these two missiles are shown in Figure 15 where  $(D/L)$  is the ratio of the distance to the center of pressure or center of gravity, measured from the base of the missile, to the length of the missile.

Corresponding drag curves for the two missiles are shown in Figure 16.

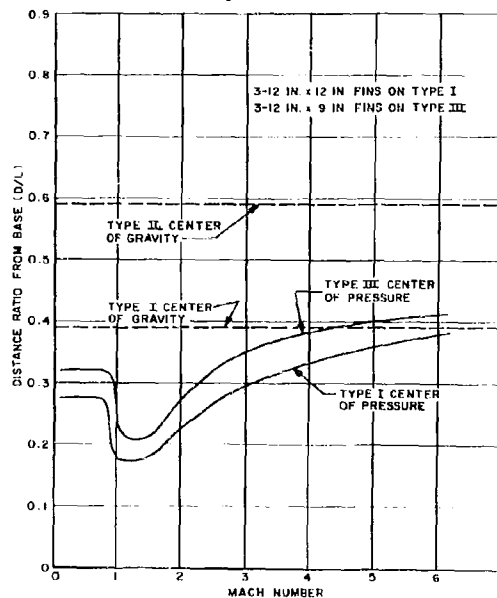


Figure 15. Type I and II Cree Missiles Center of Pressure and Center of Gravity vs Mach Number

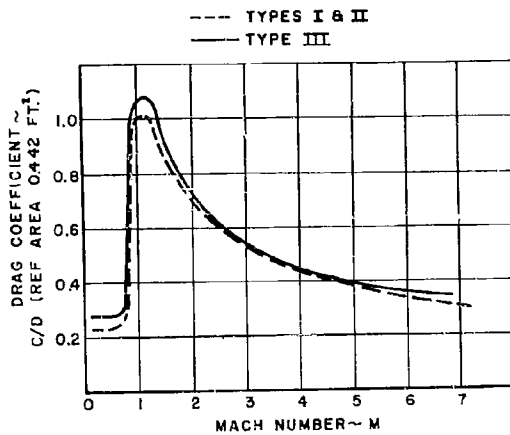


Figure 16. Drag Coefficient vs Mach Number, Cree Types I, II, and III

#### b. Single Stage Type III Configuration

Stability characteristics of this configuration are shown in Figure 17. These calculations are based upon the employment of the unfaired missile connector which was originally designed for the aircraft type of launch. The single Cree Type III missile boosted by a single stage is adequately stable with four 2.0 square foot fins on the booster. Due to the economy of the larger standard military fins, however, these are used on all first stage boosters. The drag curve for this configuration is shown in Figure 18.

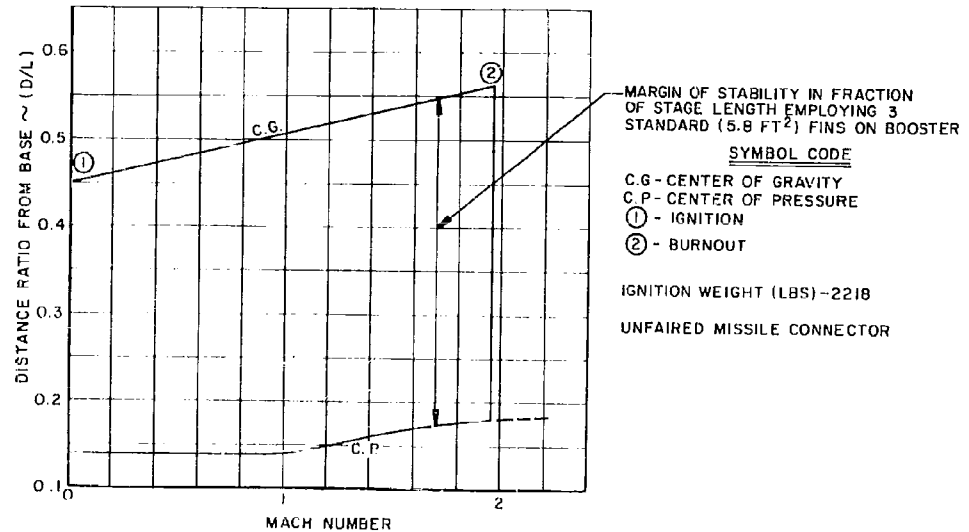


Figure 17. Single Stage Type III Cree Center of Gravity and Center of Pressure vs Mach Number

#### c. Two Stage Type III Configuration

The stability characteristics of this configuration are shown in Figure 19. As in the case of the single stage, discussed previously, 2.0 square foot fins are adequate on both stages. The



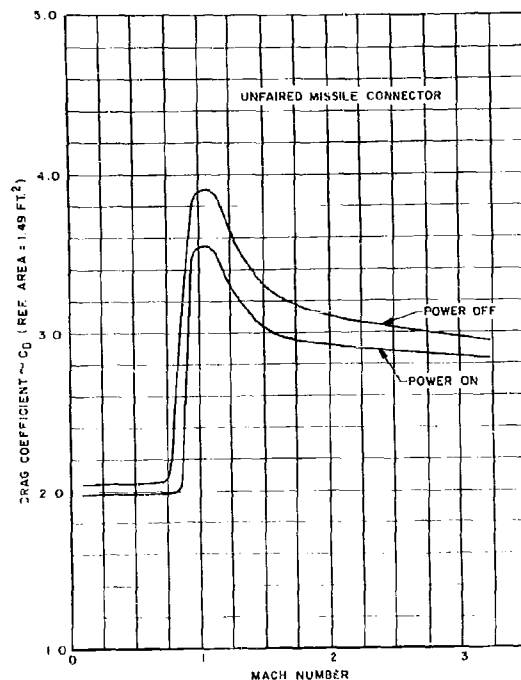


Figure 18. Drag Coefficient vs Mach Number - Single Stage Type III Cree

characteristics shown in Figure 19 are based upon the use of standard military fins on the first stage booster, and four 2.5 square foot fins on the second stage. This also is based upon the use of the unfaired missile connector. The drag curve for this configuration is shown in Figure 20.

#### d. Two Stage Type I Configuration

Stability calculations to determine the fin sizes required on the first and second stage boosters revealed that three standard Nike fins (5.8 square feet each) on the first stage booster, and four 2.5 square foot fins on the second stage would provide adequate stability throughout the Mach number range encountered in these trajectories.

The variations in location of the center of gravity and center of pressure of the first and second stage configurations are shown in Figure 21.

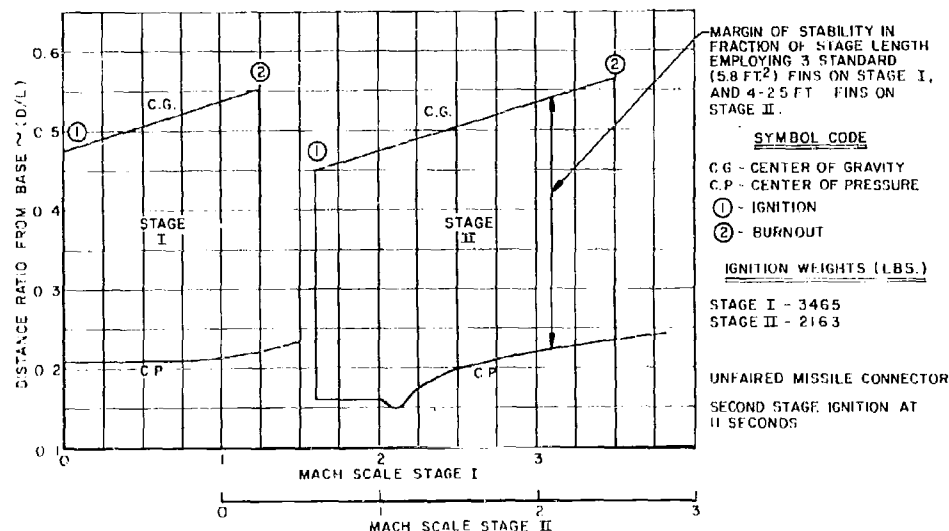


Figure 19. Two Stage Type III Cree Center of Gravity and Center of Pressure vs Mach Number

e. Three Stage Type III Configuration

The three stage type III configuration stability variation in a typical launch trajectory is shown in Figure 22. This configuration also employs standard military fins on the first stage and 2.5 square foot fins on the upper stages. Four 2.0 square foot fins are adequate for this configuration on all stages; however for purposes of standardization, the military fins and 2.5 square foot fins are used. Drag curves for the three stages of this configuration are shown in Figures 23, 24, and 25.

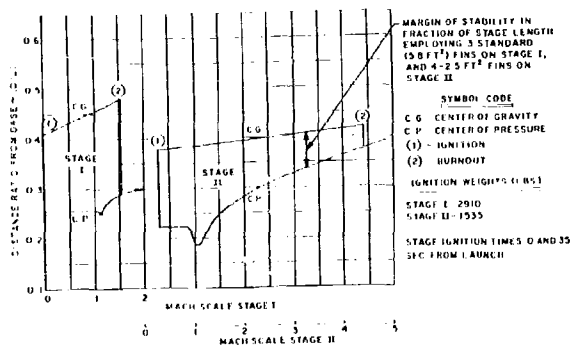


Figure 21. Two Stage Type I Cree Center of Gravity and Center of Pressure vs Mach Number

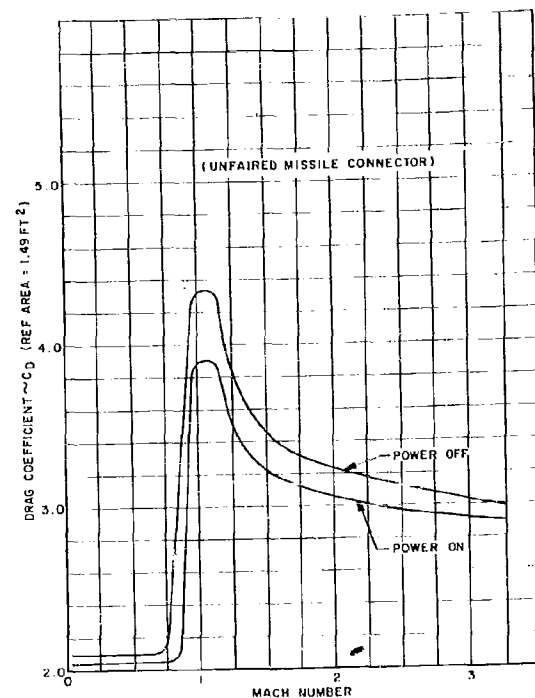


Figure 20. Drag Coefficient vs Mach Number - Two Stage Type III Cree

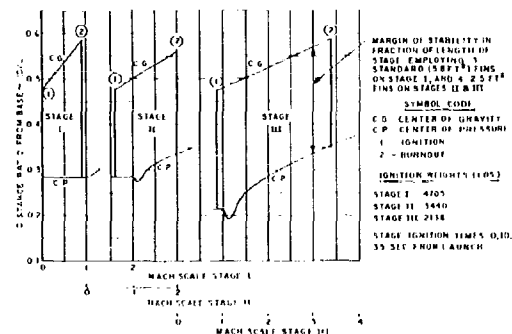


Figure 22. Three Stage Type III Cree Center of Gravity and Center of Pressure vs Mach Number

f. Three Stage Two Missile Cluster Configuration

Due to the close coupling of the missile centers of gravity with the third stage booster center of gravity and also to account

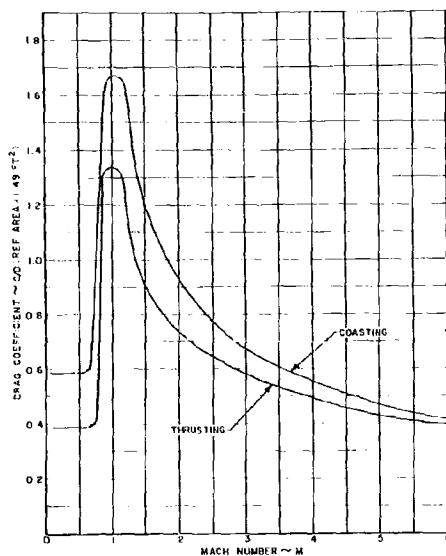


Figure 23. Drag Coefficient vs Mach Number - Cree Type III with Three Nike Stages

for possible downwash effects of the cluster, four fins of 5.0 square feet each are required for this stage. Three standard military fins are employed on the first and second stage boosters. The stability of this configuration is shown in Figure 26, for a typical launch trajectory. Drag curves for the three stages are shown in Figures 27, 28, and 29.

## 2. Dispersion

Calculations to determine the possible dispersions of the

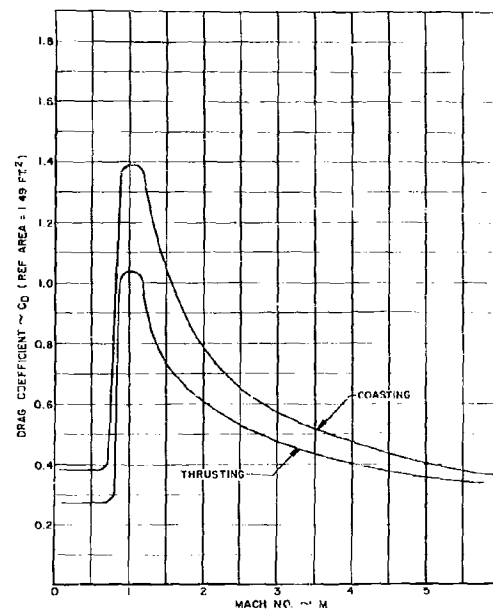


Figure 24. Drag Coefficient vs Mach Number - Cree Type III with Two Nike Stages

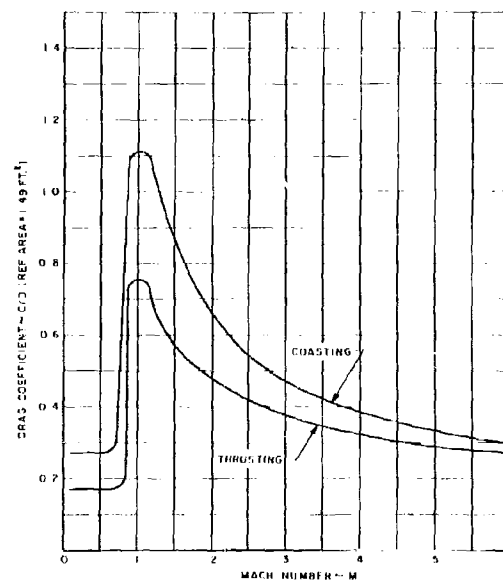


Figure 25. Drag Coefficient vs Mach Number - Cree Type III with Single Nike Stage

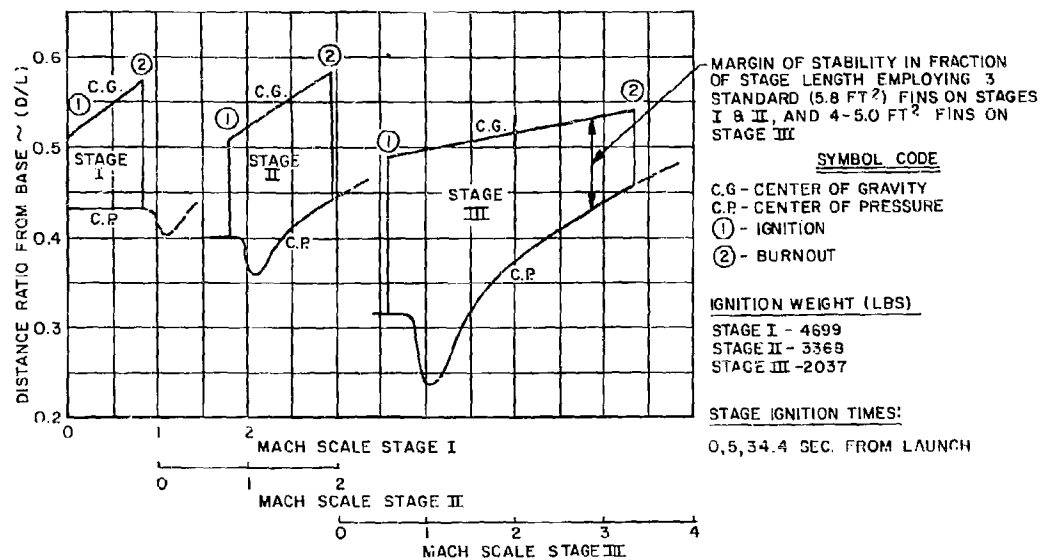


Figure 26. Three Stage Two Missile Cree Cluster Center of Gravity and Center of Pressure vs Mach Number

various ground launch configurations, particularly regarding the effects of launch angle, were performed. The various sources of dispersion in rocket motor configurations are as follows:

(a) Thrust misalignment, due to poor mechanical alignment of the nozzle causing the thrust to act off the center of gravity.

(b) Structural misalignments, caused by manufacturing tolerances of stage interconnections, misalignment with the center of gravity, or imposing a trim angle to the configuration.

(c) Wind prediction errors, which give rise to dispersions resulting from the weather cocking of the stable configuration.

(d) Launching errors, such as elevation and azimuth settings of the launcher.

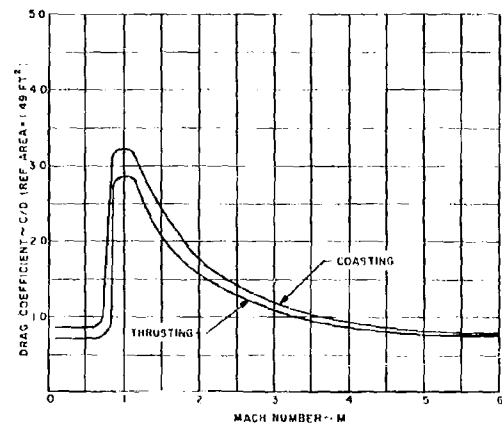


Figure 27 Drag Coefficient vs Mach Number - Cree Two Missile Cluster with Three Nike Stages

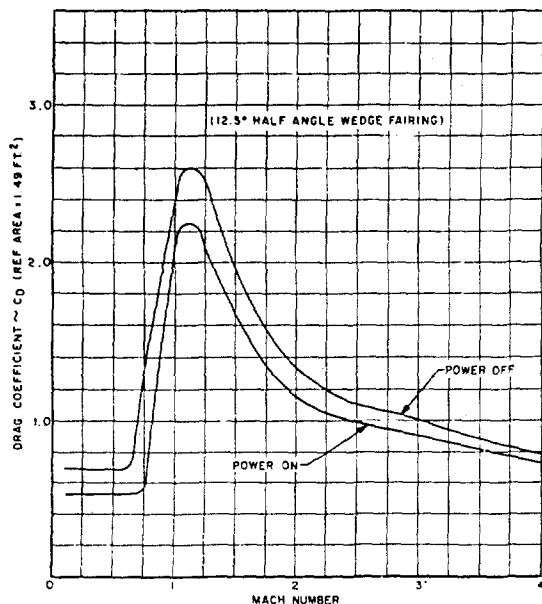


Figure 28. Drag Coefficient vs Mach Number - Cree Two Missile Cluster with Two Nike Stages

the dispersion due to thrust misalignment occurs primarily within the first second of burning, and the dispersion due to winds occurs primarily below 1000 to 2000 feet of altitude for high launch angles.

Rocket thrust misalignment are generally obtained from the rocket manufacturer. These are usually given as an angular thrust deviation which is based upon measurements made during many static firings. A typical average value of such angular misalignments is approximately 0.001 radian for a one standard ( $1\sigma$ ) deviation. All calculations are based upon this standard deviation, and employ the

(e) Errors in prediction of aerodynamic characteristics and motor thrust.

In general, analyses of the relative effects of the various sources of dispersion have indicated that the greatest sources of dispersion result from (a) and (c) above. Accordingly, the dispersion analyses performed are based on these two sources. The results of calculations which are illustrated in this report are selected on the basis of the most extreme case. This is the three stage type III missile. This configuration may be intuitively expected to be the most severe for both the dispersions due to thrust misalignment and due to winds. The former, due to the distance of the first stage nozzle from the center of gravity of the configuration, and the latter due to the relatively low first stage acceleration. It may be pointed out here that most of

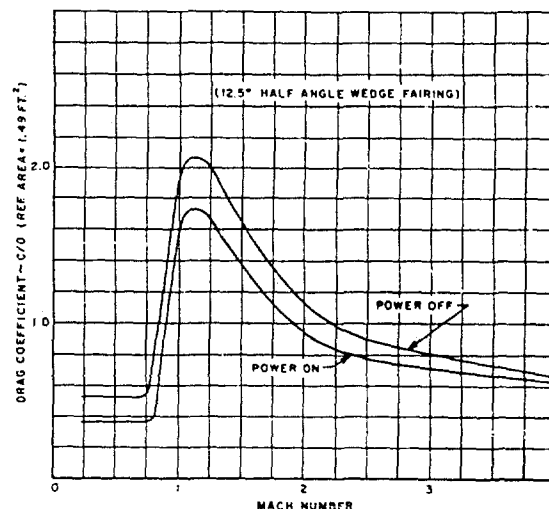


Figure 29. Drag Coefficient vs Mach Number - Cree Two Missile Cluster with One Nike Stage

methods of Reference 1 for the dispersion estimates.

Based upon the physical and aerodynamic characteristics of the three stage type III Cree configuration, the dispersion due to thrust misalignment is 1.3 degrees from the launch direction. The corresponding angular azimuth dispersion for various launch angles are listed in the following table.

Launch Angle ( $\theta_L$ ) (deg.)	Azimuth Dispersion Angle (deg.)
85	14.9
84	12.2
83	10.7
82	9.3
81	8.3
80	7.5
79	6.8

As an illustration of the azimuth deviation from the unperturbed impact point, the 79 degree launch case is used. For this trajectory, the range is approximately 30 miles (with normal parachute operation), in which case the lateral impact dispersion will be 3.6 miles.

The dispersion due to wind measurement errors for this configuration indicates that the deviation for the horizontal launch case is 0.155 degree per knot of cross wind. The azimuth error in this case for an 85 degree launch angle will be 1.8 degrees per knot of wind error. The accuracy of wind measurements depends upon the equipment employed at the launch facility and the time at which measurements are performed relative to the firing time. It is expected that wind measurement techniques should provide data which is accurate to within two to four knots. For a four knot error, the 85 degree launch azimuth error will be 7.2 degrees. The corresponding error in a 79 degree launch case is 3.3 degrees, providing a deviation of 1.75 miles laterally from the unperturbed impact point.

### 3. Aerodynamic Heating

Calculations to determine skin temperatures at various locations of the two stage Nike, Cree type I missile configuration have been performed. This configuration is selected as an illustration, since heating and loading conditions are most severe for this launch trajectory. The specific locations chosen for analysis are; the missile skin, missile nose cone, and the conical missile booster connector. Turbulent

convective heating conditions were assumed at all locations. Heat transfer coefficients were determined by the method of Reference 1. Temperature-time histories at the various locations were conservatively calculated by a one dimensional analysis neglecting radiation and heat transfer to other components.

As a result of the computations, the maximum skin temperature on the missile at a station six inches aft of the cone-cylinder junction was found to be 360°F, the temperature rise of the conical missile-booster connector was found to be 373°F, and the nose cone temperature rise was 734°F. These are shown in Figure 30. These tempera-

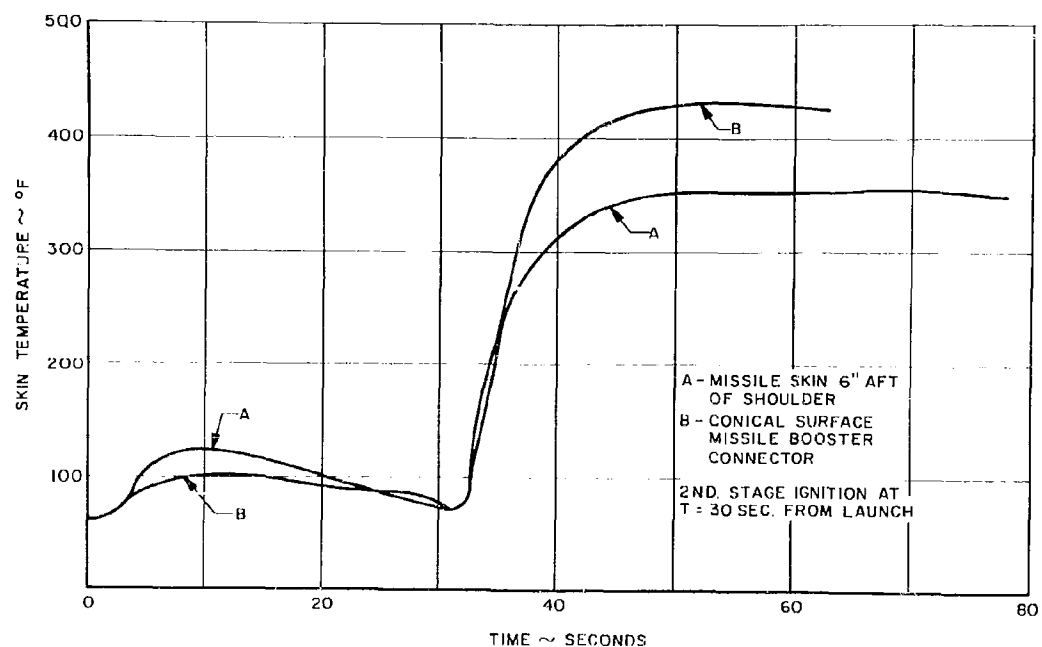


Figure 30. Skin Temperature vs. Time, Two Stage Type I Cree (Turbulent Heating)

tures are well within the allowable values for the respective component materials. In order to protect the pyrotechnic material employed for the recovery parachute door opening, a layer of insulation is required for this material to prevent it from attaining excessive temperatures. The test parachute, recovery parachute, and flotation balloon are adequately protected from surface heating conditions.

The calculations referred to above were based upon a coast period such that second stage ignition occurred at  $t + 30$  seconds. Ignition of the

second stage at an earlier time will result in more severe heating and loading conditions with small differences in performance. Corresponding reductions in peak temperatures will result with a longer coast period, and also with small differences in performance. However, the velocity of the second stage at ignition becomes quite low with increased coast time, thereby increasing the sensitivity of the configuration to high altitude winds.



## SECTION IV

### TEST METHODS, PROCEDURES AND FACILITIES

#### A. Test Facilities

##### 1. General

The Phase IV program represents the initial test effort utilizing the ground launched technique. In previous phases, both aircraft and balloons were used as launching platforms. The change to ground launching dictated the necessity of developing new test procedures and techniques. Also, a test site had to be selected and suitable launch equipment made available.

During the Phase II effort, it was determined that the test range which offered the most capability to support a Cree type research program was that of the Air Proving Ground Center, Eglin Air Force Base, Florida. While an operational launching facility did not actually exist at the Eglin range, it was evident that the problems of establishing such a facility were not severe.

##### 2. Launch Site

An excellent launch location was selected at site A-11 on Santa Rosa Island. Buildings suitable for the support activity were already in existence at this site. Building 9268 consisted of three rooms which were suitable for office space, a work and assembly area, and a control room. In addition, an adjacent building, No. 9270, was available for storage and additional work space if it should be needed.

The site for the launch pad was selected about 500 feet east of the control room. A road was built from the assembly area to the pad.

Control room equipment consisted primarily of instrumentation obtained from the mobile receiving stations used during Phases I and II of the subject program. The basic units are listed below:

- (a) Helical antennas
- (b) Telemetry receivers
- (c) Panoramic adapter

- (d) Mixer amplifiers
- (e) Recording amplifiers
- (f) Speed lock equipment
- (g) Magnetic tape recorder.

A detailed description of the various equipment can be found in Reference 2.

## B. Launch Equipment

### 1. Launcher

The Cree launcher is patterned after the NASA Wallops Island rocket launcher (NASA Dwg. No. LD-200,000). Since several changes were made to the original design, a brief description of the unit follows:

The launcher consists of a vertical mast supported by three side braces, a raisable boom, and a hoist mechanism consisting of an electric motor and a cable system. All of the above are mounted on a heavy concrete foundation. Figure 31 shows the launcher in a typical view with the boom elevated.

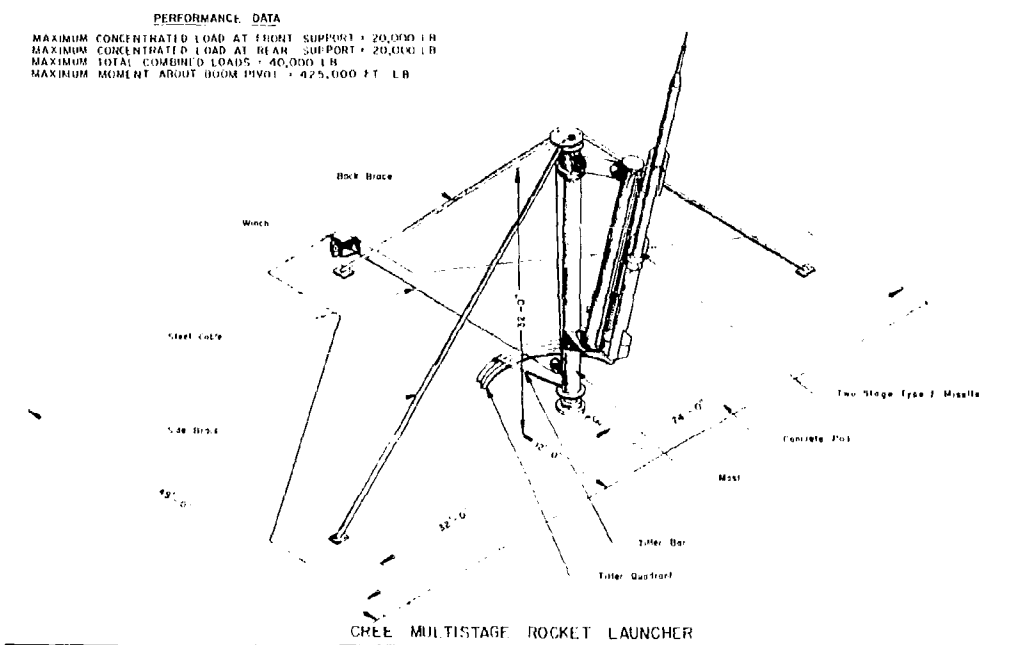


Figure 31. Cree Multistage Rocket Launcher

The foundation is a reinforced concrete pad roughly triangular in shape being 74 feet wide, 49 feet deep and two feet thick. Anchor bolts are provided where needed for tiedown of the launcher.

The single vertical mast is made from a two foot diameter steel pipe of 1/2 inch wall thickness. The mast is 32 feet tall. Nine feet from the pad surface is the attachment point for the boom. This boom is also made of two foot diameter 1/2 inch wall steel pipe. It extends outward just over 25 feet from the mast centerline. A 20 inch diameter section is available which provides a seven foot extension to the boom. A double rail was added to the lower surface of the boom along the entire length.

The boom is continuously adjustable from below the horizontal to a maximum elevation of about 83 degrees. Hoisting is accomplished through a cable and pulley arrangement. The hoist is powered by a 10 horsepower, three phase, explosion proof, electric motor.

The launcher has the capability of being rotated on its base so as to give a degree of azimuth control. A tiller bar extends outward horizontally from the mast to a quadrant which is anchored to the concrete pad. There are 12 quadrant positions for fastening the tiller bar. These positions are located at 10 degree intervals thus giving azimuth control over a 110 degree range.

The launcher has the capability of accepting a 20,000 pound concentrated load at either the front or rear supports or a total distributed load of 40,000 pounds. The maximum permissible moment about the boom pivot is 425,000 foot-pounds. The boom can be raised to its maximum elevation in less than 10 minutes. The launcher can be controlled either from an explosion proof control station at the pad or remotely from the control room.

## 2. Launch Fittings

A method had to be devised for support of the test vehicle on the launcher and here again it was decided to adopt the method used by the NASA (Reference 3). With this method, tee shaped fittings are fastened to the test vehicle at suitable locations. The first stage booster is supported both fore and aft and each succeeding stage has one additional support at its forward end. Thus, a two stage vehicle would have three support points. The payload is cantilevered from the last stage booster.

The launch tees are of graduated heights; the aft tee being the shortest, as shown in Figure 32. Each tee fits into a block which is

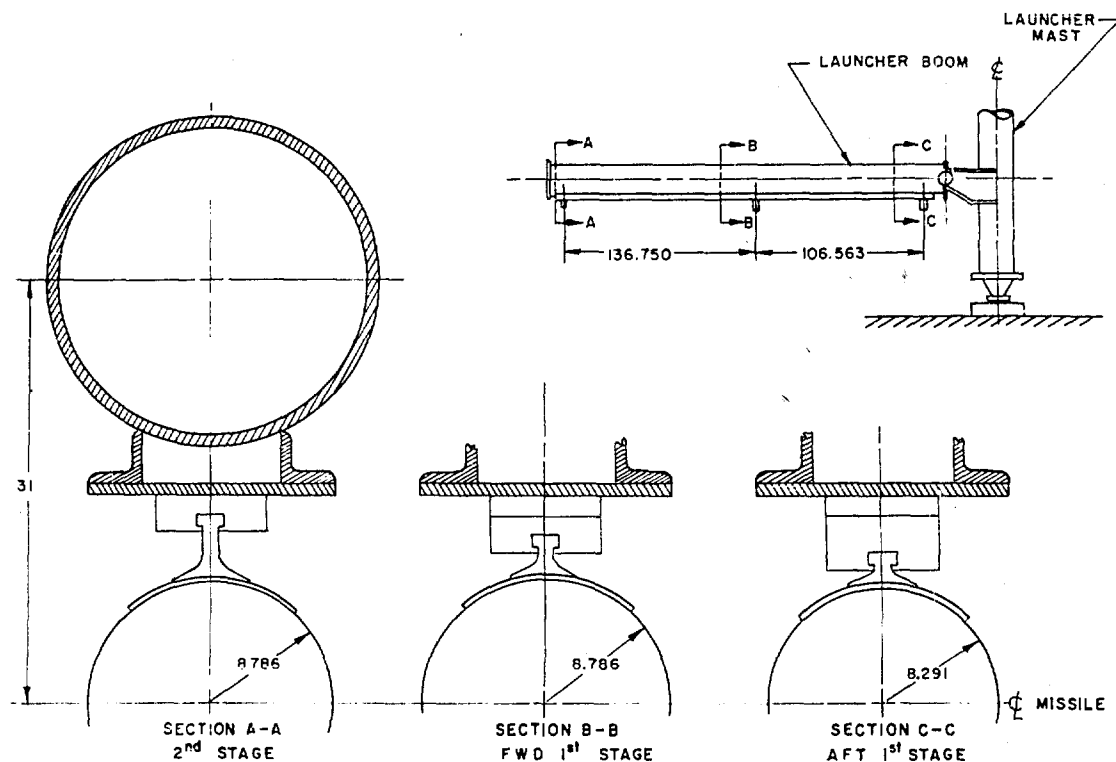


Figure 32. Cree Zero Length Launching Fittings

rigidly attached to the launcher rails under the boom. The location of these blocks is adjustable along the rail according to the type of boosters being used. The rail fittings are made to accept the launching tees in such a manner that when the test vehicle moves, the tees slide out of the blocks and the missile becomes completely unsupported. While the vehicle must move a finite distance of two inches before it becomes free of the launcher, this is still considered to be essentially a zero length launch. Stops are provided on the back side of the rail blocks so that the test vehicle can only go forward.

A capability for rail launching was added to the launcher during the Phase IV program. A typical view of the launcher with two Nike boosters attached is shown in Figure 33.

### 3. Booster Hardware

Primarily for reasons of economy, the Nike M5E1 booster was selected to be used on all Cree ground launched test missions. While only one and two stage missions were accomplished during Phase IV, three stage missions were being planned.

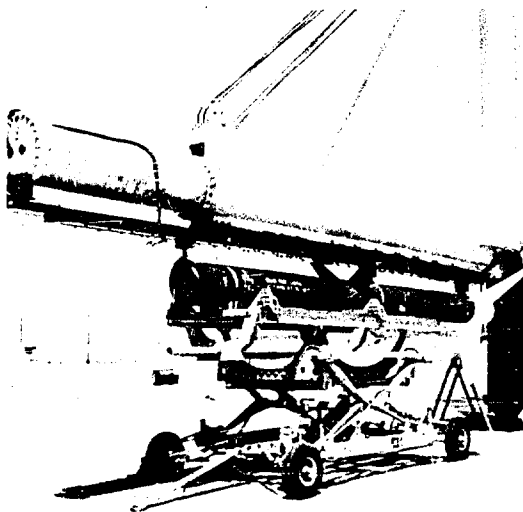


Figure 33. Cree Launcher with Two Nike Boosters Ready to Receive Payload

It was determined, on the basis of expected aerodynamic loads, that the standard Nike fins would be satisfactory for the booster used for first stage. This was true regardless of the number of succeeding stages. However, for upper stages, the standard military hardware would no longer be adequate. Special high strength fins were available having been developed for a similar purpose for the NASA. An arrangement consisting of four fins each of a two square foot area was selected for all stages beyond the first when only a single payload was being carried. The programmed cluster concept would require larger upper stage fins.

When more than one stage was to be used, interstage connecting hardware was required. Again, a

NASA design was selected. The interstage hardware consisted only of a cone shaped adapter which bolted to the front end of the first stage. This adapter was designed so as to fit snugly into the nozzle of the succeeding stage Nike booster as shown in Figure 34.

The adapter is not attached to the nozzle of the next stage but is free to slide out at any time. When the first stage fires and lifts off the launcher, the thrust of this stage keeps the adapter pressed into the nozzle of the second stage. As soon as the first stage burns out, the different weight-to-drag ratios of the two stages causes the empty first stage to decelerate more rapidly than the second. As a result, the first stage booster falls free of the test vehicle right at, or shortly after, burnout of first stage.

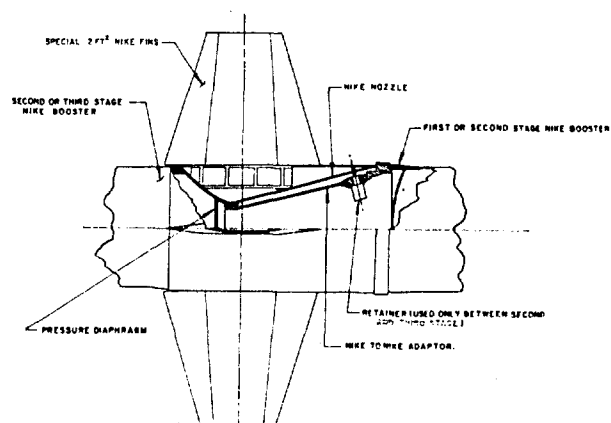


Figure 34. Nike Interstage Hardware

If a third stage is used,

the same plug type of interstage fitting can be employed. However, in this case the second and third stages must be held together until after second stage ignition in order to insure that separation of second and third stages does not occur at the time of first stage burnout. The retention system consists of a pin which is inserted through matching holes in the second to third stage adapter and the third stage nozzle (see Figure 34). The pin is extracted by a pyrotechnic device which is controlled by a variable time delay element.

#### 4. Booster to Missile Adapter

In order to expedite the work on Phase IV, it was decided that at least for the initial tests the existing booster to missile adapter would be used. This unit had been developed primarily for use in aircraft launched test missions. As a result, the design features of the structure were such that it be adaptable to those conditions anticipated for aircraft handling. The intertie structure was so designed that the Nike igniter could be easily installed as a last step just before aircraft take-off (see Figure 35). Thus, the intertie structure is of an open type of

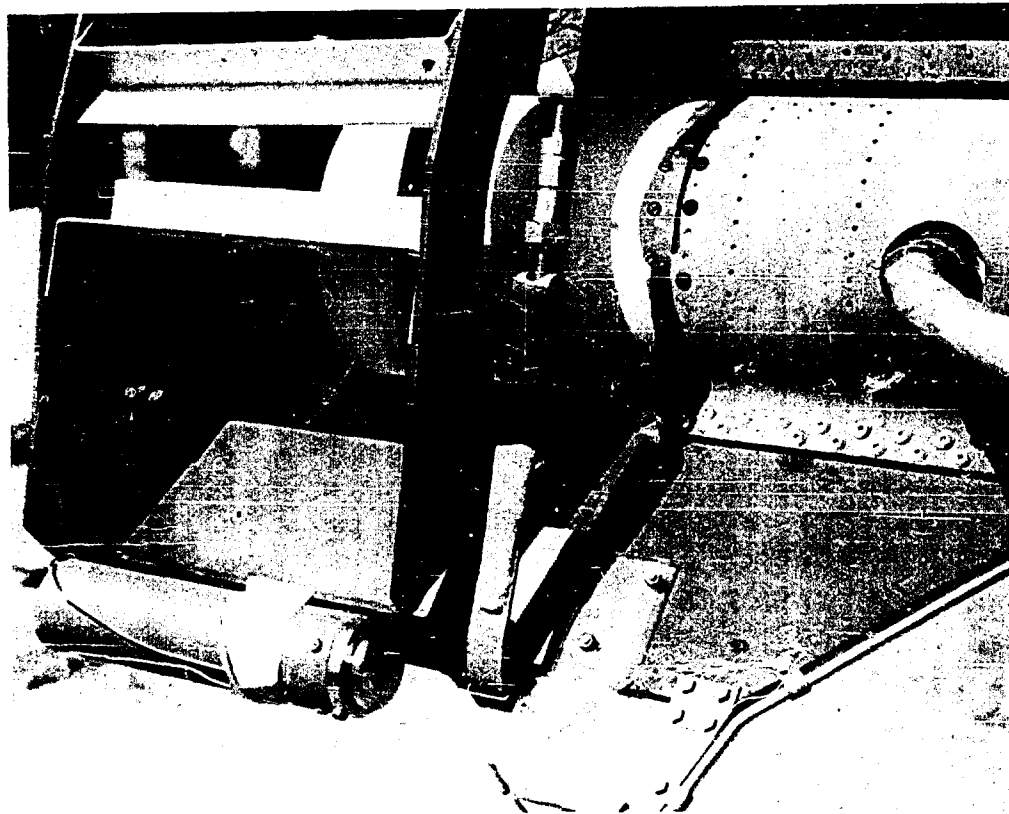


Figure 35. Missile to Booster Unfaired Intertie Structure

construction. It was designed to be strictly functional with no attempt made at streamlining.

The intertie structure bolts to the front end of the Nike booster. The test missile fins rest firmly against the forward plate of the assembly. Three groups of brackets on this plate mate with the missile fins. Both the brackets and the fins are notched to receive wedge shaped keys. When these keys are in place, the missile is securely attached to the last stage booster. The keys are held in place by a strap arrangement held together by three turnbuckles. The turnbuckles can be broken when desired by means of explosive charges stored internally.

When separation of the last stage is desired, an electric impulse sets off the charges in each of the three explosive bolts or turnbuckles. The tie band breaks apart allowing the wedge keys to fall out. The missile fins are then free to slide out of the intertie brackets.

A missile to booster connector more specifically adapted to the ground launched technique was developed during this phase. The new design, as shown in Figure 9, was of a faired conical construction nine inches in diameter at the missile end and 18 inches in diameter at the booster end.

The structure bolts permanently to the front end of the last stage booster. The small end of the adapter mates with the missile rear bulkhead. Separation is accomplished by an explosive filled groove in the mating ring. When this charge is ignited, the ring is broken and separation is achieved.

#### 5. Second Stage Igniter

The Nike boosters which were employed for all stages on all Cree test missions were supplied with standard M4 igniters. This igniter is satisfactory for the first stage booster but in order to be used for upper stages, a time delay ignition system must be added.

Such a system was developed and a schematic diagram is shown in Figure 36. The system consists of a 30 volt battery supply, a lanyard switch set to close at the first motion of the missile and two pyrotechnic time delay switches in parallel.

Safeguards, such as a battery arming plug and an igniter shorting plug, were built into the system. In addition, the lanyard switch itself provides a short across the igniter connections while in the safe position.

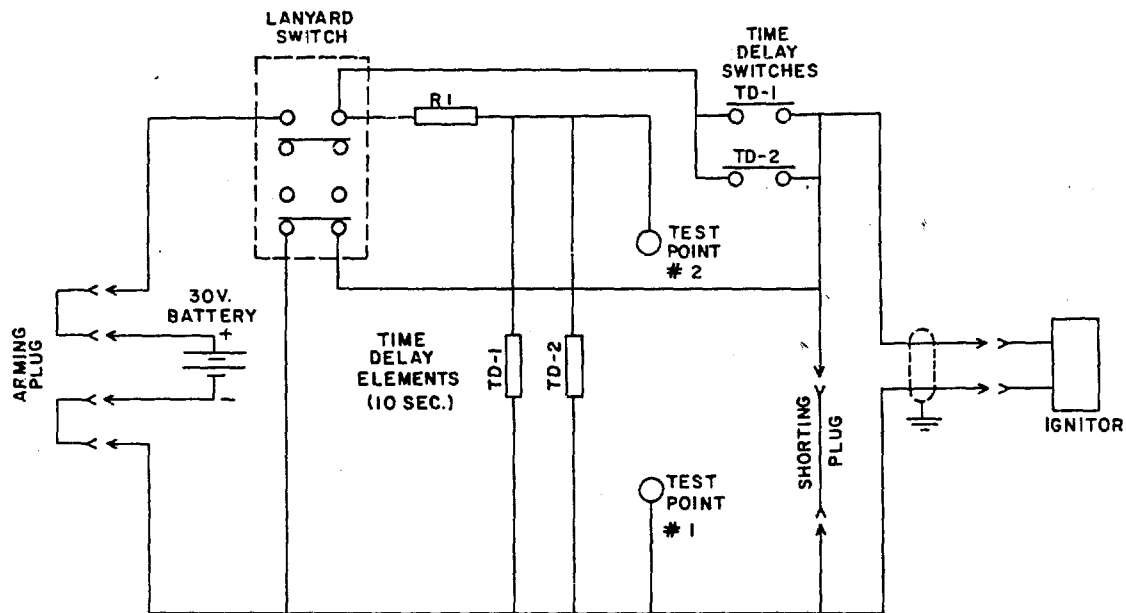


Figure 36. Schematic Diagram - Second Stage Ignition System

Test points were provided so that the condition of the package could be determined before actually connecting the igniter.

The system was housed in two containers, one of which was only a battery box while the other contained the remainder of the circuitry. The units were mounted on the missile to booster connector.

The system was placed in an operating condition by inserting the battery arming plug, removing the igniter shorting plug and connecting the igniter. When the first stage is ignited, by ground power, and the missile lifts off the launcher and the lanyard to the second stage ignition package is pulled. Pulling the lanyard opens one circuit, thus removing the final electrical short across the igniter, and closes a second putting battery power across the two pyrotechnic time delay elements (TD-1 and TD-2 in Figure 36). When the time delay elements have burned through their preset time periods, the two time delay switches are closed. The closing of either one of these two switches causes battery voltage to be impressed across the igniter thus accomplishing second stage ignition.

### C. Test Procedures

#### 1. Preparation

The boosters which will be used on the test mission are built up



in building 9270. Fins are assembled to the bottles and interstage adapters mounted on the forward end of all but the last stage. At some time before the scheduled launch time, loading of the boosters on the launcher is accomplished. If the launch is to be a two stage type, the first stage igniter is installed prior to mounting of the second stage. Once the second stage has been hung, the missile or payload can be moved out to the pad.

The intertie structure which serves to attach the missile to the last stage booster is already assembled to the missile. To accomplish hanging of the payload, it is only necessary to install six bolts into the front end of the Nike.

The electrical umbilical cable can now be inserted into the payload. The connector is attached to a mechanical linkage so arranged that the umbilical cable will be pulled free with the initial motion of the missile. The two arming lanyards for the dual missile programming system are also connected to the launcher so that they will be pulled with missile first motion thus starting the two programming systems.

Other steps required to reach the "missile ready" point are:

- (a) Installation of second stage igniter
- (b) Removal of missile shorting plug
- (c) Insertion of missile arming plug
- (d) Checkout and connection of first and second stage booster igniters.

## 2. Countdown Procedure

Prior to beginning the countdown, all rocket boosters with igniters installed, with appropriate safety circuits, are mated on the launcher; the test item mated to the final stage; and the launcher elevated. All preliminary checks on the missile will have been accomplished and all personnel will have left the launch pad.

The responsible personnel in the site A-11 control room were the Launch Officer - appointed by the Munitions Test (PGW) Director - and the Controller - appointed by Cook Research Laboratories. The Launch Officer maintained the countdown at site A-11, monitored the Mission Circuit, determined the operational status of the test vehicle (from

inputs supplied by the Controller), and fired the missile. Responsibilities of the Controller included the checkout operation of the test item.

The actual countdown procedure at the launch site is as follows:

<u>Time</u>	<u>Responsibility</u>	<u>Operation</u>
T - 120 (min.)	Launch Officer	Check communications to: a. A-19 (mission control) b. Pad
	Cook Controller	Check communication to: a. A-6 (telemetry station) b. A-13 (radar site)
T - 110 "	Cook Controller	Turn on telemetry and check
T - 100 "	Cook Controller	Turn on radar and check
T - 80 "	Launch Officer	Lower launcher
T - 70 "	Launch Officer	Check all power to pad off
	Cook Controller	Remove shorting plug
T - 65 "	Cook Controller	Install battery plug
T - 60 "	Launch Officer	Sound siren for armament setup. Check CRL missile power off.
T - 50 "	Launch Officer	Check all radars off at site A-11. Complete armament setup and raise launcher to desired angle
T - 10 "	Launch Officer	Advise mission control of readiness to fire
T - 8 "	Launch Officer	Firing circuit power on
T - 6 "	Cook Controller	Turn on external power a. Check telemetry b. Check radar

<u>Time</u>	<u>Responsibility</u>	<u>Operation</u>
T - 5 (min.)	Cook Controller	Record calibration frequencies. Check telemetry signal strength at A-6. Check radar signal strength at A-13
	Launch Officer	Recheck firing circuit continuity
T - 2 "	Launch Officer	Close final safety switch a. Turn tape recorders on b. External calibrate
T - 105 (sec.)	Cook Controller	a. Switch radar beacon to internal power b. Switch radar beacon to internal power
T - 60 "	Cook Controller	a. Calibrate telemetry b. Telemetry calibrate ready c. Radar signal good
		ANY HOLD OVER ONE MINUTE MUST RETURN TO T - 6
T - 30 "	Cook Controller	Check signal strength at A-6. Advise Launch Officer as to readiness for firing
T - 15 "	Launch Officer	Initiate programmer
T - 10 "	Cook Controller	Turn on oscillograph

#### D. Data Reduction and Analysis

##### 1. General

The final evaluation of any instrumentation system can only be based upon the authenticity of the results obtained from the system. This section deals with the methods employed to obtain reliable

calibrations of both telemetry and photographic response, and the methods used to reduce line traces on oscillograph paper (telemetry signals) and photographic images of parachute performance into comprehensive data. However, it must be noted that even the most diligently acquired calibration and reduction procedures will not provide data when unforeseen instrumentation or missile performance difficulties arise during a test event.

Effort was expended to reduce collected data on all tests where it was assumed that there was even the slightest chance that such an effect would be rewarded with success. Some of the factors which contributed to the problem were as follows:

- (a) Data Incomplete - one or more channels collected no data.
- (b) Data Intermittent - one or more channels collected data for only portions of the test.
- (c) Frequency Shifts - one or more channels evidenced frequency shifts at such times as the various programming events were occurring.
- (d) Transducers - transducer range was exceeded by test conditions, resulting either in loss of sensitivity or loss of record.

In some instances the above difficulties were resolved by application of one of the following techniques:

- (a) Using theoretical trajectory data to interpolate or extrapolate measured data
- (b) Using contrave phototheodolite and radar data for velocity and altitude where such data is available
- (c) Correcting records for obvious zero shifts for that period of time that the shift apparently was in effect.

## 2. Telemetry Data

Impact and static pressure and shock and drag forces were sensed by bourns potentiometer type pressure transducers and Cook Research Laboratories' tensiometers. The output of the various sensors were directed to one of four voltage controlled, subcarrier oscillators, with center band frequencies of 14.5 kilocycles, 22 kilocycles,

40 kilocycles and 70 kilocycles. Transmission to ground facilities was accomplished by a phase modulated crystal controlled transmitter. The multiplexed subcarrier signals from the test vehicle were recorded at the receiver outputs by an Ampex model 104 four track magnetic tape recorder. Playback into the input circuits of four data discriminators and a reference discriminator was achieved by a four channel Ampex model FR 104 playback tape transport. Multiplexed FM data were converted into voltage analog form to drive galvanometers of a photographic type Midwestern Instrument model 590 oscillograph.

a. Calibration

Static load calibrations of the missile instrumentation system were performed previous to each test mission. Pressure transducers were enclosed in a bell jar (vacuum chamber) and subjected to a range of pressures simulating the expected test conditions. The sensor response to a particular pressure was induced into the missiles telemetry system. Subcarrier oscillator input voltage and output frequency were measured, recorded, and plotted. Figure 37 shows a typical static pressure calibration curve. This data were obtained from a Bourns 0-2 lbs/in<sup>2</sup> absolute transducer previous to test mission 31-4. Preceding test parachute deployment is a three step sequential calibration of all subcarrier channels. Electrical calibration steps of zero, full scale, and fractional scale are executed by substitution of transducer output with a voltage divider rendering equivalent voltage to full scale and fractional scale, and by removal of the dc input source to the transducer to obtain a zero reference. After each test mission, the oscillograph recording is examined and the electrical calibration deflections measured (in inches) and recorded. The resulting deflections are plotted against electrical calibration voltages measured before and after static calibration (see Figure 37).

A hydraulic static loading mechanism was devised to apply simulated forces to the load link assembly (tensiometer, nylon attachment loop, and parachute pin). Forces were applied in 10 equal increments to the rated tensiometer operational limit in a direction parallel to the missile axes. The tensiometer response to both load application and removal were recorded. The tensiometer signal was fed into the telemetry system in the same manner as the pressure transducer signals. The resulting calibration plots were similar in nature to those shown in Figure 37.

A three step zero, full scale, and fractional scale,

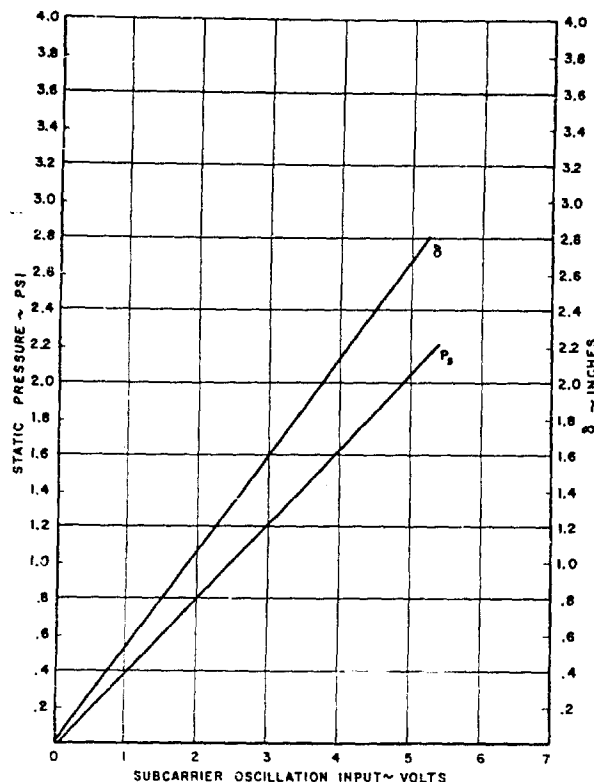


Figure 37. Typical Pressure Transducer Calibration

sequential calibration of the tensiometer subcarrier channels was obtained by unbalancing the resistance bridge, by substituting known resistance values across one bridge arm. Zero calibration was established by removing the excitation voltage from the strain gage bridges.

#### b. Data Reduction

Telemetry data were obtained in the form of oscillographic records. Appearing on each record were four data channels, showing the response of two pressure transducers and two strain gage bridges; one channel showing telemetry signal strength; and three reference traces. A 100 cycle per second oscillation, superimposed on a pressure trace, and the oscillograph timing lines (1/10 and 1/100 second) provided a timing standard for data correlation.

Progressing from a time prior to missile launch, each oscillograph record shows:

- (1) Calibration sequence on external power
- (2) Calibration sequence on internal power
- (3) In-flight calibration
- (4) In-air operate
- (5) Test parachute deployment
- (6) Recovery parachute deployment.

In addition, indications of programmed events (launch, second stage firing, separation, etc.) are seen on the various data channels.

Data editing, at the test site facilities immediately following test operation, provided explanations for data discontinuities resulting from known electrical or mechanical malfunctions or from unusual missile performance characteristics. Further, the data channels were identified and instrument calibration deflections read. Preliminary test data were calculated for in-field comparison with predicted performance values. The records were forwarded to Cook Research Laboratories for final reduction.

The initial step of the final reduction program was a careful check of the channel identification and data editing done at the test site. All traces were inspected closely to determine the actual time sequence of programmed events.

Data reading was accomplished manually with a 12 inch special purpose scale graduated in 1/50 inch. Accuracy attained would approach plus or minus 0.005 inch.

The position of all data traces relative to a particular reference trace (static reference trace, usually the uppermost on the record) was measured during the missile coast period at a time immediately before initiation of the calibration cycle. This measurement was denoted as " $\Delta_0$ ". Trace deflections at three intervals during each of the calibration steps (50 percent scale, full scale, zero) were measured from the same reference trace and their values recorded as  $\Delta_{cal}$ ". During the interim between end of electrical calibration and test parachute deployment, sample trace displacements ( $\Delta_0$ ) and corresponding time lapse from launch were recorded. If channel drift were apparent, the rate of drift per unit time was calculated and would be used later as a correction. In most cases where good test data were obtained, little or no channel drift was evidenced. Data trace displacements were measured at 0.01 second prior to test parachute deployment, in the case of force channels, and 0.01 second prior to the pressure system safety valve opening, in the case of static and impact pressures. Measurements (displacement in inches from the uppermost reference trace) were taken at 0.1 second intervals from deployment to snatch and recorded as " $\Delta_{act}$ " together with corresponding time lapse from deployment. Commencing with time of snatch, readings were made at 0.02 second intervals until a steady state force condition was attained usually by deployment plus two or three seconds. During this time, additional readings were taken wherever necessary to show peak or minimum loads. Steady state performance

measurements were taken at 0.05 second intervals to deployment  $t + 5$  seconds; at 0.10 second intervals from  $t + 5$  to  $t + 10$  seconds; at 0.5 or 1.0 second intervals from  $t + 10$  seconds to recovery parachute deployment. All measurements of force and pressure channels during the test interim were recorded as " $\Delta_{act}$ ".

To develop measurements from a reference trace into usable calibration data, the data trace displacement ( $\Delta_o$ ) immediately prior to initiation of the calibration sequence was subtracted from the various calibration deflections ( $\Delta_{cal}$  full scale,  $\Delta_{cal}$  zero) to yield  $\delta_{cal}$  which represents galvanometer response to a known electrical unbalance (see Fig. IV-37). A similar procedure was applied to attain usable force and pressure deflections ( $\delta_{act}$ ). That is, the data trace displacement ( $\Delta_o$ ) immediately prior to test parachute deployment was subtracted from all values of  $\Delta_{act}$ . The resulting deflection ( $\delta_{act}$ ) represented the galvanometer response to an unknown electrical unbalance created by the test environment. Since the calibration shows that a similar unbalance will occur as a result of particular voltage input to the subcarrier oscillator, the test data deflections ( $\delta_{act}$ , in inches) can be converted into voltage input to the oscillator, or voltage output of the sensor. Following is a typical procedure by which static pressure was attained (impact pressures and forces are determined in a similar manner). Assume the measured galvanometer deflection  $\delta_{act}$  ( $\Delta_{act} - \Delta_o$ ) to be 1.17 inch. Using the  $\delta$  curve of Figure 37 it can be seen that a corresponding subcarrier oscillator input voltage is 2.2. From the  $P_s$  curve of Figure 37, an equivalent static pressure of 0.88 psi is obtained. By entering the calibration curve with each galvanometer deflection, any nonlinearity of the calibration will be accounted for. The static (or ambient) pressure was converted from pounds per square inch to millibars and the corresponding altitude found in the meteorological data measured on shot day. It was found that an ambient 0.88 pounds per square inch existed at an altitude of 64,100 feet - peak altitude attained during mission 31-4.

With measured impact and static pressures and Rayleigh's pitot tube formula (Reference 4),

$$\frac{H_i}{P_o} = \frac{\gamma + 1}{2} M_o^2 \left[ \frac{\frac{\gamma + 1}{2} M_o^2}{\frac{2\gamma}{\gamma + 1} M_o^2 - \frac{\gamma - 1}{\gamma + 1}} \right]^{\frac{1}{\gamma - 1}}$$



where

$H_i$	=	Pitot pressure (behind a detached shock)
$P_o$	=	Free stream ambient pressure
$M_o$	=	Free stream Mach number
$\gamma$	=	$C_p/C_v$
$C_p$	=	Specific heat of dry air at constant pressure
$C_v$	=	Specific heat of dry air at constant volume

free stream Mach number was determined.

### 3. Film Data

High speed (200 frames per second) film coverage was provided during each test mission. A Fairchild Model HS100 16 mm camera equipped with 13 mm, f:1.5 wide angle lens was focussed through the aft bulkhead of the test missile. Coverage was initiated immediately prior to parachute deployment and provided photographic documentation of parachute performance. In order that a comparison of camera film and telemetry data could be made, the 100 cycle per second oscillator, which provided a time standard for telemetry data, also provided a 100 cycle input to the camera timing light. Thus, the margin of each film record was marked at 1/100 second intervals. This method of data acquisition, though providing the most dramatic results, is considered to be the least reliable of the two methods used since it depends entirely on recovery. When recovery is realized, the accuracy of data obtained is largely dependent on the presence of timing marks - there is no accurate backup reference such as oscillograph timing lines - to aid the data analyst in his evaluation of the record. The following subsections will define the method by which film calibration is provided and the method by which inflated area and parachute oscillation are obtained.

#### a. Calibration

A calibration of the Fairchild camera and lens was accomplished prior to the field test operations. The camera was mounted in a missile. Two seven foot crossed poles (calibrated at one foot intervals) were located 10 feet aft of the missile with the intersection point of the poles and the missiles centroidal axis coincident. Calibration pictures were taken. The operation was repeated with the poles placed 20 feet aft of the missile. The film, when projected on a screen or data reader, would furnish an image calibration (that is, x inches of image length would be equivalent to one foot of pole length) such that projected film exposures of any other object (for example, a parachute) that was at a distance of 10 or 20 feet from the camera could be measured

directly. The same projector placed at a fixed distance from a viewing plane must be used for observing both calibration film and parachute test film. Since it is unlikely that a deployed test parachute will be operating at exactly 10 or 20 feet aft of the missile, a correction was applied which would in effect bring the calibration poles into the plane of the test parachute.

b. Data Reduction

A specially constructed reading table (see Figure 38) was used to reduce film data. The photographic image was projected by a Bell and Howell film analyst horizontally to a front surface mirror fixed at 45 degrees to the projector axis and reflected vertically to a frosted glass panel in the table top.

With the 20 foot calibration film in the projector, the pole graduations (one foot) were measured in inches to determine the projected image length relative to the pole length ( $x$  inches image length per seven foot of pole length). The projector was moved fore and aft until an image-to-pole ratio of one inch to one foot was attained. Thus, the projected image of any object photographed with a Fairchild camera equipped with a 13 millimeter wide angle lens could be measured in inches, readily converted to feet, and later corrected for the difference between the calibrate distance of 20 feet and the distance of the object from the camera.

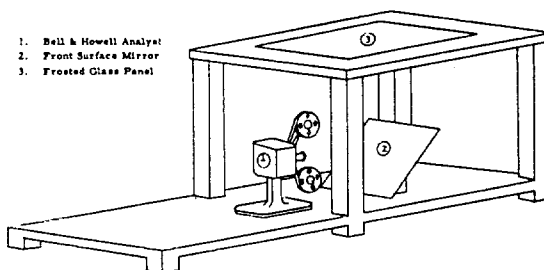


Figure 38. Film Data Reduction Table

Following is the procedure used to reduce the camera film of typical test mission:

- (1) Projected image calibration was obtained for camera subjects at a distance of 20 feet as mentioned in the preceding paragraph.
- (2) Without moving the projection equipment, the change was made from calibration film to test film.
- (3) The film was projected at slow speed; significant events and general over-all parachute performance noted. Camera

speed was calculated by noting the film frames per timing mark interval at various times throughout the test.

(4) The film was run through again and the precise instant of test parachute deployment determined. The camera was activated prior to deployment, but because of the parachute package's location at the aft end of the missile, no light was allowed to enter the camera compartment and no film was exposed. At the instant of deployment, light enters the compartment and distinctively marked frame number one of the test film sequence. The projector was stopped at deployment and the frame counter set to zero.

(5) Film was advanced manually until parachute snatch was seen to occur; the corresponding frame number was recorded.

(6) Film was advanced manually from snatch until evidence of parachute opening was observed and the corresponding time recorded.

(7) Film was again advanced manually until the parachute attains an inflated shape. The projected area of the test parachute was measured with an Ott planimeter and recorded as "Sp'" in square feet (image calibration was one inch square = one foot square). Position of the parachute relative to the left and bottom edges of the film frames was recorded as  $\Delta_{x_0}$  and  $\Delta_{y_0}$  measured in feet.

(8) Film was advanced, area and position were measured at four frame intervals through the time of parachute's full open (maximum load). Canopy position was recorded as  $\Delta_x$  and  $\Delta_y$ . Corresponding frame numbers were recorded.

(9) The remaining record was read at time intervals similar to those used in reducing telemetry data.

(10) Data available at the conclusion of the film reading operation were: time-histories of uncorrected projected areas (Sp'), and parachute deflections  $\Delta_x$  and  $\Delta_y$ . Displacements ( $\delta_x = \Delta_x - \Delta_{x_0}$  and  $\delta_y = \Delta_y - \Delta_{y_0}$ ) of the parachute from its zero position (determined in item (7) above) were calculated and resolved into an absolute displacement,  $\delta_{xy}$ .

(11) Both projected areas and absolute displacements

were corrected for the difference between the calibrate distance ( $d'$ ) and the distance of the parachute from the camera ( $d$ ) by multiplying  $S_{p'}$  by  $(d/d')^2$  and  $x_{y'}$  by  $(d/d')$ . Absolute displacement, expressed in feet, was converted to angular displacement (or oscillation angle) expressed in degrees).

## SECTION V

### DISCUSSION OF TEST RESULTS

#### A. General

The field test program of Phase IV of the subject contract consisted of a total of five test missions. All tests were of the single-missile ground launch configuration. The first mission (28-1) utilized a single booster stage while the remaining four missions employed two booster stages. Theoretical missile performance for the two basic launch configurations is presented in Figures 39 and 40.

All missiles were instrumented to collect data. However, the degree of data acquisition successfully accomplished during the test program varied significantly between the various missions. The collected data were spread throughout the test regime as illustrated by Figure 41. It should be noted that Figure 41 also includes the 29 data points collected in Phases I and II, thus making a total of 34 points.

Physical details of the parachute types tested through Phase IV are presented in Table 3. All parachutes were designed in compliance with References 5, 6 and 7.

Data collected during Phase IV consists of:

- (1) Missile performance information
- (2) Parachute performance information.

These are summarized in Table 4 and presented graphically in Figures 42 through 58. Missile performance (altitude, velocity, Mach number, and dynamic pressure) information was derived from tracking data obtained by contrave phototheodolite, by MSQ 1-A radar, by FPS16 radar, and by reduced telemetry data. Drag forces, where available, were obtained by reduction of telemetry data. In all cases drag coefficients presented were calculated on the basis of parachute design surface area,  $S_0$ .

#### B. Missile Performance

##### 1. Test Mission 28-1

This mission was intended to be a shakedown type test and as such a minimum range trajectory was obtained by utilizing only one stage of boost and a single 800 pound missile. Figure 42 compares the predicted

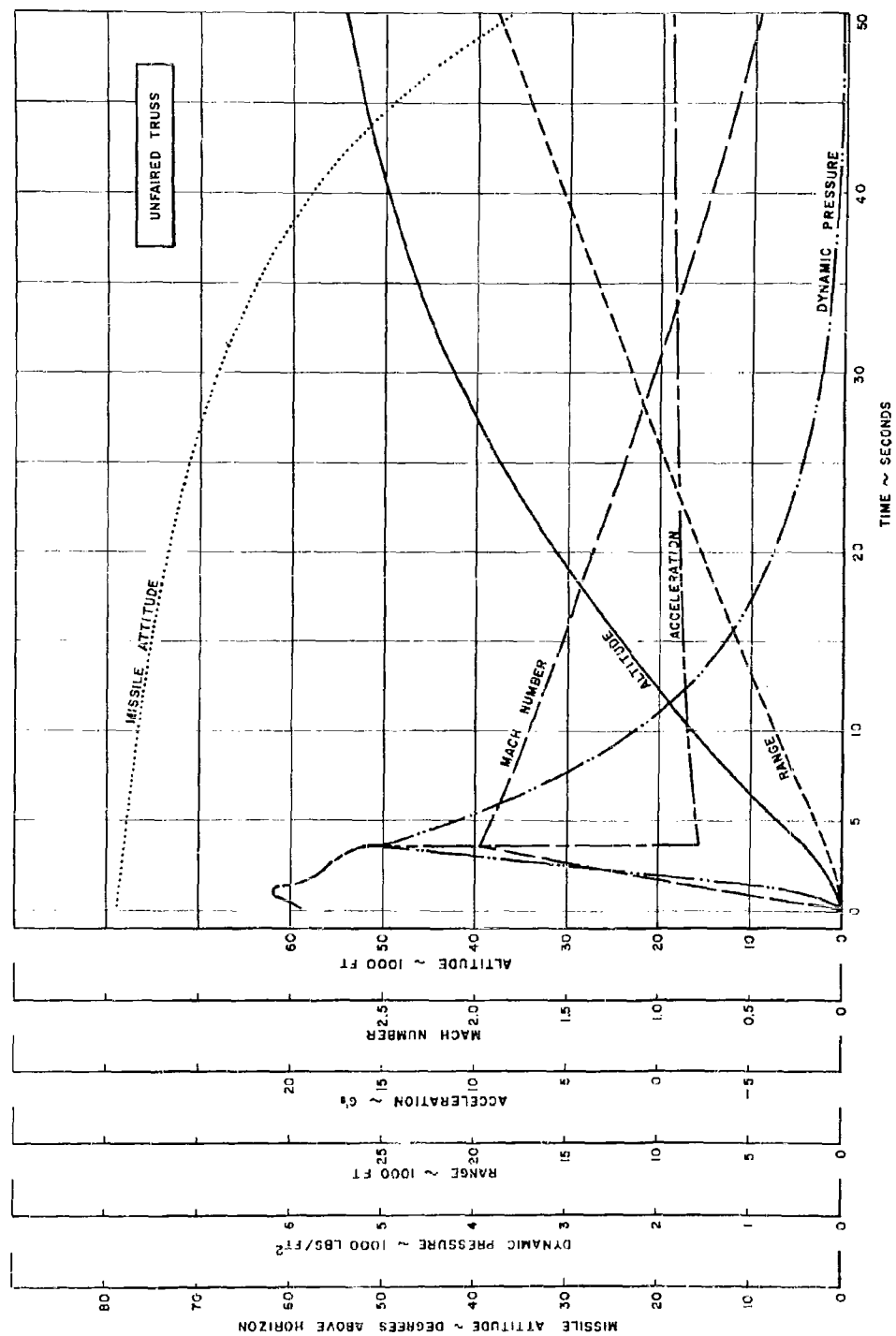


Figure 39. Predicted Missile Performance for a Single Stage, Type III Configuration

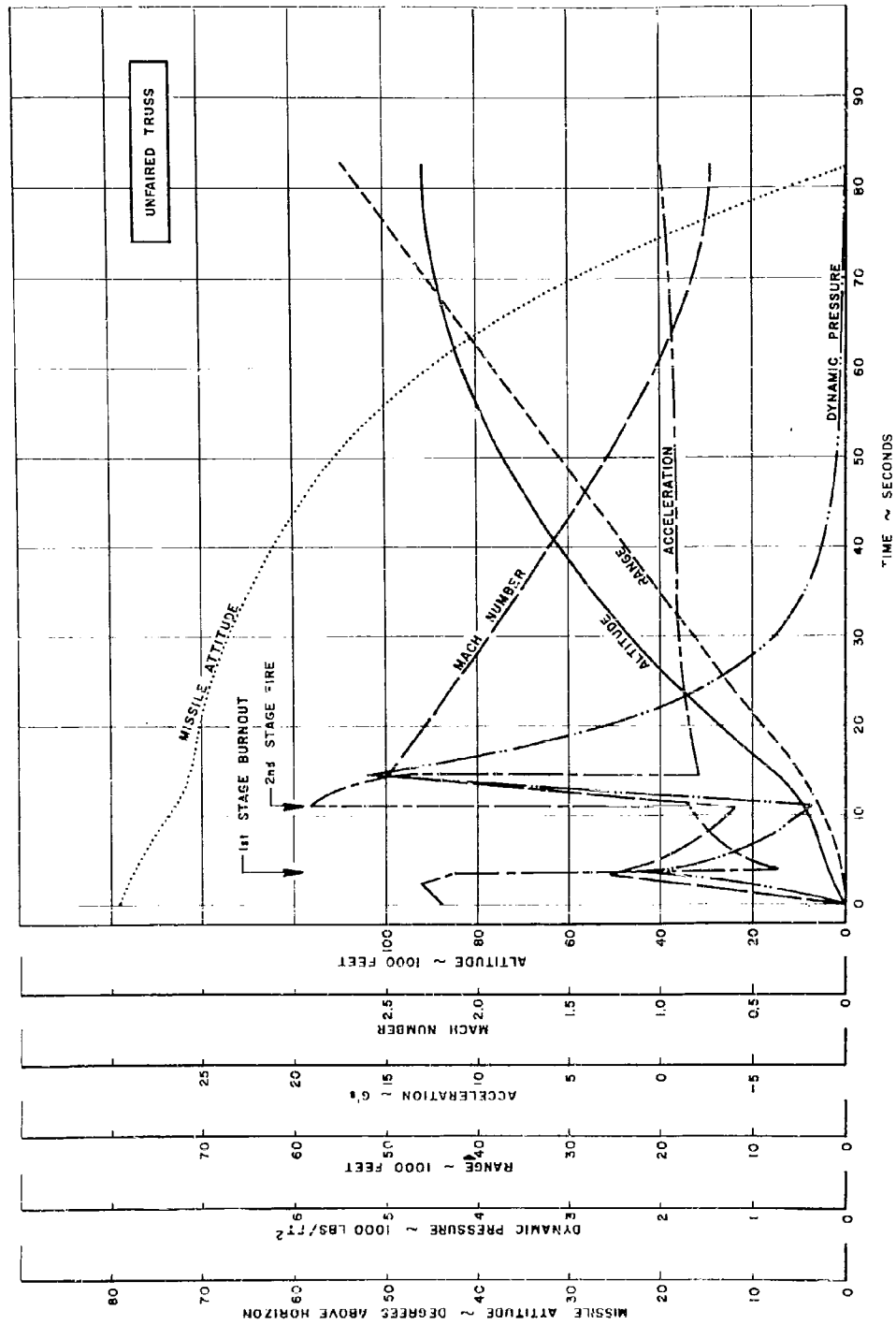
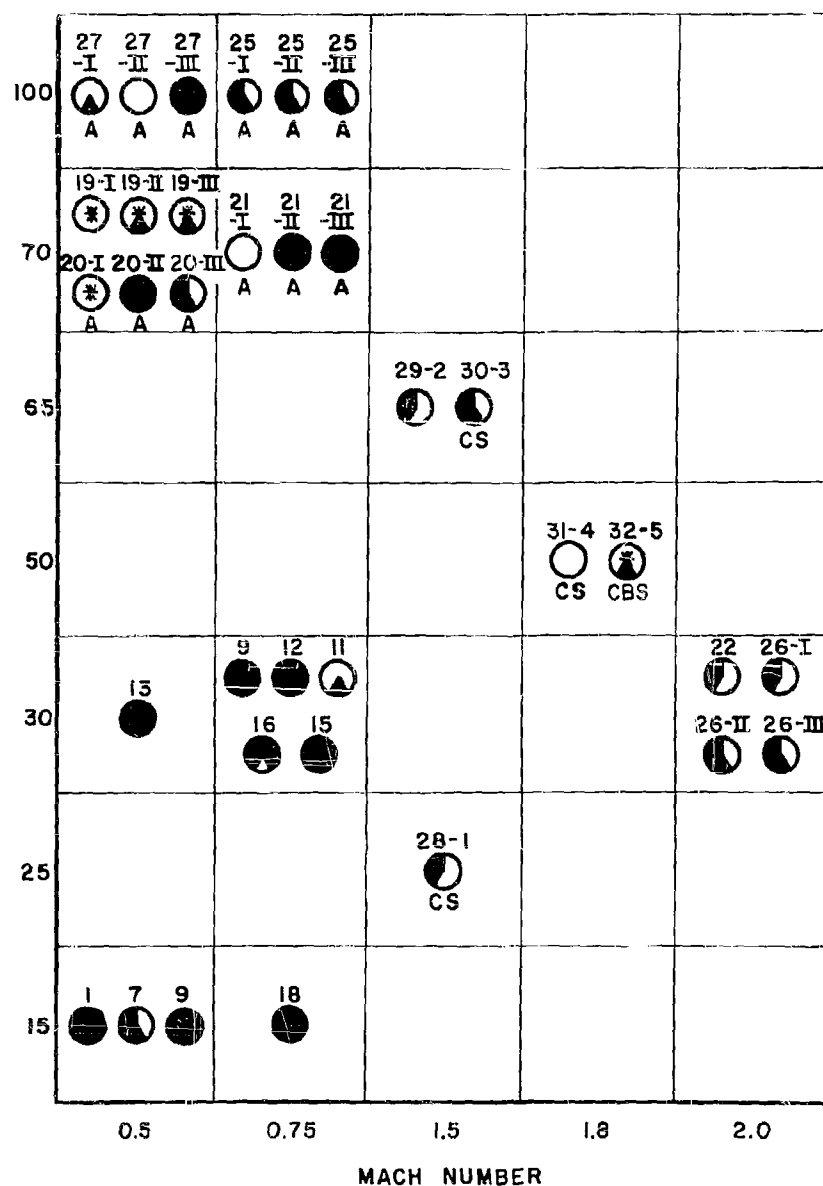


Figure 40. Predicted Missile Performance for a Two Stage, Type III Configuration



- NO DATA
- ◐ PARTIAL TELEMETRY
- FULL TELEMETRY
- ◑ CAMERA DATA
- FULL DATA
- \* INTERFERENCE ON TELEMETRY
- A ASKANIA PHOTOHEADLITE
- C CONTRAVE PHOTOHEADLITE
- B BEACON TRACK (RADAR)
- S SKIN TRACK (RADAR)

Figure 41. Data Collected on Phase I, Phase II, and Phase IV



TABLE 3

## PARACHUTE PHYSICAL DETAILS

Parachute Type	30 Conical Ribbon	FIST Ribbon	10 % Equiflo Ribbon	10 % Equiflo Ribbon	10 % Ext. Hemisflo Ribbon
Fabricator	CRL	Radioplane	CRL	CRL	CRL
Parachute Number	III-C	-	III-A	III-B	III-B
1. Nominal diameter - $D_0$ (ft)	4.03	6.0	4.03	4.03	4.12
2. Design projected area - $S_P$ (ft) <sup>2</sup>	-	33.19	-	-	-
3. Nominal area - $S_0$ (ft) <sup>2</sup>	12.76	28.26	12.76	12.76	13.32
4. Geometric Porosity - $\lambda_g$ (%)	27.2	19.5 & 23.3*	26	26	
5. Number of gores	16	8	16	16	16
6. Suspension line material (width & tensile strength - in. & lb)	1 3000	N.A. 1000	Cord 375	1/2 1000	1/2 1000
7. Horizontal ribbon material (width, B, inches and tensile strength - lb)	1 525	N.A. 460	1-1/4 120	1-1/4 280	1-1/4 280
8. Vertical ribbon material (width, A, inches and tensile strength - lb)	3/8 200	N.A.	3/8 33	3/8 58	3/8 58
9. Radial ribbon material (width, C, inches & tensile strength - lb)	2 1000	N.A.	1-1/4 280	1-1/4 280	1-1/4 280
10. Space between horizontal ribbons - b(in.)	1.0	N.A.	0.95	0.95	0.564
11. Horizontal ribbon ratio - (RHR = b/3)	1.0	N.A.	0.75	0.75	0.456
12. Vertical ribbon spacing - a(in.)	Midgore	N.A.	1.5	1.5	Midgore
13. Weight - (-b)	3.19	2.8	1.06	2.12	3.38
14. Packing density - (lbs/ft <sup>2</sup> )	20	20	20	20	20
15. Drawing number	SK18122	P/NR-5103	597-9752	597-6440	596-0327
16. Used on test number	28-1	29-2	30-3	31-4	32-5

\*Constructed  $\lambda_t$  and reefed  $\lambda_t$  porosity

N.A. - Not Available

TABLE 4  
SUMMARY OF TEST RESULTS

Mission No.	28-1	29-2	30-3	31-4	32-5
First Stage Ignition	Normal	Normal	Normal	Normal	Normal
First Stage Burnout Time	3.5 sec	separated at 0.050 sec	3.4 sec	3.4 sec	3.5 sec
Velocity	2,229 fps	N.A.	1,265 fps	1,265 fps	1,365 fps
Altitude	4,013 ft	N.A.	2,200 ft	2,000 ft	2,700 ft
Second Stage Ignition Time	-	0.050 sec	8.8 sec	8.5 sec	10 sec
Velocity	-	N.A.	840 fps	865 fps	745 fps
Altitude	-	N.A.	7,500 ft	7,000 ft	8,700 ft
Second Stage Burnout Time	-	3.55 sec**	12.2 sec	11.9 sec	14.5 sec
Velocity	-	N.A.	2,920 fps	2,764 fps	2,970 fps
Altitude	-	N.A.	13,000 ft	12,604 ft	16,889 ft
Second Stage Separation	4.0 sec*	15 sec**	14 sec	12.3 sec	12.1 sec
Test Parachute Deployment Time	4.0 sec**	43 sec**	42.94 sec	32 sec	32 sec
Velocity	2,200 fps**	N.A.	1,015 fps	N.A.	1,760 fps
Altitude	4,013 ft**	N.A.	59,000 ft	49,100 ft	53,800 ft
Snatch Force	N.R.	200 lbs	300 lbs	N.R.	N.R.
Opening Force	N.R.	1,130 lbs	665 lbs	N.R.	N.R.
Peak Altitude Attained	33,400 ft	N.A.	N.A.	64,000 ft	74,600 ft
Recovery Parachute Deployment Time	28.5 sec	75.6 sec	66.74 sec	56.5**	56.8**
Altitude	32,700 ft	N.A.	N.A.	N.A.	73,500 ft
Velocity	660 fps	N.A.	N.A.	N.A.	440 fps
Impact Time	288 sec	N.A.	473 sec	397.4 sec	491 sec
Impact Range	23,600 ft	N.A.	53,000 ft	33,400 ft	31,600 ft

\*First stage separation

N.R. - Not recorded

\*\*Approximate

N.A. - Not available

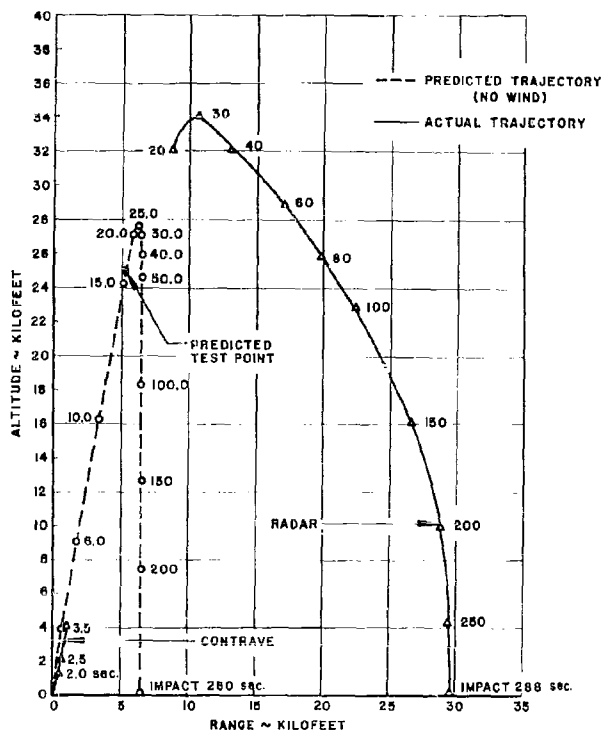


Figure 42. Predicted and Actual Trajectories for Cree Mission 28-1

and actual trajectories, obtained from reduced contrave phototeodolite and radar tracking data, for a missile launched from an angle of 79 degrees. Contrave coverage from launch to  $t + 3.5$  seconds indicated close agreement between the missile track and predicted trajectory. Burn-out occurred at  $t + 3.5$  seconds at an altitude of 4,013 feet and velocity of 2,229 feet per second. No radar beacon signal was obtained; however, a radar skin track was established at  $t + 20$  seconds and maintained throughout the remaining flight time. The recovery sequence was initiated at  $t + 28.5$  seconds with deployment of an eight foot diameter FIST ribbon recovery parachute. As can be seen from Figure 42, a considerable difference between actual track and predicted trajectory exists. This variation from the predicted is most evident during missile coast time (time after booster burnout and separation) and especially during descent at equilibrium velocities with recovery system deployed. The greater range attained during missile flight can be wholly attributed to drift created by excessively high wind velocities. Wind speeds aloft taken from meteorological data measured at noon on 10 March 1959 (shot day for test mission 28-1) are presented graphically as a function of altitude in Figure 43. The wind speeds in all probability changed somewhat during the time interval from noon to shot time (2:00 P. M.) but for purposes of discussion herein any change is ignored. Consider the flight time interval  $t + 100$  seconds to  $t + 150$  seconds of Figure 42. The predicted trajectory shows the missile to be in vertical descent while actually the missile has traveled 4,280 feet in a horizontal direction while descending from an altitude of 22,863 feet to an altitude of 16,122 feet or 6,741 feet. Between these altitudes, it can be seen from Figure 43, the average wind velocity was approximately 90 feet per second. The resulting calculated drift would be approximately 4,500 feet which is in close agreement with the actual value.

and actual trajectories, obtained from reduced contrave phototeodolite and radar tracking data, for a missile launched from an angle of 79 degrees. Contrave coverage from launch to  $t + 3.5$  seconds indicated close agreement between the missile track and predicted trajectory. Burn-out occurred at  $t + 3.5$  seconds at an altitude of 4,013 feet and velocity of 2,229 feet per second. No radar beacon signal was obtained; however, a radar skin track was established at  $t + 20$  seconds and maintained throughout the remaining flight time. The recovery sequence was initiated at  $t + 28.5$  seconds with deployment of an eight foot diameter FIST ribbon recovery parachute. As can be seen from Figure 42, a considerable difference between actual track and predicted trajectory exists. This variation from the predicted is most evident during missile coast time (time after booster burnout

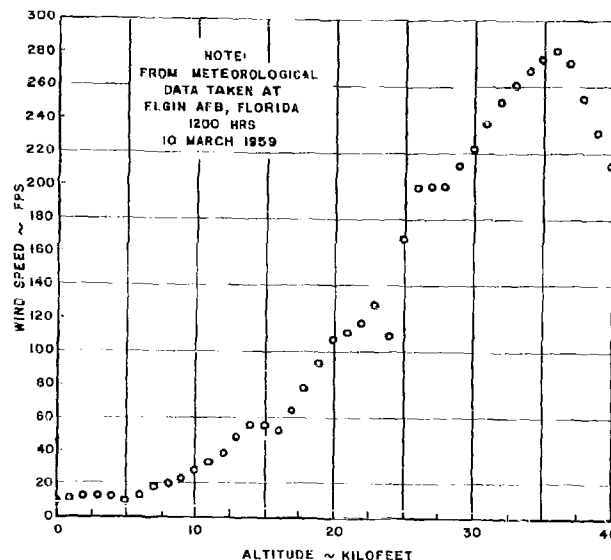


Figure 43. Wind Velocity vs Altitude  
During Cree Mission 28-1

Figure 44 displays missile performance data for Cree test mission 28-1. Shown are time-history plots of altitude, velocity, dynamic pressure, and Mach number from launch to water impact ( $t + 288$  seconds). These represent data accumulated by contrave and radar skin tracking and by the telemetering of measured static and dynamic pressures. As explained earlier, contrave phototheodolite tracked for the initial 3.5 seconds and radar skin track was established at 20 seconds and maintained to water impact. However, the radar data obtained during the interval of  $t + 20$  to  $t + 60$  seconds proved to be very erratic and consequently of little value for purposes of data presentation

On Figure 44 the missile performance data obtained from telemetry records are shown with dashed lines. Missile altitude was determined from recorded static pressures and corresponding pressure altitudes obtained from meteorological data taken on shot day (10 March 1959). Rayleigh's pitot tube formula, Reference 4, and measured impact and static pressures were employed to ascertain supersonic free stream Mach number while subsonic pressures were corrected for compressibility of air and used to determine the lower free stream values. To calculate missile velocity corresponding Mach numbers were multiplied by sonic velocities at test altitudes. These sonic velocities were analytically determined from ambient temperatures appearing on the meteorological records. Impact pressures in Figure 44 are a direct representation of the recorded values; no corrections were applied. Further investigation of the performance plots will show that altitude and velocity derived from radar skin track have been presented in their entirety, thus showing graphically the difference between the radar measurements and the telemetry data during the time interval of  $t + 20$  to  $t + 63$  seconds. The altitude data, while reasonably smooth, shows evidence of a searching or homing-in process during the earlier tracking stages. This phenomenon was effectively demonstrated in the excessive data scatter apparent in the time history of velocity from  $t + 10$  to  $t + 60$  seconds. At approximately 60 seconds the almost random oscillations in velocity resolve into a sinusoidal oscillation of decaying

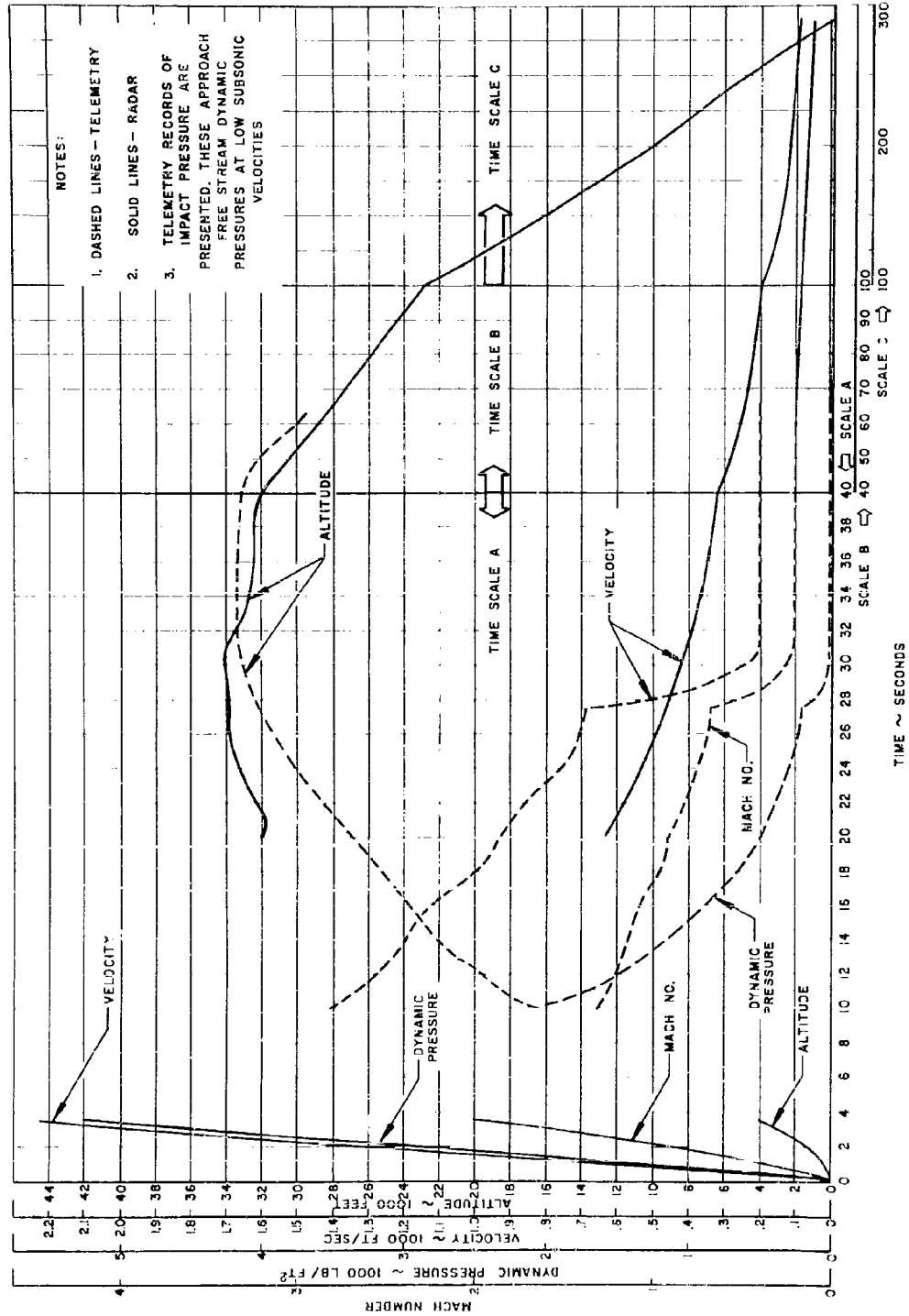


Figure 44. Missile Performance Data for Cree Mission 28-1

amplitude and frequency. The portion of the velocity curve shown during these times represents average values only and does not reflect sudden velocity change such as at the time of recovery parachute deployment.

Telemetry static and impact pressure data are available for approximately 53 seconds (from  $t + 10$  to  $t + 63$  seconds) of the total flight time. At  $t + 63$  seconds the signal became indistinguishable. Inspection of the velocity, impact pressure, and Mach number profiles shows inflection points at  $t + 27.5$  seconds (recovery parachute deployment) and rapid decay to new equilibrium conditions. Both impact pressure and Mach number derived from telemetry data agree very well with radar results at  $t + 63$  seconds.

Peak altitude attained during Cree test mission 28-1 was 33,400 feet; total flight time was 288 seconds.

## 2. Test Mission 29-2

Cree test mission 29-2 represents the first attempt, under the subject contract, to obtain high Mach, high altitude test points by utilizing a two stage Nike booster, ground launched configuration. A single type III (800 pound) missile was used.

During this mission the following boost sequence was programmed to provide a Mach 1.5 condition at an altitude of approximately 66,000 feet:

- (a) Launch, first stage ignite
- (b) First stage burnout at  $t + 3.5$  seconds
- (c) Coast, both stages, to  $t + 11$  seconds
- (d) Second stage ignite at  $t + 11$  seconds
- (e) Second stage burnout at  $t + 14.5$  seconds
- (f) Second stage separation at  $t + 15$  seconds
- (g) Payload coast to  $t + 43.09$  seconds (test parachute ejection).

These firing conditions would have provided a normal two stage trajectory. However, during the launching operation, premature ignition of the second stage booster occurred at approximately  $t + 50$  milliseconds.

Separation of the stages occurred almost immediately and second stage and missile proceeded on a nearly normal trajectory.

Neither contrave phototherdolite nor radar provided usable missile's performance data. Contrave tracked from launch to  $t + 1$  second. Radar tracked the missile beacon for the first five seconds, and skin tracked until  $t + 63$  seconds when the beacon was again received. Intermittent beacon operation occurred thereafter resulting in a partial trajectory. All radar data received was exceedingly erratic. Due to the premature second stage firing and resulting low altitude operation, the pressure range of the static transducer was not reached and ambient pressures were not recorded. Thus test altitudes were unobtainable.

Attempts were made to compute a post test trajectory using phototherdolite data for the first second, to establish initial flight conditions, and theoretical inputs up to test parachute deployment. From this point on, the impact pressure and parachute drag force were known and the trajectory could be continued to impact. The post test plot shown on Figure 45 is representative of the trajectories resulting from this approach and is shown here for illustrative purposes. Both the peak altitude attained and the total flight time indicated on the predicted post test trajectory are expected to be over-conservative, but the general profile of the actual flight should be somewhat similar in nature.

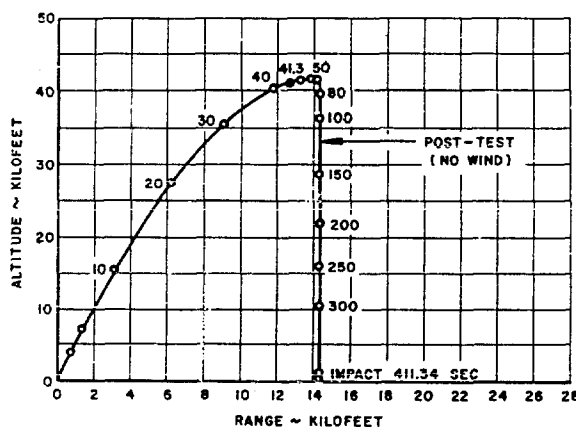


Figure 45. Predicted Trajectory for Cree Mission 29-2

With the exception of the static pressure data, which measured full scale during the entire flight, excellent telemetry data were obtained on this test. The initial impact pressure, at time of test parachute deployment, was found to be 266 pounds per square foot. A time-history plot of impact pressure will be presented later in this section together with the parachute performance obtained during mission 29-2.

### 3. Test Mission 30-3

A fully instrumented type III (800 pound) missile was assembled with two stages of Nike boosters and launched from an angle of 79 degrees. The anticipated test conditions were to be Mach 1.5 at an altitude of 66,000 feet. Figure 46 shows the predicted trajectory to

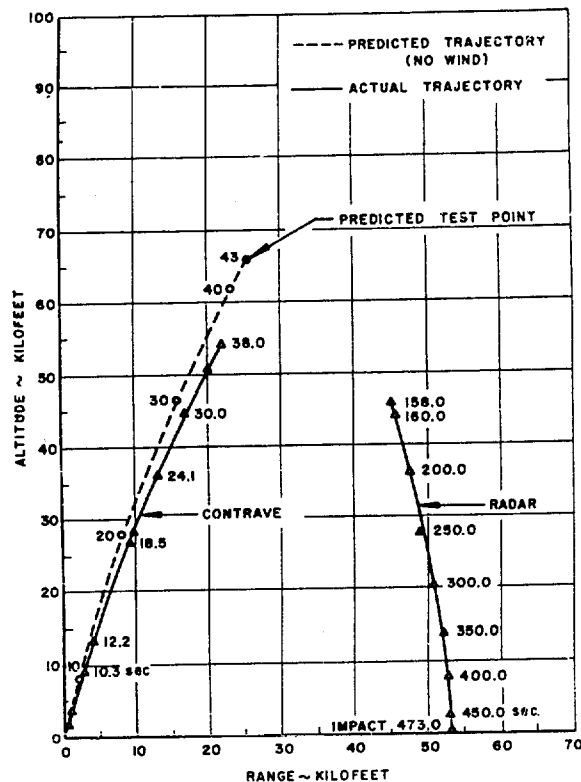


Figure 46. Predicted and Actual Trajectories for Cree Mission 30-3

the time of test parachute deployment. Actual launch was observed to be smooth and normal. First stage burned evenly and some rotation was noted. Burnout of the first stage at  $t + 3.4$  seconds, ignition of second stage at  $t + 8.8$  seconds, and burnout of second stage at 12.2 seconds occurred as programmed. The actual trajectory also presented in Figure 46 shows reasonably close agreement with the predicted for the initial 38 seconds of flight. Contrave phototheodolite intermittently tracked the missile during this time interval yielding data from launch to  $t + 12.2$  seconds, from 18.5 to 19.4 seconds, from 24.1 to 25.0 seconds, and from 30.0 to 38.0 seconds. The contrave trajectory at launch and 38 seconds showed the missile to have attained an altitude of 54,239 feet. Time-history plots of missile performance (Figure 47) showed the velocity, Mach number, and dynamic pressure at  $t + 38$  seconds to be 1,198 feet per second, 1.1, and 250 pounds per square foot, respectively. Though the beacon was functioning intermittently, limited data were obtained. However, radar skin track was established during descent at an altitude of 46,000 feet ( $t + 153.0$  seconds) and maintained to water impact and yielded the remaining data of Figure 47. A strong telemetry signal was recorded, but both pressure channels remained at 100 percent calibrate position and pressure data were not recorded. Total flight time was 473.0 seconds and missile impacted at a range of 53,000 feet.

In addition to the reduced contrave phototheodolite and radar data (shown as solid lines in Figure 47) analytical values (dashed lines) are presented to show missile performance (altitude, velocity, dynamic pressure, and Mach number) at the time of test parachute deployment. Dynamic pressure presented in the three aforementioned figures are based on free stream conditions. To obtain velocities, Mach numbers, and dynamic pressures at time intervals when contrave data were unobtainable (i. e., 12.0 to 18.5 seconds, 19.4 to 24.1 seconds, and 25.0 to 30.0



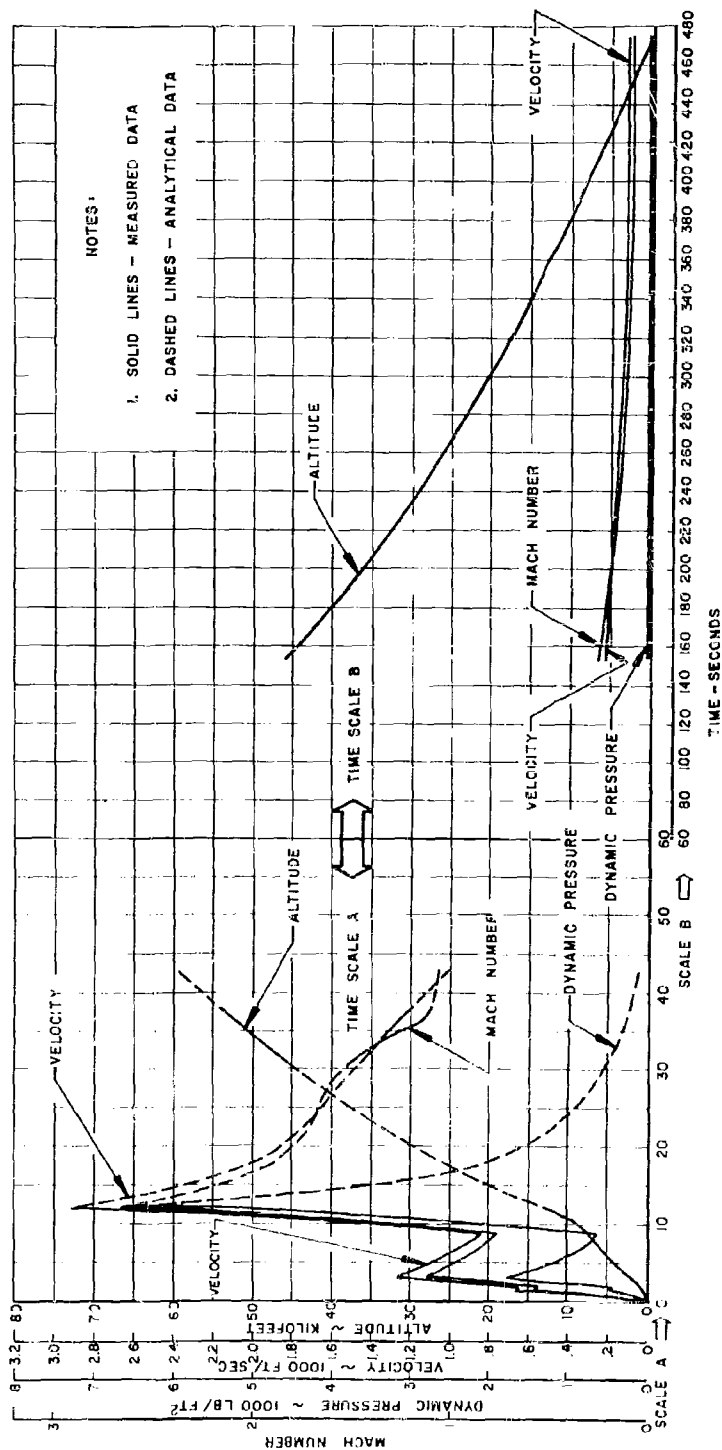


Figure 47. Missile Performance Data for Cree Mission 30-3

seconds) the following procedure was adopted:

- (a) Since the altitude profile is usually a curve of gradually changing slope and free of inflection points and since the contrave altitude data (where it existed) were comparatively smooth, the missing segments of the curve were filled in by maintaining the previously measured change in curve slope. This method was also used to extend the altitude data to the time of test parachute deployment.
- (b) To attain analytical values of missile velocities where measured data were not available, distance traveled during various time increments was determined from the altitude curve of Figures 46 and 47 and the average velocities calculated.
- (c) Thus, knowing both altitude and velocity, dynamic pressure and Mach number were determined with the aid of meteorological data (air density and ambient temperatures at altitude) taken on the shot day. From Figure 47 the missile performance at the time of test parachute deployment ( $t + 42.94$  seconds) was:

Altitude - 59,000 ft

Dynamic pressure - 135 psf

Velocity - 1,015 fps

Mach Number - 1.075

#### 4. Test Mission 31-4

The missile launch configuration for mission 31-4 was identical to that used during the previous mission, i. e., 800 pound payload with two stages of Nike boosters and launched from an angle of 79 degrees. Relatively severe test requirements necessitated test parachute deployment at  $t + 32$  seconds; missile altitude and Mach number were to be 50,000 feet and 1.87, respectively.

Launch appeared normal to personnel in attendance; however, flameout was noted at less than one second after ignition. Investigation of the contrave phototheodolite trajectory, presented in Figures 48 and 49, shows that first stage thrust was maintained for a full 3.4 seconds. The remainder of the boost phase progressed as programmed with second stage ignition at  $t + 8.5$  seconds and burnout at  $t + 11.9$  seconds. Second stage separation occurred at  $t + 12.3$  seconds. Presented in

Figure 48 for comparison purposes is a predicted missile trajectory for times to test parachute deployment. Comparison of actual and predicted trajectories shows no loss in performance as a result of the observed flameout during first stage boost. Deviation from the predicted track can be partially attributed to weather cocking due to eight knot surface winds from a direction of approximately 300 degrees. The effects of the surface winds and winds aloft to an altitude of 18,000 feet is further evidenced during descent by a drift of 1,300 feet.

Time history profiles of missile performance data taken during mission 31-4 are presented in Figure 49. Shown on an expanded time scale are reduced contrave data of altitude, velocity, free stream dynamic pressure and Mach number to  $t + 12.8$  seconds where photo-

theodolite track was lost. Radar skin track of the missile was established during descent at an altitude of 32,326 feet and maintained to water impact. The resulting radar data however, possessed scatter and the curves of Figure 49 are an average of measured values. The radar beacon did not function at any time during the mission. Altitude, velocity, dynamic pressure and Mach number at second stage burnout were 12,604 feet, 2,764 feet per second, 5,837 pounds per square foot and 2.53, respectively.

Telemetry records indicate good static pressure, but no impact data, from time of test parachute deployment through the time of recovery parachute deployment ( $t + 58.4$  seconds). From the measured static pressures, a time-history plot (Figure 50) of altitude was constructed utilizing pressure altitudes from meteorological data obtained prior to launch. Actual missile altitude at the test point was 49,100 feet.

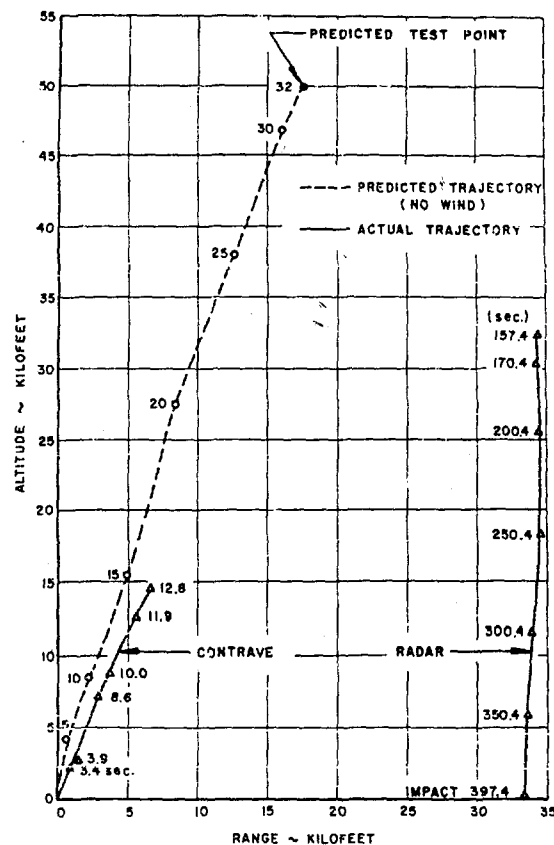


Figure 48. Predicted and Actual Trajectories for Cree Mission 31-4

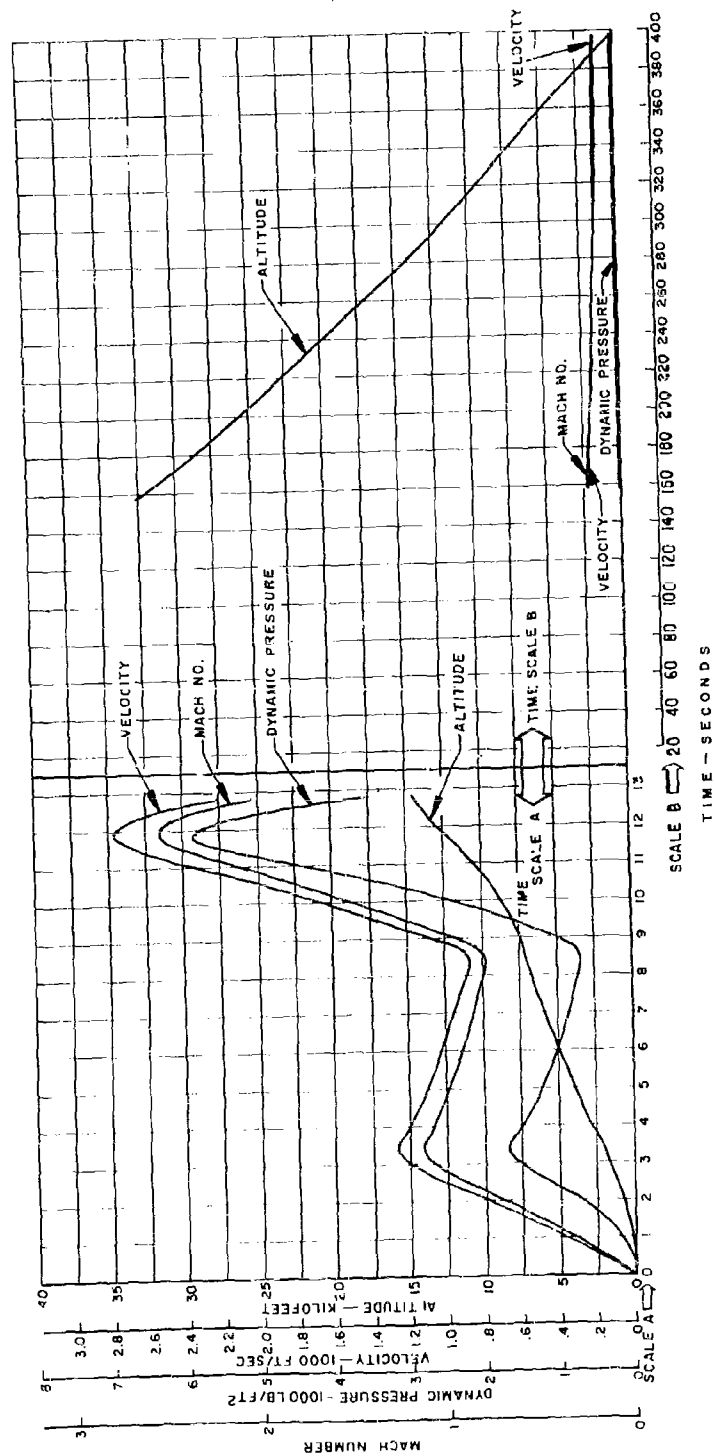


Figure 49. Missile Performance Data for Cree Mission 31-4

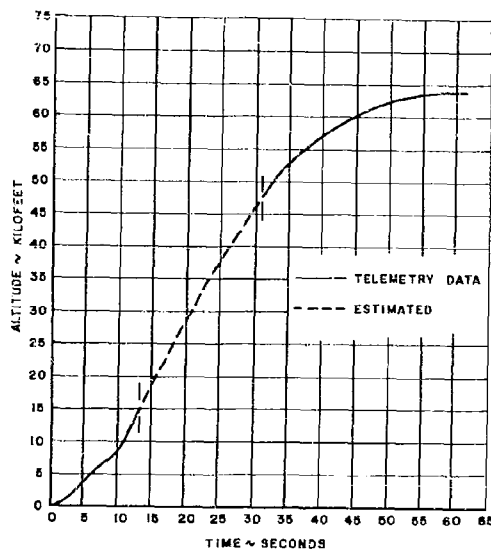


Figure 50. Altitude vs Time  
for Cree Mission  
31-4

beacon trajectories during boost substantiated the late ignition. Little data evidence is available that indicates intermittent burning of the second stage, but excessively long burning was noted. Figure 51, a comparison of predicted and actual trajectories, shows graphically that the actual missile performance exceeded anticipated performance by attaining a test altitude of 54,300 feet rather than 50,000 feet at  $t + 32$  seconds. Drift during descent is quite evident and resulted from six to 19 knot winds from approximately 250 degrees. Radar beacon track was maintained from launch to  $t + 103.6$  seconds. Radar skin tracked from  $t + 177.7$  seconds to water impact at  $t + 491.7$  seconds and a range of 31,700

A favorable comparison of missile performance exists between tests 3 and 4. For example, at second stage burnout the performance of the vehicle during test 4 was approximately 95 percent of corresponding values for test 3.

#### 5. Test Mission 32-5

A fully instrumented type III (800 pound) was launched from an angle of 79 degrees with two stages of Nike boosters. The anticipated test altitude and velocity were to be 50,000 feet and Mach 1.87. First stage booster functioned normally. However, observers at the test site noted late ignition as well as rough and uneven burning of the second stage booster. Investigation of the contrave photodolite and radar

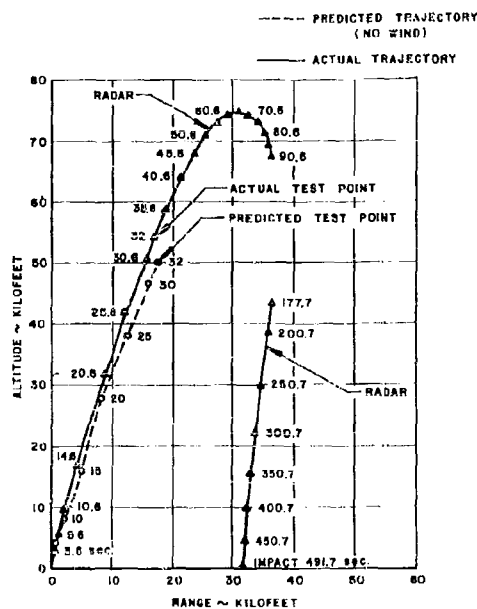


Figure 51. Predicted and Actual  
Trajectories for Cree  
Mission 32-5

feet. Contrave phototheodolite tracked from launch to  $t + 72.8$  seconds. Telemetry functioned to peak altitude; however, usable pressure data were unobtainable.

Figure 52 presents time-history profiles of altitude, velocity, dynamic pressure, and Mach number on an expanded time scale to  $t + 60$  seconds and a compressed scale from  $t + 60$  seconds to water impact. Missile performance at first and second stage burnout was obtained from reduced radar beacon track while the remaining portions of the curves represent data accumulated by both radar and contrave phototheodolite. First stage burnout occurred at  $t + 3.5$  seconds. Second stage ignition and burnout were estimated at  $t + 10$  and  $t + 14.5$  seconds, respectively. Radar beacon tracking records were obtained at 1.0 second intervals; thus the booster burning time presented may be slightly long. Total boost time of the second stage was then approximately 4.5 seconds, and would provide a possible explanation for the higher than anticipated performance as evidenced by Figure 51. At second stage burnout, an altitude of 16,889 feet, a velocity of 2,970 feet per second, a dynamic pressure of 6,059 pounds per square foot, and a Mach number of 2.75 were attained. Satisfactory test parachute deployment at  $t + 32$  seconds was exhibited by inflections in the velocity, dynamic pressure, and Mach number curves. At the test point missile performance was as follows:

Altitude - 53,800 ft

Velocity - 1,670 fps

Free stream dynamic pressure - 530 psf

Mach number - 1.83

#### C. Test Parachute Performance

During Phase IV, tests were conducted on four parachute types. These were: a 30 degree conical ribbon with a 4.03 foot nominal diameter; a FIST ribbon Project Mercury drogue parachute with a 6.0 foot nominal diameter; a 10 percent Equiflo ribbon with a 4.03 foot nominal diameter; and a 10 percent extended Hemisflo ribbon with a 4.12 foot nominal diameter. Typical gore layouts are shown in Figure 53. Data were gathered for all parachute types except the 30 degree conical. This data, however, varies in scope for each test item and is in no instance considered to be complete. In the following subsections, each parachute type is discussed separately.

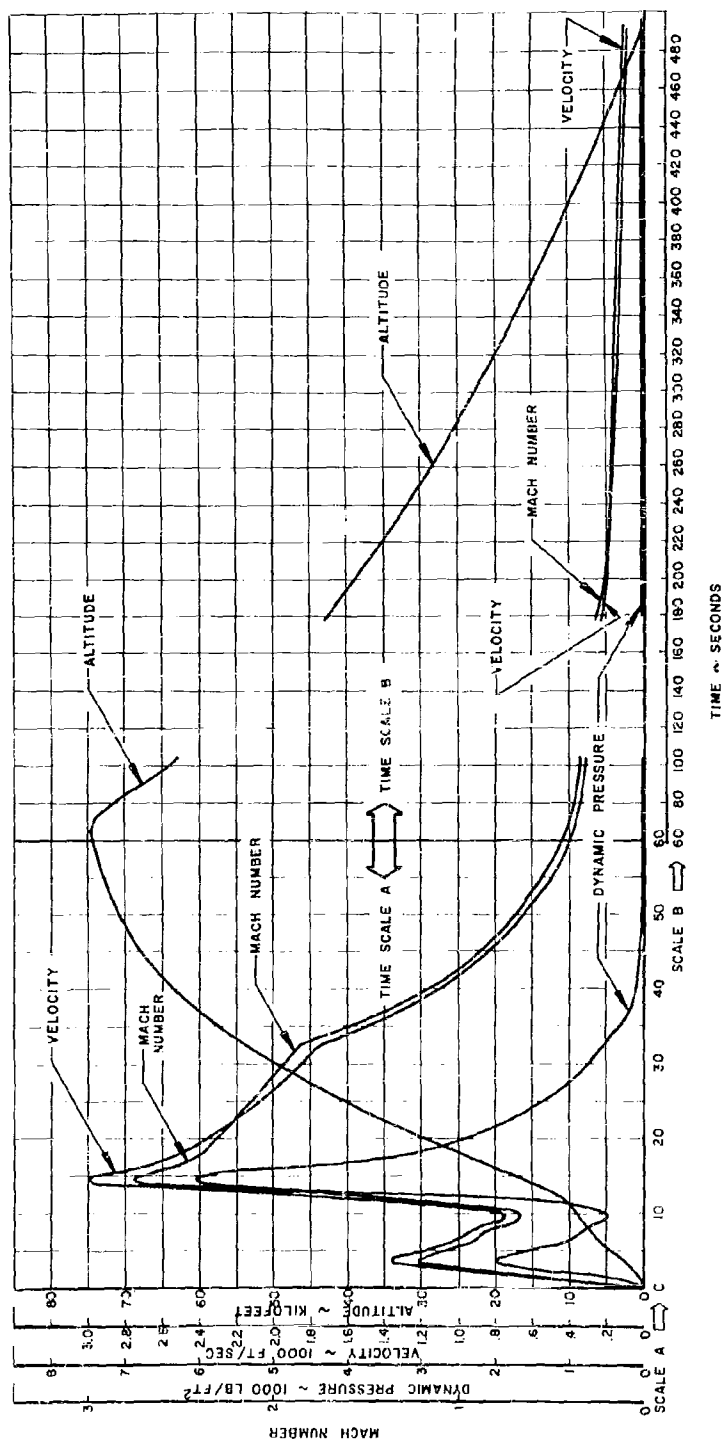
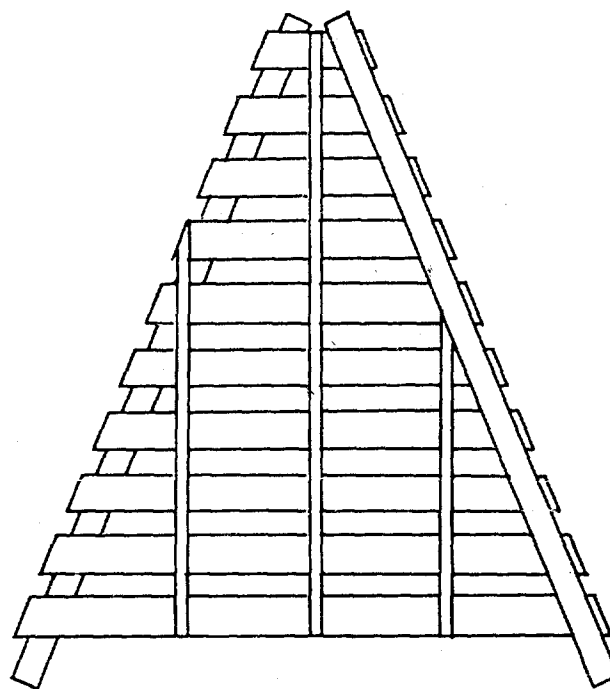
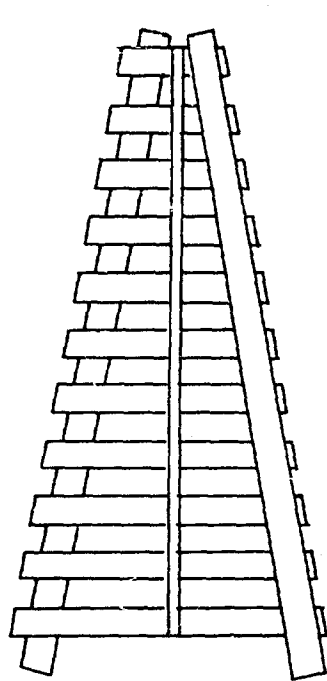
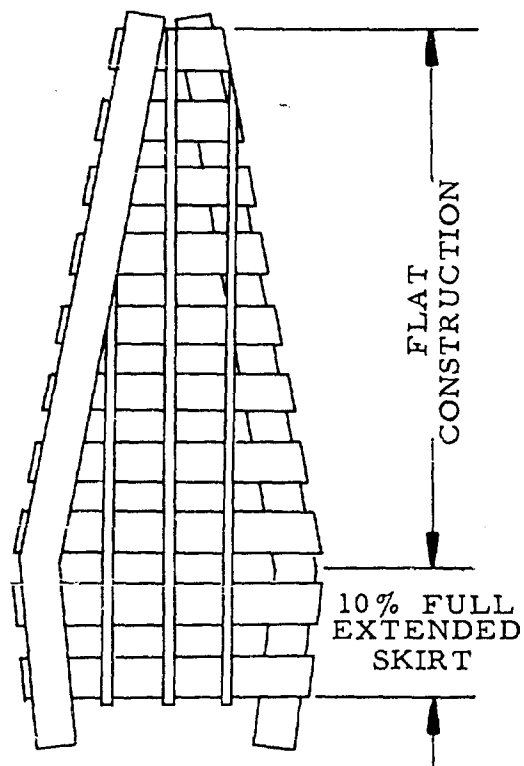


Figure 52. Missile Performance Data for Cree Mission 32-5

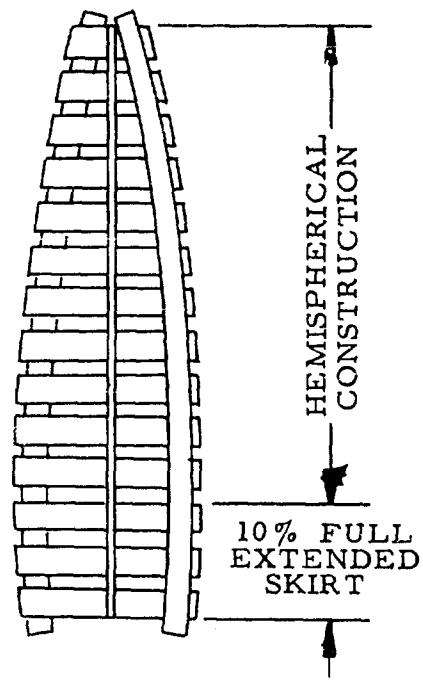


30° CONICAL GORE ASSEMBLY

FIST RIBBON GORE ASSEMBLY



EQUIFLO GORE ASSEMBLY



HEMISFLO GORE ASSEMBLY

Figure 53. Typical Test Parachute Gore Layouts



# 1. Ten Percent Equiflo Parachute

Two test missions were initiated to determine performance characteristics of a 4.03 foot nominal diameter Equiflo ribbon parachute. The test point for the earlier test (mission 30-3) was to have been Mach 1.5 at an altitude of 66,000 feet with a dynamic pressure of 190 pounds per square foot. Under performance of the missile yielded an extrapolated test point dynamic pressure of 135 pounds per square foot. A strong telemetry signal was received and good force data was recorded. Missile camera film was obtained for approximately 20 seconds. Throughout the time the parachute canopy appeared to be stable and exhibited little breathing or flutter; inflation was noted to be somewhat prolonged. The instantaneous area ratio and the parachute displacement angles together with drag forces are presented as a function of time lapsed from deployment in Figure 54.

Area ratio ( $S_p/S_o$ ) was derived by measuring the canopy's inflated or projected area, shown on photographic records of the test, and by comparing these with the nominal, or flat, parachute area. A flat parachute normally inflates to a diameter which is two thirds of its nominal diameter; thus the ratio of inflated area to nominal area becomes  $(2/3)^2$  or 0.445. This value of area ratio is then representative of a theoretical 100 percent inflation. For an Equiflo, a flat ribbon parachute with extended skirt, ( $S_p/S_o$ ) could be expected to be somewhat different.

Close investigation of the data presented in Figure 54 imparts reasonably complete parachute performance information. It can be seen from the force profile that a 300 pound snatch force occurs at deployment plus 0.25 second. The time from snatch to initial opening shock ( $t_f$ ) for a flat ribbon parachute can be expressed by:

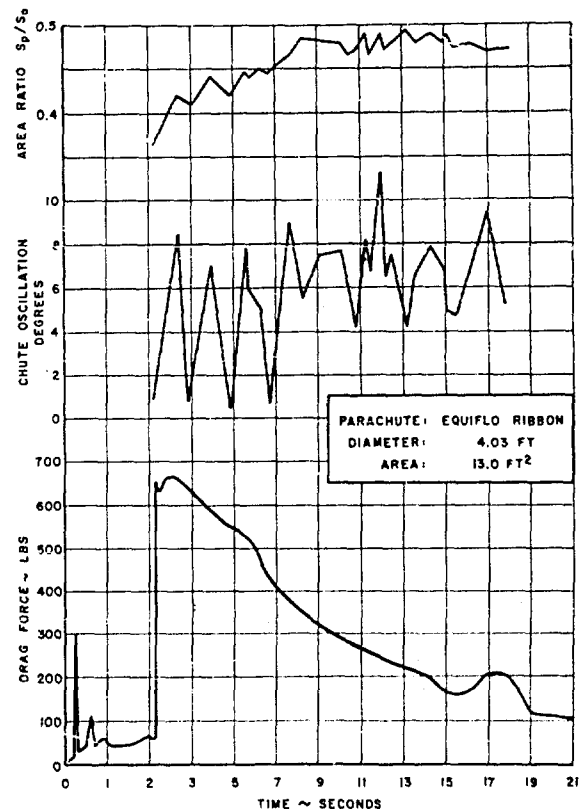


Figure 54. Parachute Test Data vs Time for Cree Mission 30-3

$$t_f = \frac{12 D_0}{V_s \sigma^{0.2}} \quad (\text{from Reference 8})$$

where:

$D_0$  = nominal diameter of the parachute

$V_s$  = velocity at time of snatch

$\sigma$  = density ratio.

Assuming the above expression to apply equally well to basically similar Equiflo parachutes, the theoretical filling time would be:

$$t_f = \frac{12 \times 4.03}{1015 \times 0.09877^{0.2}} = 0.0758 \text{ second}$$

However, line twist as evidenced by film coverage resulted in a delayed opening time of 1.88 seconds; notice should be taken of the fact that when canopy opening is initiated (at deployment plus 2.1 seconds) a very short time was expended (0.05 second) during inflation. The measured opening force was 665 pounds. Since time-histories of static and impact pressures were unobtainable, drag coefficients could not be determined directly. However, estimates of the drag coefficient at the time of full open force can be ascertained by using the extrapolated dynamic pressure of 135 pounds per square foot (from Figure 47). This was found to be 0.379. Instantaneous area ratio at the corresponding time was 0.40. Increase in area ratio is evident for approximately four seconds where an average value of  $S_p/S_0$  was 0.480 and represents 100 percent inflation. It has been found during earlier testing (during Phase II, the results of which are presented in detail in Reference 8) that when the inflation of a flat ribbon parachute is between 75 and 100 percent, the drag coefficient varies almost linearly with area ratio. If this premise is assumed to hold time in the case of Equiflo ribbon parachutes, a steady state drag coefficient of 0.455 results.

Figure 55 shows a series of views of the 10 percent Equiflo ribbon during deployment and opening.

A second test (mission 31-4) at an altitude of 50,000 feet and Mach number of 1.87 provided no additional data on the performance of a 10 percent Equiflo ribbon parachute. A type IIB (higher strength) modification of previously tested parachutes was used.



32



332



340



51



335



341



58



336



342



62



337



343



65



338



350



68



339



600

TIMES SHOWN ARE FROM START OF DEPLOYMENT  
CAMERA SPEED IS APPROXIMATELY 200 FRAMES PER SECOND.

Figure 55. Equiflo Parachute Inflation Characteristics

A good telemetry signal was obtained for about three minutes; however, the only data resulting was static pressure. Since the test vehicle was not recovered, no onboard film record was acquired. Telemetry record show evidence of test parachute deployment at the proper time but no conclusions can be drawn concerning performance.

## 2. FIST Ribbon

During Phase IV (mission 29-2) a 6.0 foot diameter FIST ribbon Project Mercury drogue parachute was to be tested at Mach 1.5 and 66,000 feet. Premature ignition of the second stage resulted in a much lower test altitude. No reliable records of actual missile trajectory were obtained, and ambient pressures at test altitude exceeded the range of the static pressure transducer. Excellent telemetry signal was received and good measurements of drag force and impact pressure recorded (see Figure 56).

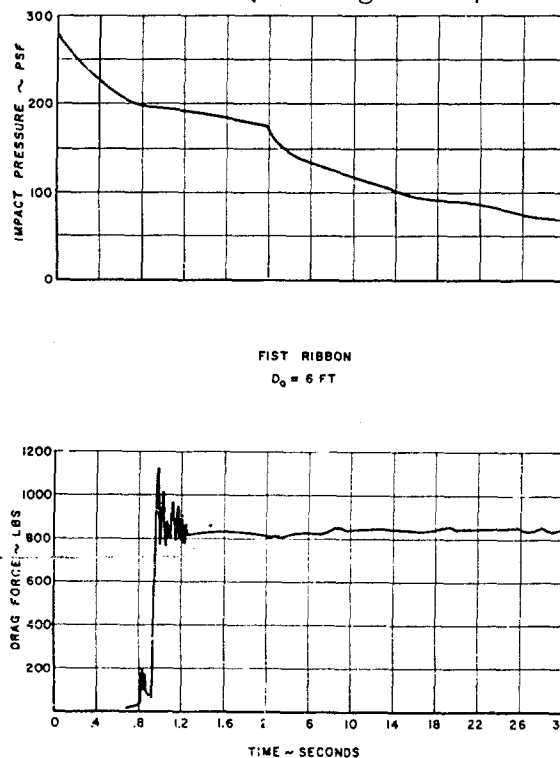


Figure 56. Parachute Test Data vs Time for Cree Mission 29-2

the missile had decelerated to an equilibrium velocity. The force level at this time was 840 pounds. Though velocity was not measured, it can be safely assumed to fall within a Mach number of 0.6. The ratio of

The two force channels were in almost exact agreement. Snatch force was 200 pounds and occurred at 0.97 after deployment. Therefore, filling time was 0.13 second. Drag force reached a value of 840 pounds at deployment plus 10 seconds where it remained until the end of the record 23 seconds later. Without records of static pressure, altitude could not be determined and the parachute drag coefficient could not be calculated. Investigation of the drag force profile would seem to indicate that test parachute deployment had occurred during ascent but very near the peak altitude and that by deployment plus 10 seconds descent had begun. At deployment plus 28 seconds, the impact pressure reached a steady state value of 68 pounds per square foot indicating that

compressible to incompressible dynamic pressures ( $q_c/q_{inc}$ ) could then be expected not to exceed the limits of  $q_c/q_{inc} = 1$  (at Mach number = 0) and  $q_c/q_{inc} = 1.1$  (at Mach number = 0.62). Thus, for an average value of  $q_c/q_{inc} (= 1.05)$  the free stream dynamic pressure was found to be 64.7 pounds per square foot. The resulting subsonic drag coefficient would not be less than  $CD_0 = 0.437$  nor exceed  $CD_0 = 0.482$  with an average value of  $CD_0 = 0.459$ .

### 3. Ten Percent Extended Hemisflo Ribbon

A 4.12 nominal diameter, 10 percent extended skirt Hemisflo ribbon parachute was tested during the final mission (32-5) of Phase IV. The planned test point conditions were attained, parachute was deployed at an altitude of 53,800 feet and velocity of Mach 1.83. Reliable radar trajectories at test altitude show evidence of satisfactory test parachute deployment at  $t + 32$  seconds. Telemetry functioned through parachute test but no usable data were acquired. Camera operated for about seven seconds, yielding approximate time-history profiles of area ratio ( $S_p/S_0$ ) and parachute oscillation (see Figure 57). Malfunction of the timing light or 100 cycle per second oscillator resulted in an absence of timing marks on the film record.

Investigation of Figure 57 shows that the area ratio increases from an initial value of 0.30 (at approximately deployment plus 0.2 second) to 0.34 at deployment plus 4.4 seconds where steady state parachute performance is attained. Area ratio was derived by measuring the canopy's inflated or projected area shown on photographic records of the test and by comparing these to the parachute's nominal area of 13.33 square feet. In the case of a Hemisflo parachute, the theoretical ratio of projected area to nominal area would be 0.386. High frequency canopy breathing was evidenced during the first second of test operation. For very brief periods (about five milliseconds), the area ratio attained a maximum value of 0.34 and a minimum value of 0.275. This breathing is not presented as data in Figure 57.

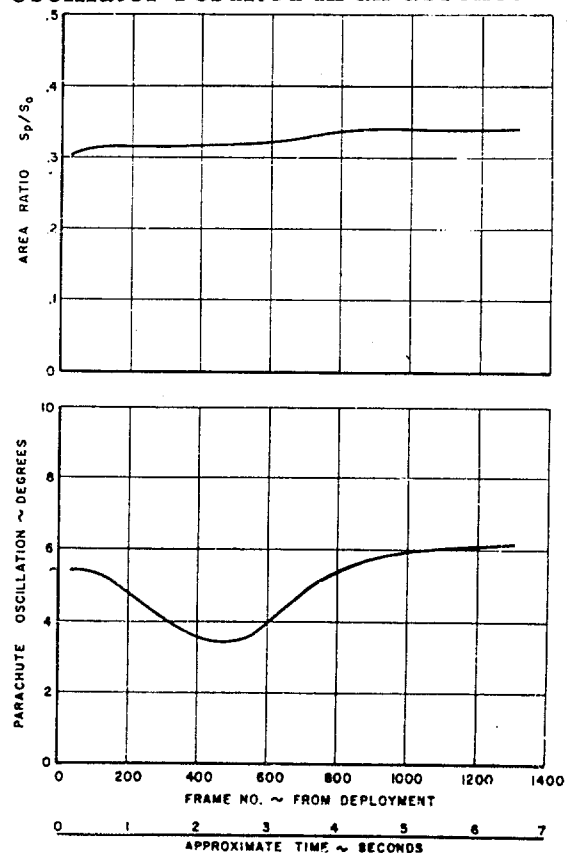
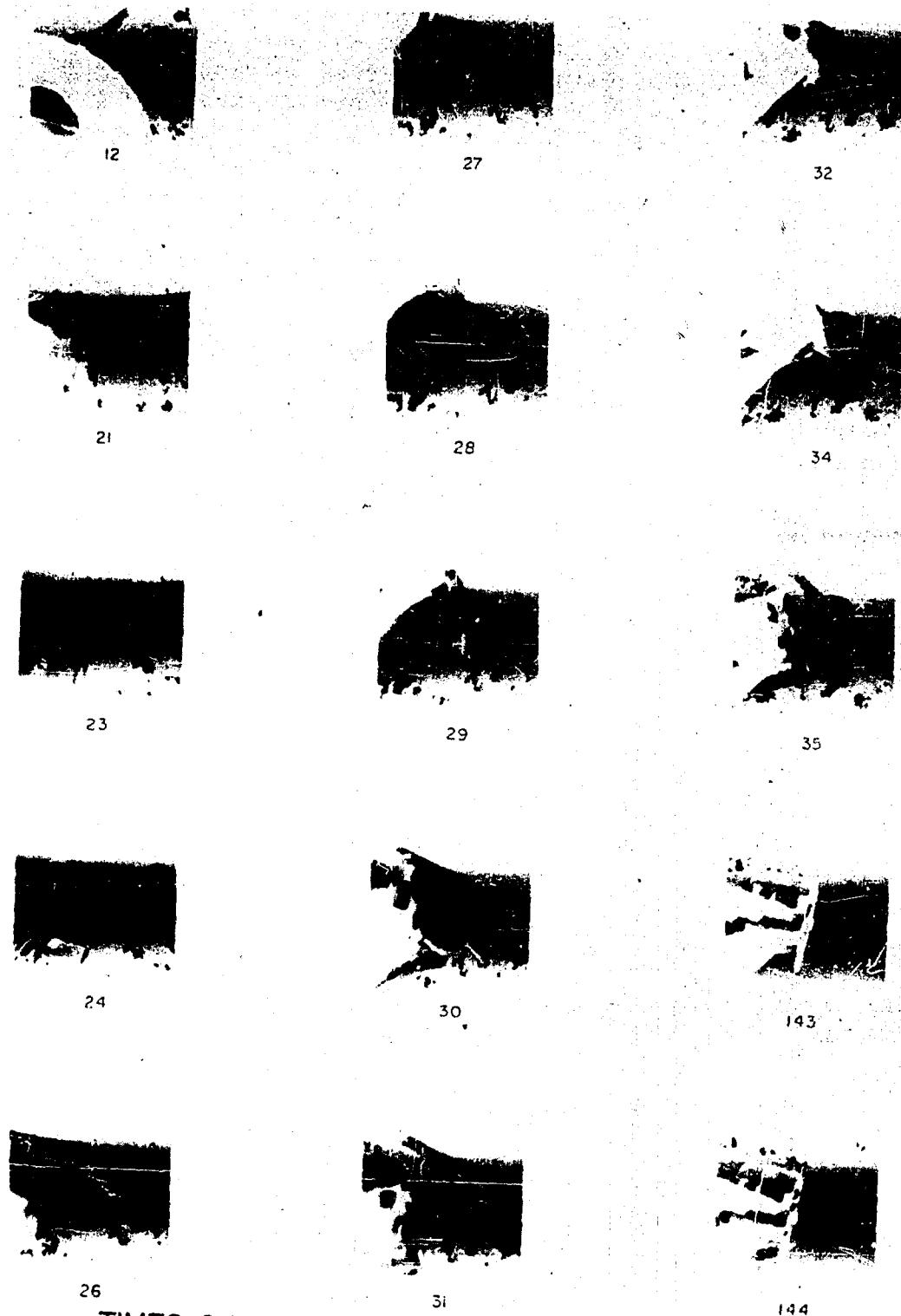


Figure 57. Film Data for Cree Mission 32-5



TIMES SHOWN ARE FROM START OF DEPLOYMENT  
CAMERA SPEED IS APPROXIMATELY 200 FRAMES PER SECOND

Figure 58. Hemisflo Parachute Inflation Characteristics

Parachute oscillations were measured in degrees displacement from the canopy location at estimated time of snatch. Though the data is presented as an oscillation, the parachute movement was actually rotational in nature, with the center of rotation being a point possessing what appears to be random movement. An approximate period of rotation, not evidenced by inspection of Figure 57 was 0.06 second (once every 12 frames) during the first 0.50 second of test and decaying to once every 57 frames (0.28 second) at the end of the record. As time, from deployment, progresses the radius of rotation diminished but never reached zero. The random movement of the center of rotation did not seem to be effected significantly by lower velocities. Thus a time-history of instantaneous oscillation (or displacement) does not in this particular case present a rigorous evaluation of parachute stability. Shown in Figure 57 are average values of parachute displacement. At no time did the parachute displace more than 8.25 degrees (2.32 feet). Figure 58 illustrates the Hemisflo parachute inflation characteristics.

## SECTION VI

### CONCLUSIONS AND RECOMMENDATIONS

#### A. Conclusions

Examination of the results obtained during the Phase IV test program lead to a number of conclusions which are as follows:

- (1) A method for the testing of aerodynamic decelerators at high Mach numbers and high altitudes, in addition to those employed in previous phases, was developed. The ground launch technique is practical, reasonably economical, and offers a potential for future development.
- (2) A modified Cree test vehicle was developed which was suitable for an over water type of operation. The flotation capability, which was added to the basic land type vehicle, was developed to the point where successful operation could be expected under normal operating conditions. This was evidenced by the recovery of the test vehicle during two of the last three test missions.
- (3) Parachutes with shaped canopies, such as the Equiflo and the Hemisflo, show promise for supersonic operation. The Hemisflo particularly functioned well at Mach numbers as high as 1.83. The canopy had excellent shape, was steady, and was fully inflated.
- (4) While only limited testing was accomplished during the Phase IV field effort, it should be recognized that on future programs it will be possible to test at an increased rate. Any scheduling rate will be dependent mainly upon the work load at the test range and the priority assigned to the parachute test program.
- (5) The ground launch technique while eliminating or reducing some of the problems attendant with aircraft and balloon launching does introduce some entirely new problem areas. However, none of these problem areas appear to offer any serious restriction to the eventual development of equipments and techniques for testing at conditions far beyond the capabilities of either of the other two launch methods.

#### B. Recommendations

Since the Cree missile program has been one of a continuing nature, it can be logically assumed that the test methods developed during the Phase IV program would be extended into future phases.



Based upon the results of the effort reported herein and the conclusions drawn, a number of recommendations can now be made. These are:

- (1) Parachute testing utilizing the ground launch technique should be continued.
- (2) Effort should be directed towards tests at higher Mach numbers and higher altitudes. If necessary, boosters other than the M5E1 Nike should be employed.
- (3) The investigation of shaped parachute canopies should be continued. Other more exotic configurations should also be tested if preliminary wind tunnel investigations indicate satisfactory operation.
- (4) The free flight test program should be augmented by a wind tunnel study with effort directed towards the development of new concepts in the field of aerodynamic decelerators.
- (5) The various facets of the test effort such as test vehicle design, launch hardware and fittings, checkout and launch techniques and missile tracking and search activity should be reviewed with the aim of improving over-all range coordination and both the quality and the quantity of the test data collected.

## REFERENCES

1. Davis, L. Jr., Follin, J.W. Jr., Blitzer, L., Exterior Ballistics of Rockets, D. Van Nostrand Company, Inc., New York, 1958
2. Engstrom, B.A., Performance of Trailing Aerodynamic Decelerators at High Dynamic Pressures, Part I Development of Test Method and Test Equipment, WADC TR 58-284, Wright-Patterson Air Force Base, Ohio, June 1958
3. Thibodaux, J.G., A Brief Summary of Experience in Boosting Aerodynamic Research Models, NACA Research Memorandum, RM L56E28, July 1956
4. Hilton, W.F., High Speed Aerodynamics, First Edition, Longmans, Green and Co., New York
5. United States Air Force Parachute Handbook, WADC TR 55-265.
6. FIST Ribbon Parachute: Design, Construction, and Use of, MCR EXE-672-19LL
7. Parachute, FIST Ribbon General Specifications for Construction of, MIL-P-6635.
8. Engstrom, B.A., Performance of Trailing Aerodynamic Decelerators at High Dynamic Pressures, Part II, Phase II, Test Results, WADC TR 58-284, Wright-Patterson Air Force Base, Ohio, January 1960.

This Document  
Reproduced From  
Best Available Copy